A STUDY OF MAGNETIC AND ELECTRICAL PROPERTIES OF SOME SPINELS

A Thesis

submitted to the

UNIVERSITY OF POONA

for the degree of

DOCTOR OF PHILOSOPHY
IN CHEMISTRY

By

SOMARAJU SUSEELA,
M. Sc.

National Chemical Laboratory,
Poona 8.

April 1971

ACKNOWLEDGEMENT

I express my sincere thanks to Dr. A.P.B. Sinha, for his help in selecting the problem and for his guidance and helpful suggestions in carrying out the work.

Thanks are due to the Director, Bhabha Atomic Research Centre, Bombay, for the X-ray spectrograms.

Thanks are also due to the Director, National Chemical Laboratory, Poona for allowing this work to be submitted in the form of a Thesis.

S. Suseela.
(S. Suseela)

C O N T E N T S

GENERAL INTRODUCTION

In spinels containing magnetic ions at both octahedral and tetrahedral sites, the much stronger A-B interaction controls the magnetic behaviour of solids and it is not possible to get any idea of B-B interaction. However if the tetrahedral 'A' sites are occupied by diamagnetic ions, then the 90° B-B interactions become quite significant.

The 90° Mn^{4+}-Mn^{4+} interactions are known to be ferromagnetic and 90° Cr^{3+}-Cr^{3+} interactions in oxides are known to be antiferromagnetic. With a view to compare the behaviour of isoelectronic ions Cr^{3+} and Mn^{4+} both having the $3d^3$ configuration, this work was taken up. Solid solutions containing diamagnetic ions at tetrahedral sites and Mn^{4+} and Cr^{3+} ions at octahedral sites have been prepared. The concentrations of Cr^{3+} and Mn^{4+} have been varied in a regular manner and the paramagnetic susceptibility of the compounds has been measured.

The valence state of copper ions in manganites has been a subject of considerable interest. Whereas the magnetic susceptibility and electrical conductivity results suggest that copper in copper manganite is present as Cu^{1+}, the X-ray absorption data indicate the presence of Cu^{2+}. We have therefore studied the electrical properties of several chromite-manganite solid solutions. The work can be divided into two systems: the first system containing Li^{1+} and Zn^{2+} at tetrahedral sites and Mn^{4+}, Cr^{3+} and Li^{1+} at octahedral sites, and the second system containing Cu^{1+}, Li^{1+} and Zn^{2+} at tetrahedral sites and Mg^{2+}, Mn^{4+} and Cr^{3+} at octahedral sites.

In Chapter I, the crystallographic, magnetic and electrical properties of manganites are discussed. In Chapter II, the experimental techniques are described. In Chapter III, the results are presented and in Chapter IV, the results are discussed in detail.

CHAPTER - I

INTRODUCTION

1.1 CRYSTAL STRUCTURE OF MANGANITES

Crystallographically manganites belong to the family of substances having the spinel structure. This name was originally given to a cubic mineral of composition $MgAl_2O_4$ by Bragg[1].

Many oxides crystallise in a face centred cubic structure where the O^{-2} ions which form a close packed assemblage are held together by the interstitial cations. There are two kinds of interstices: tetrahedral with four nearest neighbours and octahedral with six nearest neighbours. If only the octahedral sites are filled the crystal has the rock salt structure and if only the tetrahedral sites are occupied the crystal has the zinc blende structure. The spinel is an ordered mixture of zinc blende and rock salt structures in which there are cations in each type of interstice. Each unit cell contains eight AB_2O_4 molecules. The 32 oxygen ions form a nearly close packed structure containing 64 tetrahedral interstices and 32 octahedral interstices. In the spinel structure eight of these tetrahedral holes and sixteen of the octahedral holes are occupied by cations.

The space group is $Fd3m, O_h^7$. The atomic positions in the spinel structure are: 8 metal ions at 8(a) sites: 0,0,0; 1/4, 1/4, 1/4 (+f.c.c.), 16 metal ions at 16(d) sites: 5/8,5/8,5/8; 5/8,7/8,7/8; 7/8,5/8,7/8; 7/8,7/8,5/8 (+f.c.c.) 32 oxygen ions at 32(c) sites:

u,u,u; u,$\bar{u}$,$\bar{u}$; $\bar{u}$,u,$\bar{u}$; $\bar{u}$,$\bar{u}$,u;

1/4-u,1/4-u,1/4-u; 1/4-u,1/4+u,1/4+u;

1/4+u,1/4-u,1/4+u; 1/4+u,1/4+u,1/4-u;(+f.c.c.).

The f.c.c. translations are:

+(0,0,0; 0,1/2,1/2; 1/2,0,1/2; 1/2,1/2,0).

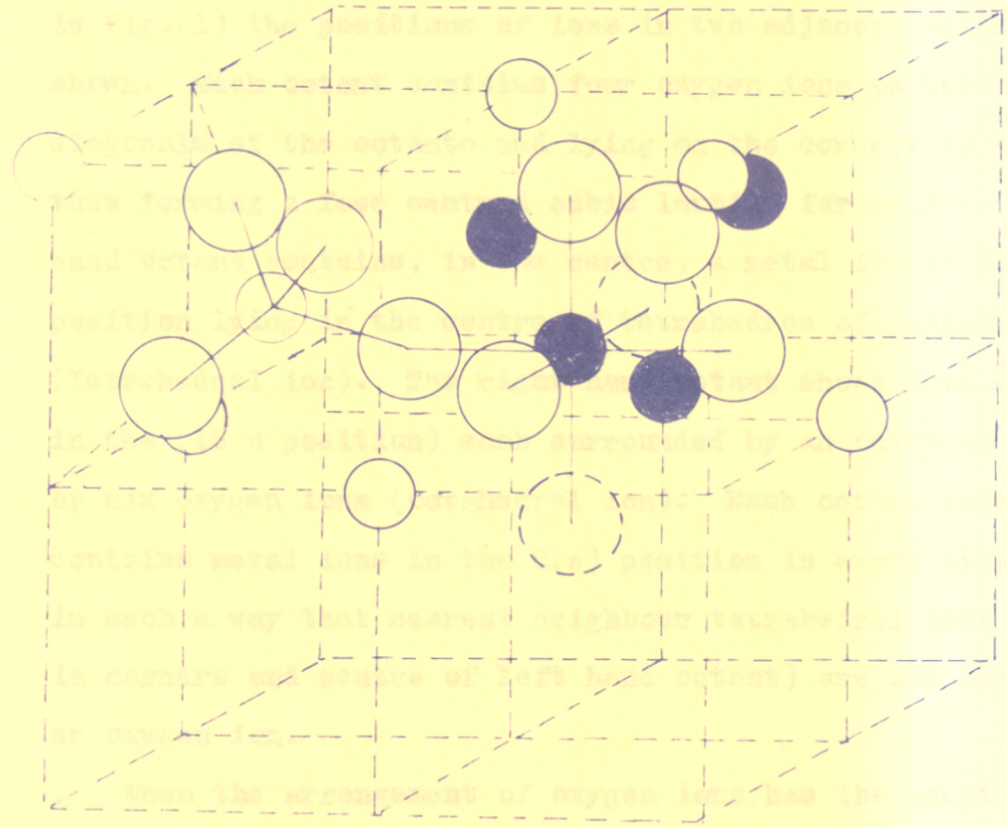

Oxygen ions

Tetrahedral cations

Octahedral cations

UNIT CELL OF AN IDEAL SPINEL SHOWING ONLY TWO OCTANTS

Fig. 1.

The unit cell with a cube edge 'a' consists of two different groups of four cubes with edges 1/2 a (octants) with identical positions. Ionic positions are different in two octants sharing a face and identical in two octants sharing an edge. In Fig.(1) the positions of ions in two adjacent octants are shown. Each octant contains four oxygen ions on the body diagonals of the octants and lying on the corners of a tetrahedron, thus forming a face centred cubic lattice for u=3/8. The left hand octant contains, in the centre, a metal ion in the (8a) position lying in the centre of tetrahedron of oxygen ions, (Tetrahedral ion). The right hand octant shows four metal ions in the (16 d position) each surrounded by an octahedron formed by six oxygen ions (Octahedral ion). Each octant moreover contains metal ions in the 8(a) position in every other corner in such a way that nearest neighbour tetrahedral ions (those in corners and centre of left hand octant) are not separated by an oxygen ion.

When the arrangement of oxygen ions has the exact cubic close packing, the oxygen parameter 'u' has a value 3/8. However in actual spinel lattices 'u' is slightly larger than 3/8. In that case the tetrahedral sites are expanded by an equal displacement of four oxygen ions outwards along the body diagonals of the cube. Since these four oxygen ions still occupy the corners of enlarged tetrahedron, the surrounding of each A ion retains cubic symmetry. But the oxygen surrounding of the B ion has no longer cubic symmetry, but has a symmetry similar to that of neighbouring B ions.

Tetragonal Spinel Structure

Some manganites such as Mn_3O_4 and $ZnMn_2O_4$ do not crystallise in cubic spinel structure but crystallise in tetragonal spinel structure. The unit cell contains four molecules of the formula unit $X Y_2O_4$. Usually $c \simeq 9\text{Å}$, $a \simeq 5.5\text{Å}$ and $\frac{c}{a} \simeq 1.6$. The space group assigned to this structure is $I4_1/amd$-D_{4h}^{19} and the positions of the ions in the unit cell are as follows:

4(a) position: 0,0,0; 0,1/2, 1/4 ;+ b.c.

8(d) position: 0,1/4,5/8; 0,3/4,5/8; 1/4,0,3/8; 3/4,0,3/8; +b.c.

and oxygen ions at 16(h) position:

$0,\bar{x},z$; $0,x,z$; $0,1/2+x,1/4-z$; $0,1/2-x,1/4-z$; $x,0,\bar{z}$;

$\bar{x},0,\bar{z}$; $x,1/2,1/4+z$ and $\bar{x},1/2,1/4+z$ + b.c.

The b.c. translations are +0,0,0 and 1/2,1/2,1/2.

A body-centered tetragonal spinel can be changed to a larger face-centered tetragonal spinel on its 'c' face diagonals and the new parameters for this cell are $a' = a\sqrt{2} \approx 8\text{Å}$ and $c' = c \simeq 9\text{Å}$. The volume of this cell is double the original cell. The atomic positions are similar to those in a cubic spinel in case of tetragonally distorted spinel containing 8 molecules of Me_3O_4. The metal ions in this tetragonal structure are distributed over the two types of sites. One type has the tetragonally distorted octahedral surrounding and the other type, the tetragonally distorted tetrahedral surrounding. Each ion at the former set has six oxygen neighbours, four of which are in the plane defined by the axes a and b and the rest two oxygen ions along the normal to

this plane. The four oxygen ions in the plane a-b are closer to the metal ion than the remaining two oxygen ions by a factor a'/c'. The metal ions at the tetrahedral positions, however, have their four oxygen neighbours all at the same distance.

Cation Distribution in Spinels

Spinels are classified as normal, inverse and random by Barth and Posnjak[2]. If all the A ions are in tetrahedral and B ions in octahedral interstices, the spinel is called normal, whereas the spinel is inverse if all the A ions and half of the B ions occupy octahedral sites and rest of the B ions occupy tetrahedral sites. The random spinel is one in which both the A and B ions are distributed equally and randomly between the two sites. Spinels can be further classified depending on the valency of the cations as 2-3, 1-3, 1-4 and 1-6 spinel type. All the aluminates, chromites and ferrites of divalent metals are examples of 2-3 spinels. Stannates and several titanates belong to the 2-4 class. The ferrites and aluminates of Lithium [$LiFe_5O_8$, $LiAl_5O_8$] are examples of 1-3 spinels, while some molybdates and tungstates of monovalent elements such as Na_2MoO_4 belong to the group of 1-6 spinels.

The formula of a spinel can be written by putting the cations situated at the octahedral sites in square brackets, tetrahedral ions and oxygen ions outside the bracket on the left and right respectively. The variation in the distribution of cations in tetrahedral and octahedral positions causes a marked change in some of the physical properties such as electrical and magnetic.

The distribution of cations can be determined with the help of X-ray diffraction, provided the scattering power of these is sufficiently different. If the scattering of X-rays by the two cations is nearly the same then the X-ray diffraction fails to decide the ionic arrangement. Neutron diffraction studies can often facilitate the determination of cation distribution. The study of electrical and magnetic properties throw light on the cation distribution.

Individual Site Preference of Cations

The distribution of cations over the tetrahedral and octahedral sites is governed by the minimization of total energy. If the chemical bonding in the spinel lattice is treated as ionic, there is an equilibrium of coulomb forces described by the Madelung potential and Born repulsive forces roughly determined by the size of different cations. The ionic radii will not vary over a wide range because the spinel structure is stable only if the cations are medium sized and in addition the radii of the different ionic species in the same compound do not differ too much.

Verwey and Heilmann[3] and Verwey, DeBoer and Vansanten[4] tried to explain the cation distribution taking into account static coulomb interaction and overlap forces. The coulomb potential energy per molecule $V_c = \frac{-Me^2}{a}$ is dependent on charge distribution, on the oxygen parameter 'u' and on the celledge 'a'. Madelung constants (M) have been calculated by Verwey, DeBoer and Vansanten as a function of 'u', for an average ionic charge of 4, 3 or 2 in tetrahedral position and 2, 2.5 and 3 in

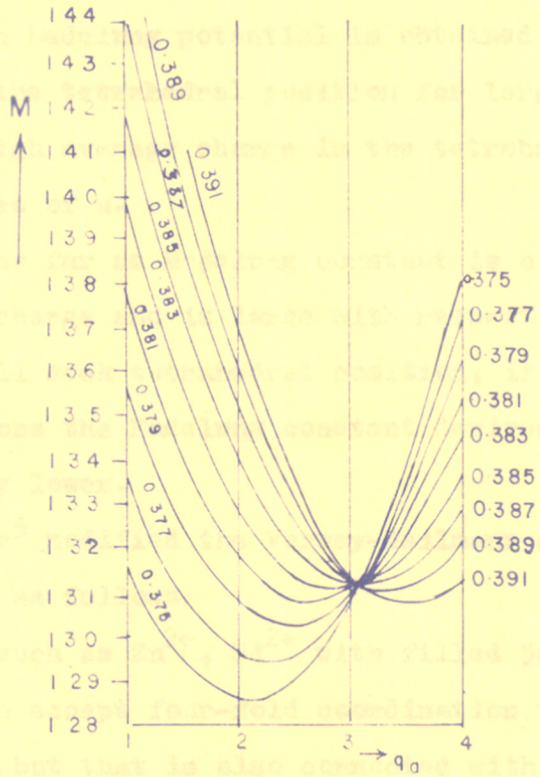

FIG 2. MADELUNG CONSTANT (M) AS A FUNCTION OF THE IONIC CHARGE IN THE 'A' POSITION (q_a) FOR DIFFERENT VALUES OF THE OXYGEN PARAMETER (u) (GORTER 5)

octahedral position.

Gorter[5] has considered the case of mixed crystals containing fractional number of charges per formula unit in both positions. He has given the Madelung potentials expressed in units e^2/a as a function of q_a for different values of 'u' by a set of parabolas represented in Fig.(2). From the figure, it is clear that a high Madelung potential is obtained (1) with low average charge in the tetrahedral position for large values of u, (2) with high average charge in the tetrahedral position for small values of u.

Thus as far as Madelung constant is concerned, an ion that has a low charge and is large with respect to other cations present will seek tetrahedral position, if for other cation distributions the Madelung constant derived from figure (2) is appreciably lower.

Gorter[5] modified the Verwey-Heilmann scheme and has summarised as follows:

(a) Ions such as Zn^{2+}, Cd^{2+} with filled 3d shells have a tendency to accept four-fold coordination, thus, forming covalent sp^3 bonds, but that is also connected with the dependence of lattice energy on the lattice parameter a, the oxygen parameter u, and q_a the average ionic charge per formula unit in such a site.

(b) The ions such as Li^{1+}, Mg^{2+}, Al^{3+} and Ti^{4+} which have a noble gas configuration do not show any preference for either coordination.

(c) The ions with half filled 3d shells exhibit spherical symmetry and so they do not possess any individual preference.

(d) Transition metal ions such as Cr^{3+}, Ni^{2+} or Mn^{4+} with $3d^3$

and $3d^8$ configuration have a marked preference for octahedral positions. Other transition metal ions do not have any individual preference.

Goodenough and Loeb[6] explained the site preference on the basis of covalent bond formation. The ions with a full d shell, which is separated in energy by only a small interval from the next empty s and p shells form tetrahedral orbitals resulting from the hybridisation of sp^3 orbitals. The strength of the covalent bonds decreases with increasing atomic number of the cation and decreasing atomic number of the anion in any one column of the Periodic Table. The octahedral hybrid d^2sp^3 orbitals occur in the transition metals which have partially filled d shells especially with d^3 or d^6. So ions like Cr^{3+} are stabilized in the octahedral site by partial covalent bond formation, and also ions with d^4, d^8 or d^9 can form square covalent bonds and can be accommodated in an octahedral site. The covalent bond strength depends on the relative sizes of the cations and interstices, the electronegativity difference between anions and cations and also on the strength of the covalent bond in the opposite set of lattice sites.

Some workers[7,8,9] applied the crystal field theory for explaining the cation distribution. When a transition metal ion is surrounded by six negative ions in a regular octahedral arrangement, the five d orbitals no longer have the same energy but are split into two groups a lower triplet t_{2g} and an upper doublet e_g. The physical basis for this splitting is simply the electrostatic repulsion between the d electrons and the surrounding negative ions. The e_g orbitals $d_{x^2-y^2}$ and d_{z^2}

point directly at these ions and are thus destabilized. The t_{2g} orbitals (d_{xy}, d_{xz} and d_{yz}) point in directions where the field is least i.e. between the ions and are thus stabilized. In the tetrahedral environment a similar splitting occurs but here $d_{x^2-y^2}$, d_{z^2} have lower energy than d_{xy}, d_{yz} and d_{zx}. The difference between the energy values for octahedral and tetrahedral stabilization has been used by Dunitz, Orgel and McLure[9] as a measure of octahedral site preference. While calculating they ignored the variation of the difference in Madelung energy with the nature of metal ions between normal and inverse spinels. Another factor that they have ignored is that the irregular variation of crystal field stabilizations must be superimposed on a steady variation with atomic number of the difference in energy between octahedrally and tetrahedrally coordinated compounds.

More complete work has been done by Miller[10]. He calculated site preference energies P_J of various ions taking into account (a) the coulomb energy, (b) the short range energy which is assumed to result from central forces effective only between nearest neighbour atoms and includes repulsion and covalent bonding effects and ~~the~~ (c) crystal field stabilization energy.

A cation with a larger value of P_J displaces a cation having a smaller value of P_J from the octahedral spinel sites. He has not tabulated the P_J's computed for tetravalent cations because the effects of angular orientation other than crystal field become important enough to overwhelm other terms and they have been neglected in this treatment. He has also observed that the cation pairs in spinels whose ionic distributions are

Table - 1

Octahedral Site Preference Energies for Various Cations. Values of P_J are in K.cal/g. atomic weight

Ion	P	Ion	P	Ion	P	Ion	P
Li^{+}	- 3.6	Mn^{++}	-14.7	Zn^{++}	-31.6	Cr^{+++}	16.6
Cu^{+}	- 8.6	Fe^{++}	- 9.9	Cd^{++}	-29.1	Mn^{+++}	3.1
Ag^{+}	-19.6	Co^{++}	-10.5	Al^{+++}	- 2.5	Fe^{+++}	-13.3
Mg^{++}	- 5.0	Ni^{++}	9.0	Ti^{+++}	-21.9	Ga^{+++}	-15.4
Ca^{++}	-30.7	Cu^{++}	- 0.1	V^{+++}	-11.6	In^{+++}	-40.2

intermediate between normal and inverse have values of P_J which differ from each other by less than 3 K.cal/g. atomic weight which is of the order of magnitude of RT at effective temperature determining the ionic distribution. (Table 1).

Goodenough[11] has corrected the site preference energies given by Miller. He used a different expression for Madelung energy. (Table 2).

He commented that while calculating polarization energies earlier workers considered only crystal fields but actually the centre of gravity of the d state manifold is shifted by the polarization effect and the ratio of τ_5 stabilization to τ_3 stabilization of octahedral cations is not known. He says that d state polarizations must be considered while calculating site preference energies.

Table - 2

Spinel Octahedral Site Preference Energies for Various Cations

Ion	$(O-T)^{a-b}$ K.cal/gm.	P^c K.cal/gm.	Ion	$(O-T)^{a-b}$ K.cal/gm.	P^c K.cal/gm.
Li^+	0	5.9	Cd^{2+}	0	-10.1
Cu^+	0	0.9	Al^{3+}	0	26
Ag^+	0	-10.1	Ti^{3+}	7.7	6.6
Mg^{2+}	0	14	V^{3+}	12.3^d	16.9
Ca^{2+}	0	-11.7	Cr^{3+}	46.7	45.1
Mn^{2+}	0	4.3	Mn^{3+}	25.3	31.6
Fe^{2+}	3.9	9.1	Fe^{3+}	0	15.2
Co^{2+}	2.1	8.5	Co^{3+}	?	?
Ni^{2+}	22.8	28.0	Ga^{3+}	0	13.7
Cu^{2+}	15.6	18.9	In^{3+}	0	-11.7
Zn^{2+}	0	-12.6	-	-	-

a = D.S.McClure Physics and Chem.Solids, 3, 311 (1957)

b = Weak field limit $\beta=0$.

c = A.Miller. J.Appl.Physics Suppl. 24S (1959) but corrected by 9.5 Zi because a different expression for EM was used

d = Strong field limit ($\beta= \frac{1}{4}$)

A Review of the Work done on Crystal Structure of Manganites Containing Mn^{4+}

Till now we have considered the site preference energies in spinels. From these arguments it is quite clear that Mn^{4+} which is isoelectronic with Cr^{3+} also prefers octahedral sites. Quite a good amount of work has been done on the crystal structure of manganites containing tetravalent manganese. The compounds along with their cell edges are presented in a table below:

Table - 3

Compound	Ionic distribution	a	Ref.
$CuMn_2O_4$	$Cu^{1+}[Mn^{3+}Mn^{4+}]O_4$	8.33	12
$ZnNiMnO_4$	$Zn^{2+}[Ni^{2+}Mn^{4+}]O_4$	8.31	13
$LiMn_2O_4$	$Li^{+}[Mn^{3+}Mn^{4+}]O_4$	8.246	14
$CuMg_{0.5}Mn_{1.5}O_4$	$Cu^{+}[Mg^{1+}_{0.5}Mn^{4+}_{1.5}]O_4$	8.31	15
$CuNi_{0.5}Mn_{1.5}O_4$	$Cu^{+}[Ni^{2+}_{0.5}Mn^{4+}_{1.5}]O_4$	8.31	15
$LiNi_{0.5}Mn_{1.5}O_4$	$Li^{1+}[Ni^{2+}_{0.5}Mn^{4+}_{1.5}]O_4$	8.17	15
$LiZn_{0.5}Mn_{1.5}O_4$	$Li^{+}_{0.5}Zn^{++}_{0.5}[Li^{+}_{0.5}Mn^{4+}_{1.5}]O_4$	8.19	15
$CuMgMnO_4$	$Cu^{1+}[Mg^{2+}_{0.5}Mn^{4+}_{1.5}]O_4$	8.31	15
$Cu_{1.5}Mn_{1.5}O_4$	$Cu^{+}[Mn^{4+}_{1.5}Cu^{2+}_{0.5}]O_4$	8.28	15
$CuCrMnO_4$	$Cu^{+}[Cr^{3+}Mn^{4+}]O_4$	8.31	15
$LiMg_{0.5}Mn_{1.5}O_4$	$Li^{+}[Mg^{2+}_{0.5}Mn^{4+}_{1.5}]O_4$	8.18	15

cont....

Table - 3 (cont.)

Compound	Ionic distribution	a	Ref.
$LiCo_{0.5}Mn_{1.5}O_4$	$Li^{1+}[Co^{2+}_{0.5}Mn^{4+}_{1.5}]O_4$	8.16	15
$Cu_1Mn_1Cr_1O_4$	$Cu^{1+}_{0.5}Cu^{2+}_{0.5}[Mn^{3+}_{0.5}Mn^{4+}_{0.5}Cr^{3+}]O_4$	8.35	16
$LiCrMnO_4$	$Li[Cr^{3+}Mn^{4+}]O_4$	8.19	17
$LiRhMnO_4$	$Li[Rh^{3+}Mn^{4+}]O_4$	8.30	17
$Li_{4/3}Mn_{5/3}O_4$	$Li[Li_{1/3}Mn^{4+}_{5/3}]O_4$	8.19	17
$FeMnCuO_4$	$Fe^{3+}[Mn^{3+}_{0.1}Mn^{4+}_{0.9}Cu^{2+}_{0.1}Cu^{1+}_{0.9}]O_4$	8.40	18
$CuMnCrO_4$	$Cu^{1+}_{0.5}Cu^{2+}_{0.5}[Mn^{3+}_{0.5}Mn^{4+}_{0.5}Cr^{3+}_{1.0}]O_4$	8.32	18
$ZnNi_{0.1}Mn_{1.9}O_4$	$Zn^{2+}[Ni^{2+}_{0.1}Mn^{3+}_{1.8}Mn^{4+}_{0.1}]O_4$	Tetragonal	19
$ZnNi_{0.5}Mn_{1.5}O_4$	$Zn^{2+}[Ni^{2+}_{0.5}Mn^{3+}_{1}Mn^{4+}_{0.5}]O_4$	8.245	19
$ZnNi_{0.7}Mn_{1.3}O_4$	$Zn^{2+}[Ni^{2+}_{0.7}Mn^{3+}_{0.6}Mn^{4+}_{0.7}]O_4$	8.275	19
$ZnNi_{0.9}Mn_{1.1}O_4$	$Zn^{2+}[Ni^{2+}_{0.9}Mn^{3+}_{0.2}Mn^{4+}_{0.9}]O_4$	8.263	19
$ZnNi_{0.8}Mn_{1.2}O_4$	$Zn^{2+}[Ni^{2+}_{0.8}Mn^{3+}_{0.4}Mn^{4+}_{0.8}]O_4$	8.267	19
$Zn\ Li_{0.4}Mn_{1.6}O_4$	$Zn^{2+}[Li^{1+}_{0.4}Mn^{3+}_{0.8}Mn^{4+}_{0.8}]O_4$	8.19	19
$Zn\ Li_{0.5}Mn_{1.5}O_4$	$Zn^{2+}[Li^{1+}_{0.5}Mn^{3+}_{0.74}Mn^{4+}_{0.76}]O_4$	8.24	19
$Zn\ Li_{0.6}Mn_{1.4}O_4$	$Zn^{2+}[Li^{1+}_{0.6}Mn^{3+}_{0.58}Mn^{4+}_{0.82}]O_4$	8.23	19

1.2 MAGNETIC PROPERTIES OF MANGANITES

The magnetic properties of any individual atom or ion result from the spin moment of the electron and the orbital moment resulting from the motion of the electron around the nucleus. A multielectron atom is assumed to have the quantum numbers:

$$n, L = \sum_i li,\ M_L,\ S = \sum_i si \quad (\text{or } n,\ L,\ J = |L + S| \text{ and } M_J)$$

It follows from the Pauli's principle that for a closed shell $\sum_i li = \sum_i si = 0$ and the quantum numbers for the atom are determined by electrons outside the closed shells. The total angular momentum J has possible values $|L+S|$ -- $|L-S|$ so that the multiplicity of terms corresponding to a given J is either $(2S+1)$ or $(2L+1)$ whichever is smaller. The degeneracy of these multiplets is removed by the interaction of the magnetic moment associated with the angular momentum with that associated with spin. Electron correlations determine the magnitude of the quantum number J and spin orbit coupling gives rise to multiplets associated with J. Both the angular momentum and spin contribute to the permanent magnetic moment.

When the separation of the multiplet components $\Delta >> K T$ then the effective magnetic moment of the atom is given by:

$$\mu_{eff} = g[J(J+1)]^{1/2} \mu_B$$

In cases where multiplet separation $\Delta << K T$

$$\mu_{eff} = [4S(S+1) + L(L+1)]^{1/2} \mu_B$$

where g is the spectroscopic splitting factor falls within the

limits of $1 \leqslant g \leqslant 2$

where $g = 1$ for $S = 0$

and $g = 2$ for $L = 0$ (spin only value)

μ_B = Bohr magneton = $\frac{eh}{4\pi mc} = 9.27 \times 10^{-21}$ erg.gauss^{-1}

In the special case where $L = 0$ then,

$$\mu_{eff} = 2\,[S(S+1)]^{1/2}\mu_B \quad \text{(spin only value)}$$

If atoms are condensed into a molecule or a crystalline array, the outer electrons in partially filled shells are strongly perturbed by the neighbouring atoms. Character of a bonding electron is quite different in a crystal from what it is in a free atom. The observed magnetic moment exceeds the spin only value quite often, but it is not as high as μ_{L+S}. This is because the electric fields of other atoms, ions or molecules surrounding the metal ion in its compound restrict the orbital motion of the electron so that orbital angular momenta are partially or completely quenched. In the case of a d^3 ion in an octahedral environment the orbital contribution is introduced in opposition to the spin contribution and moments slightly below the spin only values are observed as for Cr^{3+}.

If a substance is placed in a field of H, the intensity of magnetization induced is M, then $\chi = M/H$ is called the susceptibility per unit volume. Depending on the sign and magnitude of χ three cases arise:

(1) Diamagnetism: where χ is negative in sign, is. independent of temperature and field strength.

(2) Paramagnetism $\chi > 0$ but is very small. In this case the magnetic moments which are already present but which have a

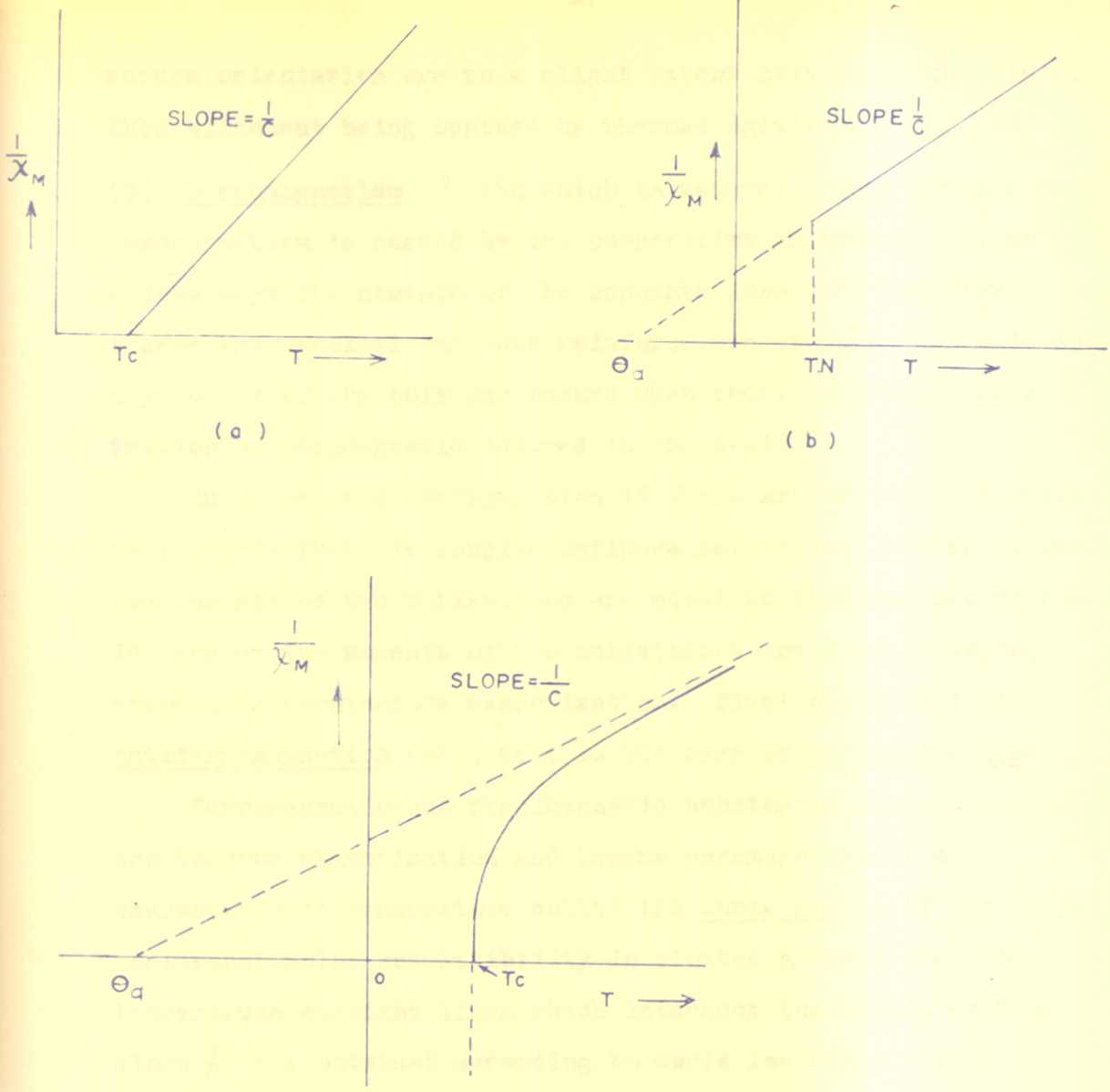

FIG. No. 3. $1/\chi_M$ vs. T CURVES FOR (a) FERROMAGNETIC (b) ANTIFERROMAGNETIC (c) FERRI MAGNETIC MATERIALS.

random orientation are to a slight extent aligned in the field, this alignment being opposed by thermal agitation.

(3) Ferromagnetism $\chi >> 0$ which is several orders greater than paramagnetism is caused by the cooperative phenomena i.e. it arises when the moments of the separate ions tend to align themselves parallel and thus reinforce one another. Thus it is a property of the bulk and occurs when there is a high concentration of paramagnetic centres in the solid.

In an ordered configuration if there are two ferromagnetic sublattices that are coupled antiparallel to one another, either the moments of two sublattices are equal so that the net moment is zero, or the moments of two sublattices are unequal so that there is a spontaneous magnetization. First one is called antiferromagnetism and second is the case of ferrimagnetism.

Ferromagnetic and ferrimagnetic substances loφse their spontaneous magnetization and become paramagnetic at a characteristic temperature called the Curie point. If paramagnetic reciprocal molar susceptibility is plotted against absolute temperature, straight lines which intersect the origin with a slope $\frac{1}{C}$ are obtained according to Curie law, where C is a Curie constant. But many substances do not give straight lines that pass through origin but they cut either x or y axis. So the equation can be represented as $\chi_M = \frac{C}{T - \theta}$ where θ is the temperature at which the line cuts the T axis. This is known as the Curie-Weiss law and θ is known as Weiss constant.

Neel[20] has formulated the equation for ferrimagnetic

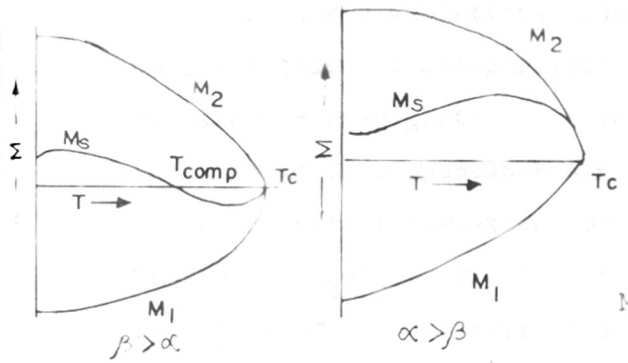

SCHEMATIC M_S vs T CURVES ACCORDING TO THE NÉEL THEORY.

FIG 4 (a).

$M_S = M_2 - M_1$ is the resultant magnetization.

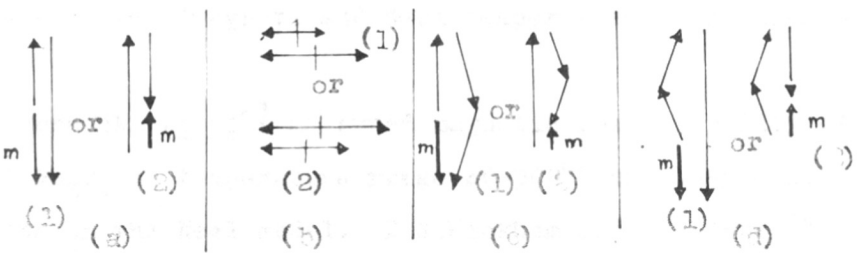

FIG No 4 b FOUR DIFFERENT THEORETICALLY POSSIBLE ORIENTATIONS OF THE MOMENTS IN THE SUBLATTICES 'A' AND 'B' FOR DIFFERENT RATIOS BETWEEN AA, AB AND BB INTERACTIONS.

(a) Interactions AA and BB both small with respect to AB.
(b) Interactions AA and BB large with respect to AB.
(c) Interactions BB comparable to AB , and AA small with respect to AB.
(d) Interactions AA comparable to AB, and BB small with respect to AB.

compounds:

$$\frac{1}{\chi_M} = \frac{T}{C_M} + \frac{1}{\chi_0} - \frac{S}{T-\theta}$$

assuming a sublattice model in which the magnetization of one sublattice is antiparallel to other (they are called collinear ferrimagnets). Below the transition temperature T_C there would be a spontaneous magnetization M_S which is given as the resultant magnetization of two antiparallel sublattices. Thus $M_S = |M_1 - M_2|$. The temperature dependence of M_S is the resultant of the temperature dependences of M_1 and M_2 (Fig.4a). The order-disorder transition temperature is called Curie temperature in ferrimagnets and Néel temperature in antiferromagnets.

A.S.Borovik *et al*[21] measured magnetic susceptibility of Mn_2O_3 and Mn_3O_4 in temperature range 20-300°K and they explained the results on the Néel model. D.G.Wickham and W.J.Croft[14] have prepared $Zn_xGe_{1-x}Mn_2O_4$, $Zn_xGe_{1-x}Co_{2-x}O_4$, $Zn_xLi_{1-x}Mn_2O_4$ and $Co_{3-x}Mn_xO_4$. In that paper they concluded that the magnetic property measured for cubic materials is the result of Néel type magnetic coupling between Co^{2+} ion on tetrahedral site and Mn^{3+} ion on octahedral sites.

In 1952 Yafet and Kittel[22] extended the Néel theory to take into account the antiferromagnetic exchange interaction within the two sublattices. The Yafet-Kittel's theory is based on the assumption that 'A' lattice is divided into two (A' and A") face centered cubic lattices and B lattice into four ($B_1B_2B_3B_4$) face centered cubic lattices all having the same cube edge as the spinel cell. They showed that the ground

state may have an antiparallel arrangement of the spins on the two sites, or consist of a triangular arrangement of the spins on the sublattices, or have an antiferromagnetism in each of the two sites separately (Fig.4b). It is not necessary to have two crystallographically different sites in order to have antiferromagnetism.

The triangular arrangement of moments of Y.K. model has been supported by E.Prince[23] who studied the crystal structure and magnetic structure of copper chromite by Neutron diffraction. The pattern below a Curie point at about 135°K indicated a triangular arrangement of moments. Another evidence for Y.K. model has been provided by Jacobs[24] who studied the compounds of the type $Mo.Mn_2O_3$. A linear increase in net magnetization with field at high fields and low temperature is expected for the triangular arrangement but not for Neel model. They have measured upto 4.2°K in pulsed fields upto 140 K.oe on compounds $Mo.Mn_2O_3$ where M is Mn, Co, Zn and Mg. A high field susceptibility is observed in these and is absent in Fe_3O_4, thus supporting a triangular model.

E.W.Gorter[5] has considered the experimental findings on chromites as well as his own results on lithium chromite-ferrite systems and has attempted to explain the results on the basis of non-collinear spins suggested by Y.K.model. He postulated that angles are present between B-site moments both in pure $MnCr_2O_4$ and in chromium rich solid solutions with lithium ferrite and manganese ferrite. F.K.Lotgering[25] applied Yafet-Kittel theory to normal spinels and showed that both $MnCr_2O_4$ and $FeCr_2O_4$ are consistent with triangular arrangement of

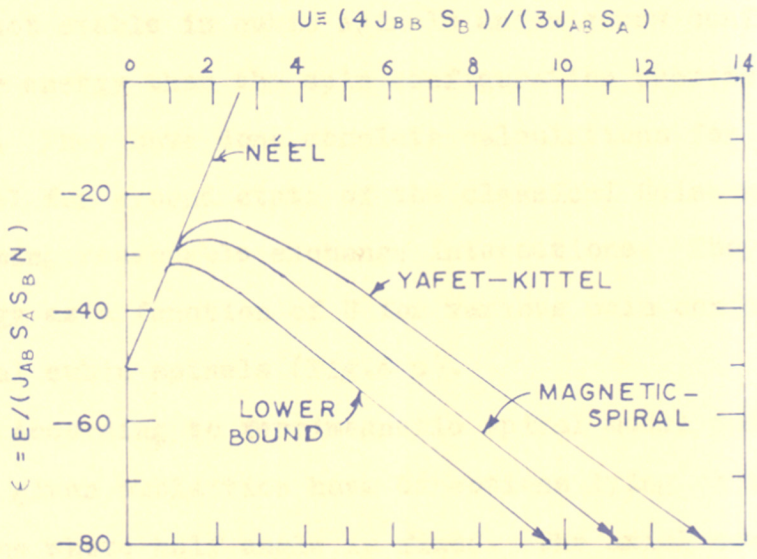

FIG No 4 (c) NORMALISED ENERGY vs. RELATIVE INTERACTION STRENGTHS FOR THREE SPIN CONFIGURATIONS IN CUBIC SPINELS
(After Kaplan ; et. al.,[28])

J_{BB} = B-B exchange constant, J_{AB} = A-B exchange constant,
S_A - Spin angular momentum at A site,
S_B = Spin angular momentum at B site.

moments in which angles occur at B-sites.

However, Dwight and Menyuk[26] who studied the magnetic properties of Mn_3O_4 single crystals between 4.2°K and 41.9°K found that several of the observed properties of Hausmanite disagree with the calculations based on Y.K.theory. They concluded that the concept of canted spin is essentially correct but specific Y.K.model involves oversimplification which limits its applicability.

T.A.Kaplan[27,28] has shown that Yafet-Kittel arrangements are not stable in cubic spinels and a screw configuration has a lower energy than the spin configuration proposed by Y.K. and Neel. They have done complete calculations for normal cubic spinel for ground state of the classical Heisenberg energy assuming reasonable exchange interactions. They have plotted energy as a function of U for various spin configurations in normal cubic spinels (Fig.4 c).

According to ferrimagnetic spiral model, spins belonging to a given sublattice have directions lying on the surface of a cone whose half angle is fixed. The axial components of the spins on one sublattice are constant, but transverse components rotate in discrete steps under translation to equivalent sites in other unit cells along a fixed direction in the crystal (Propagation direction). In the general case each sublattice is characterized by a cone angle and a phase angle for the rotation of the transverse components. The axes of the cones corresponding to different sublattices are parallel but need not coincide with the direction of propagation of spiral. The magnetic spiral model has been supported by Hastings and

Corliss[29] for $MnCr_2O_4$, who investigated the magnetic structure of the spinel by neutron diffraction. They found that Néel model and Y.K.model fail to account for the major qualitative features of diffraction results.

Sinha and Sinha[30] have made a theoretical study of antiferromagnetism of some normal spinels in which the cations occupying the tetrahedral sites are diamagnetic while the cations occupying the octahedral sites are paramagnetic. Using molecular field approximation they have found that the arrangement, in which, each <IIO> and <II$\bar{O}$> row is antiferromagnetically ordered with the spin vectors pointing along these directions, is the most stable arrangement. They have predicted temperature independence of magnetic susceptibility below the transition temperature for such an arrangement.

This model has been supported by M.Rosenberg and I.Nicolae[31] who studied the temperature dependence of magnetic susceptibility of the tetragonalized normal spinels $Zn_xMn_{3-x}O_4$, $Cd_xMn_{3-x}O_4$ (with $0.2 \leqslant x \leqslant 1.0$) and of normal and inverted $MgMn_2O_4$. In the case of tetragonalised spinels with paramagnetic ions on octahedral sites and diamagnetic ions on tetrahedral sites, the values of anisotropic exchange constants were determined on the basis of Sinha's theory.

Theory of Magnetic Coupling - Various Exchange Interactions

Till now we have considered only the spin alignment in various solids. We have to consider the various mechanisms that contribute to the exchange integral. In general, there are two types of interactions: cation-cation and cation-anion-cation.

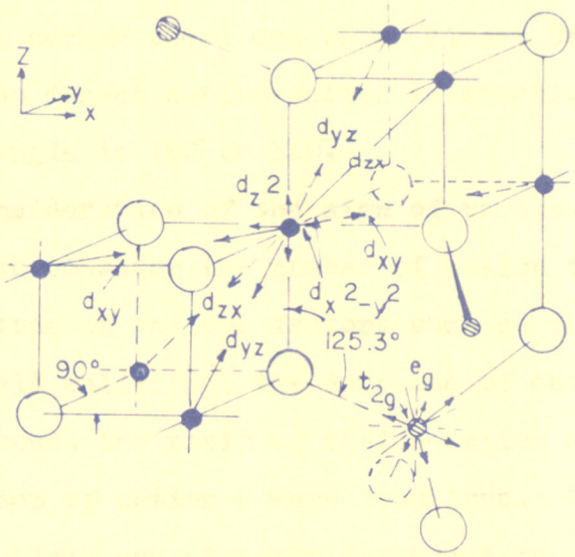

A-SITE CATION

B-SITE CATION

Fig 5 ORIENTATION OF CATION *d* ORBITALS WITH RESPECT TO THE SPINEL STRUCTURE. (GOODENOUGH[43])

Let us consider the case of a spinel where the cation is placed in octahedral environment of six negative charges. The orientation of the d orbitals is shown in the (figure 5) . The anion directed orbitals are less stable than the orbitals which are directed away from the neighbouring anions. The predominant interactions between neighbouring cations whose anion octahedra share a common face or edge are assumed to be cation-cation. On the otherhand if cation occupied octahedra share a common corner there can be no direct overlap of cation orbitals and no direct cation-cation interactions whether cation-anion-cation angle is 180° or 120°.

For a consideration of the sign of various interactions it is necessary to consider the number of cation outer electrons, and the magnitude of various factors such as the magnitude of the ligand field splitting, the decrease of covalency in the anion-cation bond, the ratio of cation-cation separation to radial extension of cation d wave functions. Cation-cation direct interactions are strongly dependent on distance and data on sulphur spinels indicate much weaker B-B interaction because of much larger B-B distances.

According to Goodenough[32,33] if both A site t_{2g} orbitals and B site e_g orbitals are half filled or less than half filled, strong antiferromagnetic AB interactions would result. If A site t_{2g} orbitals and/or the B site e_g orbitals are empty, the AB interactions are relatively weak and antiferromagnetic. If B-site t_{2g} orbitals are half filled or less than half filled and degenerate direct B-B interactions are possible. If the t_{2g} orbitals of one or both of two cations in neighbouring

B sites are full no direct B-B interactions occur between them. He has considered the relative strength of cation-cation direct interactions and cation-anion-cation interactions and pointed out that cation-cation interactions may be significant if octahedral site cations have the outer electron configuration $3d^m (m \leq 5)$ and the occupied octahedra share either a common face or a common edge. He has also mentioned that $Cr^{3+}(3d^3)$ ions are always in B-sites with empty e_g orbitals and half filled t_{2g} orbitals and hence provide optimum conditions for B-B interactions.

Cation-Anion-Cation Interactions

Zener. C.[34] has proposed theory of double exchange to explain the magnetic and electrical properties of Perovskite type manganites. According to that, the electron transfer from a Mn^{3+} ion to a Mn^{4+} ion and vice versa takes place through a O^{--} ion, and the lowest energy of the system $Mn^{3+}-O^{--}-Mn^{4+}$; $Mn^{4+}-O^{--}-Mn^{3+}$ corresponds to a parallel alignment of spins. The system is inherently degenerate owing to the presence of manganese ions of two charges and the double exchange thereby introduced leads to a ferromagnetic alignment of spins. Moreover he has shown that this ferromagnetic alignment of spins leads to an increase in the rate of migration of Mn^{4+} ions and hence an increase in electrical conductivity.

P.G.Degenes[35] studied theoretically the double exchange phenomena in magnetic compounds of mixed valency. He has shown that the double exchange phenomena must cause a distortion of the ground level spin arrangement. If the zener carriers are

mobile, the distortion would correspond to a uniform canting of the spin sublattices. On the otherhand the bound carriers are expected to give a non-homogeneous distortion even though the average effect will be the same as above. He has shown that the arrangement would be stable upto a certain temperature T , and above this temperature the systems may change to either antiferromagnetic or ferromagnetic state depending upon the number of mobile electrons.

R.R.Heikes, T.R.McGuire and R.J.Happel[36] have studied the magnetic susceptibility of lithium substituted manganese selenide at various temperatures. They have suggested that the holes introduced by the substitution of Li^{+} ions remain loosely bound to them at low temperatures. A double exchange phenomenon takes place causing local distortions (clusters) in the spin system near these Li^{1+} ions. These clusters can overlap sufficiently if the lithium ion concentration is adequately high and a magnetic field can now induce an appreciable magnetic moment.

P.W.Anderson and H.Hasegawa[37] have studied the double exchange phenomenon in more detail and they calculated the interaction for a pair of ions with general spin S, with general transfer integral b and internal exchange integral J. According to their calculations, while the states of large total spin have both the highest and lowest energies their average energy is the same as for the states of low total spin. If this theory is applicable in high temperature expansion of the susceptibility, the high temperature Curie-Weiss constant θ should be zero and $\frac{1}{\chi}$ vsT a curved line. But manganites where double exchange has

been presumed to be the interaction mechanism, obey a fairly good Curie-Weiss law.

Semi-covalent Exchange

J.B.Goodenough[6,38] proposed the theory of semicovalent exchange and applied it to perovskite type manganites. Semicovalence is defined as a bond due to the coupling of a single anion electron to the net spin of a cation. The electron that participates in semicovalence has a spin parallel to that of a cation. The other anion electron therefore has a spin antiparallel to the spin of the cation. The other electron may participate in semicovalence with a cation on the other side of anion. In that case the spins of the two cations could be coupled antiparallel to each other. This model which provides a mechanism for antiferromagnetic coupling is called semicovalent exchange. Its strength depends on the overlap between O^{-2} orbitals and the cation orbitals and on the cation-anion-cation angle. If semicovalence occurs with one cation only, the interaction between the anions and the other cations is confined to direct exchange and weak ferromagnetism may result. The necessary condition is the location of interacting cations at opposite sides of an anion. So this coupling is strongest when c-a-c bond angle is 180°. In the spinel structures neighbouring octahedral cations make an angle 90° with their common anion and the semicovalent exchange between them is small compared to that between the tetrahedral and octahedral cations. Wollan and W.C.Kochϕler[39] have done a complete study of magnetic and crystallographic lattices as a function of

Mn^{4+} content by neutron diffraction and the results were explained by Goodenough in terms of semicovalent exchange.

Super-exchange Mechanism

It was first proposed by Kramers[40]. Super exchange is due to the admixture of excited states with the ground state of the system containing two like cations separated by anion. The excited states are the result of removing an electron from the O^{-2} and placing it in an empty or half filled cation orbital. If the cation orbital is empty, the transferred electron aligns its spin parallel to the net spin already on the cation in accordance with Hund's rule. If the orbital is already half filled, the transferred electron aligns its spin antiparallel to that of the electron already there and hence to the existing net spin on the cation. The O^{-} from which the electron is transferred has a net spin which is antiparallel to that of removed electron. The net spin of oxygen ion is antiparallel to the net spin of the reduced cation if the cation d shell was originally less than half filled, parallel if the cation d shell was originally at least half filled. According to the super exchange model, the net spin on the O^{-} ion interacts directly with that of a neighbouring cation on the other side.

The super exchange mechanism originally proposed by Kramers has been extended by several workers[38,41,42] and Goodenough has summarised the work in his book[43].

Several mechanisms of comparable magnitude contribute to the exchange coupling and these contributions usually add so that qualitative criteria for the sign and relative strengths

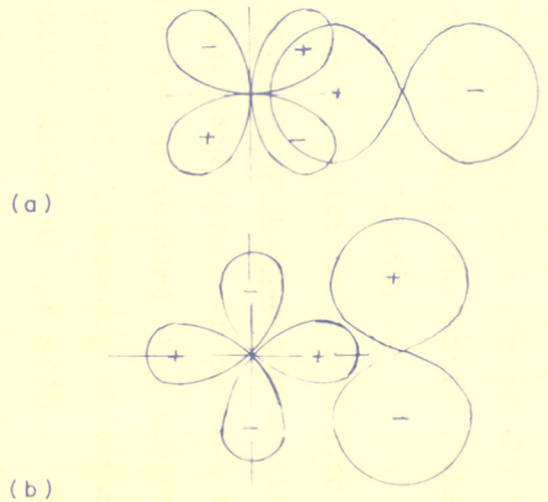

FIG. 6 : SYMMETRY RELATIONS BETWEEN (a) t_{2g} AND $p\sigma$ ORBITALS, (b) e_g AND $p\pi$ ORBITALS. (GOODENOUGH[43])

of exchange parameters can be given.

180° Cation-Anion-Cation Interactions

If we consider two transition metal cations in octahedral interstices that share a common corner as in an ideal cubic Perovskite structure, $p\sigma$ orbital is orthogonal to the t_{2g} orbital but not the e_g orbital of principal overlap, and $p\pi$ orbitals are orthogonal to the e_g orbital but not the t_{2g} orbital of principal overlap. Therefore electron transfer or partial covalence can occur only between $p\sigma$ orbital and e_g orbital of principal overlap, or between a $p\pi$ orbital and t_{2g} orbital of principal overlap. They are called a σ transfer and a π transfer. The predominant contribution to the super-exchange comes from the covalency of σ bonds. Therefore the more ionic the bonds, the smaller the 180° cation-anion-cation interaction (Fig.6).

Three mechanisms contribute to the super exchange. The correlation mechanism takes into account the simultaneous partial bond formation on each side of the anion. The cation spins are so coupled that the two $p\sigma$ electrons one of each spin can simultaneously form partially covalent bonds on opposite sides of the anion. In the delocalization mechanism an electron is assumed to drift from one cation to the other, the transfer integral b_{ij} depending sensitively on the amount of partial covalent bonding, since covalency causes the cation d orbitals to spread out over the anion. The contribution from the anion polarization is small relative to the correlation and delocalization effects.

CASE	OUTER-ELECTRON CONFIGURATION	CORRELATION SUPER EXCHANGE		DELOCALIZATION SUPER EXCHANGE		SUM	STRENGTH °K (OXIDES)
		$p\sigma$	$p\pi$	$p\sigma$	$p\pi$		
1	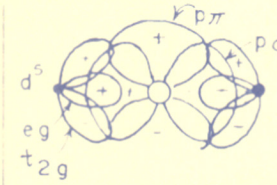	STRONG ↑↓	WEAK ↑↓	STRONG ↑↓	WEAK ↑↓	↑↓	~ 750
2	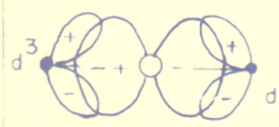	WEAK TO MODERATE ↑↓	WEAK ↑↓	—	WEAK ↑↓	↑↓	≲ 300
3	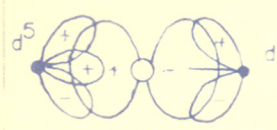	MODERATE ↑↑	WEAK ↑↓	MODERATE ↑↑	WEAK ↑↓	↑↑	~ 400

FIG No. 7. THREE POSSIBLE 180° CATION-ANION-CATION INTERACTIONS BETWEEN OCTAHEDRAL-SITE CATIONS (Goodenough[43])

In the diagram (Fig.7) three cases have been represented. Case 1 represents the coupling between cations that have a half filled e_g orbital directed towards the anion intermediary. Case 2 represents half filled t_{2g} orbitals and empty e_g orbitals directed towards the anion. Case 3 represents a cation with a half filled e_g orbital overlapping $p\sigma$ on the one side and an empty e_g orbital overlapping $p\sigma$ on the other.

90° Cation-Anion-Cation Interactions

If the octahedral interstices of two neighbouring cations share a common edge, then there is a direct overlap of the d_{xy} (or d_{yz} or d_{zx}) orbitals of the cation. In this case the anion plays a less obvious role in delocalization super exchange process. The transfer integral for t_{2g} electrons varies as the overlap of the t_{2g} orbitals of the two cations rather than as the product of their respective overlap of a given anion orbital. In this case, the direct exchange interaction is likely to be pronounced. Delocalization super exchange can also occur between e_g orbitals via the intermediate anion orbitals. As far as the correlation super exchange is concerned the interaction can take place by means of the following three sets of anion electrons:

(1) Anion s electrons
(2) Two p electrons of the same orbitals
(3) Two p electrons from different p orbitals.

The interaction via the s electrons is supposed to be weaker because of the smaller radial extension of the s orbitals. The interaction via p electrons belonging to different p orbitals

CASE	OUTER-ELECTRON CONFIGURATION	DELOCALIZATION SUPEREX			CORRELATION SUPEREX			SUM	
		$t_{2g} - t_{2g}$	$e_g - t_{2g}$	$e_g - e_g$	via s	via $p\sigma$, $p\pi$	via $p\sigma$, $p\sigma'$	OXIDES	CHLORIDES
1	d^5 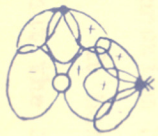 d^5	↑↓	↑↓	↑↓	↑↓	↑↓	[↑↑]	↑↓ ~200°K	↑↓ ~50°K
2	d^3 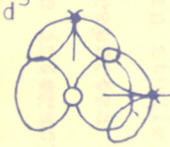 d^3	↑↓	↑↑	—	↑↓	[↑↑]	[[↑↑]]	↑↓ ~300°K	↑↑ ~50°K
3	d^3  d^5	↑↓	(↑↓)	[↑↑]	↑↑	(↑↓)	[[↑↓]]	↑↓ ~100°K	?
4	d^8 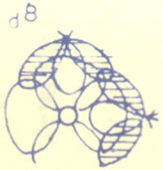 d^8	—	[↑↑]	↑↓	↑↓	—	[↑↑]	↑↓ AND ↑↑	↑↑ ~50°K

FIG. 8 FOUR ILLUSTRATIVE, 90° SUPEREXCHAGE INTERACTIONS (Goodenough 43)

is also expected to be weaker than that via the two electrons from the same p orbitals, unless the t_{2g} orbitals are more than half filled. Four illustrative 90^{o} interactions are shown in the Figure (Fig.8).

In addition to the 180^{o} or 90^{o} c-a-c angles there are other intermediate angles observed in many solids. For example, in spinel, the angle between the tetrahedral cation and the octahedral cation via the oxygen p orbital is only 125^{o}. It is expected that the interaction would vary in a regular way as the angle is varied from 90^{o} to 180^{o}. Possibilities of c-a-a-c super exchange interactions have been considered by several workers. Blasse[44] proposed an exchange mechanism involving $Co^{2+}-O^{2-}-Rh^{3+}-O^{2-}-Co^{2+}$. Bertaut[45] proposed even more distant interactions.

Some Important Studies on 90^{o} B-B Interactions in Spinels

As discussed earlier, the 90^{o} B-B interactions are determined by two main mechanisms (1) Direct exchange and (2) Super exchange. The direct exchange interaction is highly sensitive to cation-cation separation. As we are interested in the study of 90^{o} interaction between $Cr^{3+}-Cr^{3+}$, $Mn^{4+}-Mn^{4+}$ and $Mn^{4+}-Cr^{3+}$ we give a brief review of the work where both +ve and -ve interactions in spinels containing manganese and chromium have been studied.

It has been reported by T.R.McGuire and L.N.Howard[46,47] that the magnetic interaction in $Cr^{3+}-O^{2-}-Cr^{3+}$ is strongly negative. They have reported that spinels $Mg[Cr]_2O_4$ and $Zn[Cr]_2O_4$ have $\theta_A = -370^{o}K$ and $-350^{o}K$ respectively. They

have measured the saturation magnetization and the temperature dependence of paramagnetic susceptibility of Mg, Mn, Co, Ni, Cu and Zn chromites. Magnesium and zinc chromites exhibit a normal paramagnetic behaviour corresponding to a spin only moment for Cr^{3+}. Susceptibility of the remaining members of the series have the characteristic temperature dependence predicted by Néel for ferrimagnetic spinels but whereas the effective moment for Mn and Fe have the spin only value, those for Co, Ni and Cu are appreciably higher. The saturation magnetizations for Fe, Co, Ni and Cu are considerably lower than given by Néel model.

F.K.Lotgering[48] has studied some sulphur compounds which show ferromagnetic behaviour and metallic conductivity. He has discussed in detail, the sign of 90° B-B interaction for Cr^{3+}. His table which shows the variation of θ with Cr-Cr distance is given below:

Table - 4

Variation of θ with Cr-Cr distance

Compound	Curie constant per gm atom	θ°K	Cr-Cr distance
$NaCrO_2$	1.85	-354	2.96
$LiCrO_2$	1.72	-577	2.88
$ZnCr_2O_4$	1.85	-350	2.94
$MgCr_2O_4$	1.87	-350	2.94
$CrCl_3$	1.90	+ 27	3.46
$ZnCr_2S_4$	1.67	+ 18	3.53
$CrBr_3$	1.85	+ 47	3.61
$ZnCr_2Se_4$	1.77	+115	3.71
	To compare with spin only value 1.87		

θ is a measure of average exchange interaction & and a +ve θ for $ZnCr_2Se_4$ must be attributed to +ve interaction. It is seen from the table that θ shifts in +ve sense for increasing nearest neighbour distance. $ZnCr_2Se_4$ has highest +ve θ value and largest Cr-Cr distance. The change from a strongly -ve θ for Cr-Cr $\approx$ 2.9 Å (in oxides) to a weakly +ve θ for Cr-Cr $\approx$ 3.5 Å (in chlorides and sulphides) points to a -ve extra contribution to the interactions for small Cr-Cr distances. This may be due to overlap of the d functions on the neighbouring Cr^{3+} ions (Goodenough[33]). Ferromagnetic interactions between Cr^{3+} ions on B-sites in a spinel may arise from a direct exchange mechanism (Anderson[49]) and which takes place via an intermediate anion as super exchange does. According to Anderson, in the absence of overlapping d functions on neighbouring Cr^{3+} ions, the 90° exchange interaction consists of a positive direct exchange term and negative super exchange term. Both the terms are small and cannot be estimated with any accuracy. The resulting interaction may theoretically be positive or negative. Therefore assuming positive Cr-Se-Cr interaction in $ZnCr_2Se_4$ does not contradict Anderson's theory.

P.K.Baltzer, W.H.Lehman and M.Robbins[50] have reported insulating ferromagnetic spinels $CdCr_2S_4$, $CdCr_2Se_4$, $HgCr_2S_4$ and $HgCr_2Se_4$ which are both electrical insulators and ferromagnetic. They argued that metallic like conductivity is not a necessary condition for ferromagnetism. They[51] considered very distant neighbour interactions in spinels and said that they play very important role in the determination

of the type of magnetic order observed in Chalcogenide spinels.

N.Menyuk and K.Dwight[52] made a study of the magnetic properties of ACr_2X_4 where A is diamagnetic Zn or Cd and X is O, S and Se. They have found disagreement between experimental values of $\frac{T_A}{T_C}$ and theoretical values calculated by assuming nearest neighbour interactions and hence they concluded that next nearest neighbour interactions are playing a role in the ferromagnetic materials.

P.F.Bongers and E.R.Vanmeurs[53] studied the ferromagnetism in compounds with pyrochlore structure, containing chromium $[A_2B_2O_7]$. They found in accordance with Anderson's theory of exchange that the interaction between chromium ions is negative if Cr-O-Cr is 180°. If Cr-O-Cr angle is 90°, it is strongly negative in oxides and positive in sulphides and selenides. This effect is attributed to the competetion between a -ve direct exchange which is sensitive to distance and a positive interaction via an anion which is less sensitive to distance. In pyrochlore, the cation separation is large ($\approx$ 3.6 Å) and Cr-O-Cr angle is 125°.

G.Blasse[54] has discussed the 90° interactions in chromites and considered ionic radii as one of the very important deciding factors. The strength of the cation-cation interaction is determined by the overlap of t_{2g} orbitals of the cations and consequently by the size of the cation and anion involved. The strength of the c-a-c interaction is determined by the degree of covalency of cation-anion bond i.e. by the overlap of the cation and anion orbitals. Consequently, the interaction is expected to be strongly negative in the case of metal ions

which are not too small relative to the anions and are bonded ionically. He has taken the ratio between cation and anion ionic radii as a rough measure of cation-cation interaction.

G.Blasse[55] has studied the preparation and properties of many spinels containing tetravalent manganese. In one of the earlier papers[54] he reported the magnetic B-B interaction between Mn^{4+} ions in spinels to be weak and negative. But in the later papers by studying $Cu^{+}[Mg^{2+}_{0.5}Mn^{4+}_{1.5}]O_4$ and $Li_{0.5}Zn_{0.5}[Li_{0.5}Mn^{4+}_{1.5}]O_4$ he concluded that 90° $Mn^{4+}-O^{2-}-Mn^{4+}$ interactions are +ve and strongly dependent on distance. He has shown that combination of tetrahedral Cu^{1+} and octahedral Mn^{4+} is more stable than tetrahedral Cu^{2+} and octahedral Mn^{3+}. He argued that the +ve sign of $Mn^{4+}-Mn^{4+}$ interaction must be due to the orthogonality of d_{xy} orbitals of neighbouring Mn^{4+} ions. The direct overlap of these orbitals is not large enough to overcome this effect. But in the case of chromites, the direct overlap of d_{xy} orbitals overcomes the effect and the 90° $Cr^{3+}-Cr^{3+}$ interaction is strongly negative. $Mn^{4+}-Mn^{4+}$ 90° interaction also depends on distance. Increasing distance means decreasing direct overlap and consequently a stronger +ve exchange. In $LiZn_{0.5}Mn_{1.5}O_4$ and $CuMg_{0.5}Mn_{1.5}O_4$ the only paramagnetic ions present (Mn^{4+}) occupy the same crystallographic sites. The cell edge of the later compound is larger and its Curie temperature is higher. He has reported the χ^{-1}-T curve in $CuCrMnO_4$ to be convex. In the region 300-500°K it approaches a straight line with a slope calculated for $CuCr^{3+}Mn^{4+}O_4$, above 500°K it becomes more convex due to the

formation of Cu^{2+} and Mn^{3+} and below 300°K it is more or less hyperbolic. Below 45°K this compound shows saturation moment but saturation is not obtained in fields upto 30 Koe, which indicates non-collinear spin arrangement. At low temperatures the cation distribution will be approximately $Cu^{+}[Cr^{3+}Mn^{4+}]O_4$ but long range magnetic order on B sites is not easy to achieve because there is no crystallographic order.

Recently Kiyosi Motida and S.Miyahara[56] studied the 90° exchange interaction between cations [Cr^{3+}, Mn^{2+}, Fe^{3+} and Ni^{2+}] in oxides. They drew empirical relations between bond angle M-O-M and asymptotic Curie temperature Θ or Néel temperature T_N, by taking into account the direct exchange interaction and 90° superexchange interaction. They have mentioned that geometrical configurations play an important role in determining the sign of interaction. Though Mn^{2+} and Fe^{3+} have the same electronic configuration, the contribution of J_d to the total interaction is more for Mn^{2+} than for Fe^{3+}. They explained it, as the ionic radius of Mn^{2+} is larger than that of Fe^{3+}, the overlap between the cation orbitals is larger for Mn^{2+} than for Fe^{3+}.

In a short note[57] they have discussed the 90° exchange interaction between Cr^{3+}'s in sulphides and selenides. They found that there exists a definite relation between Θ and γ in each of sulphides or selenides.

1.3 ELECTRICAL PROPERTIES OF MANGANITES

E.G.Larson and others[58] prepared a complete range of solid solutions between cubic spinel $NiMn_2O_4$ and tetragonal spinel Mn_3O_4 and reported the electrical and magnetic properties of the compounds. They have assigned the formula:

$$(1-\beta)Mn_x^{2+}Mn_{1-x}^{3+}[Ni_{1-x}^{2+}Mn_{1+x}^{3+}]O_4 + \beta Mn^{2+}[Ni_{1-x}^{2+}Mn_{2x}^{3+}Mn_{1-x}^{4+}]O_4$$

They explained the conductivity results on the basis of localized electron theory that it is a result of transfer of electrons from B-site Mn^{3+} to B-site Mn^{4+}. The activation energy becomes primarily an activation energy for the jump and hence for mobility.

M.Rosenberg et al[59] prepared a series of systems : $Cu_xMn_{3-x}O_4$ ($0 \leqslant x \leqslant 0.2$), $Zn_{1+x}Mn_{2-x}O_4$ ($0 \leqslant x \leqslant 0.2$), $Mg_xMn_{3-x}O_4$ ($0 \leqslant x \leqslant 1$) and $Zn_xMn_{3-x}O_4$ ($0 \leqslant x \leqslant 1$). They noted that the conductivity data are consistent with the hopping model involving octahedral site Mn^{3+} and Mn^{4+} ions and that the materials are low mobility semiconductors. All the compounds studied showed in the variation of electrical resistance with temperature, a thermal hysteresis in the range of transition from tetragonal to cubic structure. They observed that the gradual increase of the quantity of Mn^{4+} in the octahedral sublattice causes a decrease of resistivity and activation energy since the possibility of transition between ions of the same type but of different valencies thus increases.

The presence of Mn^{3+} is associated with tetragonal distortion. So each electron exchange will have to be associated with a rearrangement of surrounding oxygen ions which would require

an additional activation energy. With a view to investigate this behaviour, P.P.Jogalekar and A.P.B.Sinha[18] have studied the electrical properties of the system $ZnLi_xMn_{2-x}O_4$ ($0.1 \leq x \leq .6$). They observed that in manganites, the activation energy for conduction is always higher than that in corresponding ferrites and activation energy depends on number of charge carriers.

Sabane[60] has studied the electrical conductivity of a number of pure and mixed manganites viz., $CuMn_2O_4$, $NiMn_2O_4$, $MgMn_2O_4$, $CoMn_2O_4$, $MnMn_2O_4$, $ZnMn_2O_4$, $CdMn_2O_4$ and $NiMn_2O_4$-$CuMn_2O_4$, $NiMn_2O_4$-Mn_3O_4, $NiMn_2O_4$-$CoMn_2O_4$, $NiMn_2O_4$-$MgMn_2O_4$ etc. From the study of electrical conductivity as a function of temperature, Sabane has found that all the compounds obey Wilson's law upto atleast 400°C. The measurements of thermoelectric coefficient showed that all these compounds except $NiMn_2O_4$ are p type.

Ghare and Sinha[19] synthesised a series of compounds of the general formula $Zn^{2+}[Ni_x^{2+}Mn_{2-2x}^{3+}Mn_x^{4+}]O_4$ containing both Mn^{3+} and Mn^{4+} ions at the octahedral sites and measured the conductivity as a function of temperature. They found that energy of activation first decreases rapidly with increasing x in the range $0 < x < 0.3$, then slowly in the range $0.3 < x < 0.7$ and becomes constant after $x = 0.7$. Similarly specific resistance first decreases with increasing x, reaches minimum at $x = 0.7$ beyond which it starts increasing again. They have also suggested hopping mechanism for conduction of electrons.

There is a lot of controversy regarding the valencies of copper and manganese in $CuMn_2O_4$. Sinha and Sanjana[12] first synthesised the compound and reported it as cubic. The absence

of Jahn-Teller distortion indicates that no appreciable concentration of Mn^{3+} ions exists at B-sites. Magnetic studies by Blasse[55] indicated that copper is monovalent at A site but E.Lopatin and P.K.Baltzer[61] argued that copper is divalent. Sabane[62] and others have done electrical conductivity and thermoelectric coefficient measurements of copper manganite as a function of temperature and supported a formula close to $Cu^{1+}[Mn^{3+}Mn^{4+}]O_4$. Naik and Sinha[63] have done a structural study of $Cu_xA_{1-x}[Mn_{2-x}Fe_{2-2x}]O_4$ ($A=Cu^{2+}$, Ni^{2+}, Co^{2+}, Zn^{2+}, Mn^{2+}), and noted that Cu^{1+} is stabilized at A site. But X-ray absorption edge measurements by Miller[64] on $CuMn_2O_4$ strongly indicate the presence of divalent copper. So the most probable ionic distribution is:

$$Cu_x^{2+}Mn_{1-x}^{2+}[Cu_{1-x}^{2+}Mn_{1-x}^{4+}Mn_{2x}^{3+}]O_4 \quad \text{where } 0 < x < 0.33$$

and the compound is not a normal spinel. This was suggested by I.T.Sheftel et al[65].

CHAPTER - II

EXPERIMENTAL TECHNIQUES

2.1 PREPARATION OF THE COMPOUNDS

To study the influence of Mn^{4+} and Cr^{3+} ion concentrations on the sign of exchange interactions in spinels, manganites represented by the formulae given below have been prepared.

Table - 5

List of the Compounds Prepared

System-I

(1) $Li^{1+}[Mn^{4+}Cr^{3+}]O_4$

(2) $Li^{1+}_{0.8}Zn^{2+}_{0.2}[Mn^{4+}_{0.8}Cr^{3+}_{1.2}]O_4$

(3) $Li^{1+}_{0.9}Zn^{2+}_{0.1}[Mn^{4+}_{1.1}Cr^{3+}_{0.8}Li^{1+}_{0.1}]O_4$

(4) $Li^{1+}_{0.6}Zn^{2+}_{0.4}[Mn^{4+}_{0.6}Cr^{3+}_{1.4}]O_4$

(5) $Li^{1+}_{0.7}Zn^{2+}_{0.3}[Mn^{4+}_{0.9}Cr^{3+}_{1.0}Li^{1+}_{0.1}]O_4$

(6) $Li^{1+}_{0.8}Zn^{2+}_{0.2}[Mn^{4+}_{1.2}Cr^{3+}_{0.6}Li^{1+}_{0.2}]O_4$

(7) $Li^{1+}_{0.4}Zn^{2+}_{0.6}[Mn^{4+}_{0.4}Cr^{3+}_{1.6}]O_4$

(8) $Li^{1+}_{0.5}Zn^{2+}_{0.5}[Mn^{4+}_{0.7}Cr^{3+}_{1.2}Li^{1+}_{0.1}]O_4$

(9) $Li^{1+}_{0.6}Zn^{2+}_{0.4}[Mn^{4+}_{1.0}Cr^{3+}_{0.8}Li^{1+}_{0.2}]O_4$

(10) $Li^{1+}_{0.7}Zn^{2+}_{0.3}[Mn^{4+}_{1.3}Cr^{3+}_{0.4}Li^{1+}_{0.3}]O_4$

(11) $Li^{1+}_{0.2}Zn^{2+}_{0.8}[Mn^{4+}_{0.2}Cr^{3+}_{1.8}]O_4$

(12) $Li^{1+}_{0.3}Zn^{2+}_{0.7}[Mn^{4+}_{0.5}Cr^{3+}_{1.4}Li^{1+}_{0.1}]O_4$

(13) $Li^{1+}_{0.4}Zn^{2+}_{0.6}[Mn^{4+}_{0.8}Cr^{3+}_{1.0}Li^{1+}_{0.2}]O_4$

(14) $Li^{1+}_{0.5}Zn^{2+}_{0.5}[Mn^{4+}_{1.1}Cr^{3+}_{0.6}Li^{1+}_{0.3}]O_4$

(15) $Li^{1+}_{0.6}Zn^{2+}_{0.4}[Mn^{4+}_{1.4}Cr^{3+}_{0.2}Li^{1+}_{0.4}]O_4$

(16) $Zn[Cr_2]O_4$

(17) $Li^{1+}_{0.1}Zn^{2+}_{0.9}[Mn^{4+}_{0.3}Cr^{3+}_{1.6}Li^{1+}_{0.1}]O_4$

(18) $Li^{1+}_{0.2}Zn^{2+}_{0.8}[Mn^{4+}_{0.6}Cr^{3+}_{1.2}Li^{1+}_{0.2}]O_4$

(19) $Li^{1+}_{0.3}Zn^{2+}_{0.7}[Mn^{4+}_{0.9}Cr^{3+}_{0.8}Li^{1+}_{0.3}]O_4$

(20) $Li^{1+}_{0.4}Zn^{2+}_{0.6}[Mn^{4+}_{1.2}Cr^{3+}_{0.4}Li^{1+}_{0.4}]O_4$

(21) $Li^{1+}_{0.5}Zn^{2+}_{0.5}[Li^{1+}_{0.5}Mn^{4+}_{1.5}]O_4$

System II

(22) $Cu^{1+}_{0.2}Li^{1+}_{0.8}[Mn^{4+}_{1.1}Cr^{3+}_{0.8}Mg^{2+}_{0.1}]O_4$

(23) $Cu^{1+}_{0.2}Li^{1+}_{0.6}Zn^{2+}_{0.2}[Mn^{4+}_{0.9}Cr^{3+}_{1.0}Mg^{2+}_{0.1}]O_4$

(24) $Cu^{1+}_{0.4}Li^{1+}_{0.6}[Mn^{4+}_{1.2}Cr^{3+}_{0.6}Mg^{2+}_{0.2}]O_4$

(25) $Cu^{1+}_{0.2}Li^{1+}_{0.4}Zn^{2+}_{0.4}[Mn^{4+}_{0.7}Cr^{3+}_{1.2}Mg^{2+}_{0.1}]O_4$

(26) $Cu^{1+}_{0.4}Li^{1+}_{0.4}Zn^{2+}_{0.2}[Mn^{4+}_{1.0}Cr^{3+}_{0.8}Mg^{2+}_{0.2}]O_4$

(27) $Cu^{1+}_{0.6}Li^{1+}_{0.4}[Mn^{4+}_{1.3}Cr^{3+}_{0.4}Mg^{2+}_{0.3}]O_4$

(28) $Cu^{1+}_{0.2}Li^{1+}_{0.2}Zn^{2+}_{0.6}[Mn^{4+}_{0.5}Cr^{3+}_{1.4}Mg^{2+}_{0.1}]O_4$

(29) $Cu^{1+}_{0.4}Li^{1+}_{0.2}Zn^{2+}_{0.4}[Mn^{4+}_{0.8}Cr^{3+}_{1.0}Mg^{2+}_{0.2}]O_4$

(30) $Cu^{1+}_{0.6}Li^{1+}_{0.2}Zn^{2+}_{0.2}[Mn^{4+}_{1.1}Cr^{3+}_{0.6}Mg^{2+}_{0.3}]O_4$

(31) $Cu^{1+}_{0.8}Li^{1+}_{0.2}[Mn^{4+}_{1.4}Cr^{3+}_{0.2}Mg^{2+}_{0.4}]O_4$

(32) $Cu^{1+}_{0.2}Zn^{2+}_{0.8}[Mn^{4+}_{0.3}Cr^{3+}_{1.6}Mg^{2+}_{0.1}]O_4$

(33) $Cu^{1+}_{0.4}Zn^{2+}_{0.6}[Mn^{4+}_{0.6}Cr^{3+}_{1.2}Mg^{2+}_{0.2}]O_4$

(34) $Cu^{1+}_{0.6}Zn^{2+}_{0.4}[Mn^{4+}_{0.9}Cr^{3+}_{0.8}Mg^{2+}_{0.3}]O_4$

(35) $Cu^{1+}_{0.8}Zn^{2+}_{0.2}[Mn^{4+}_{1.2}Cr^{3+}_{0.4}Mg^{2+}_{0.4}]O_4$

(36) $Cu^{1+}_{1.0}[Mn^{4+}_{1.5}Mg^{2+}_{0.5}]O_4$

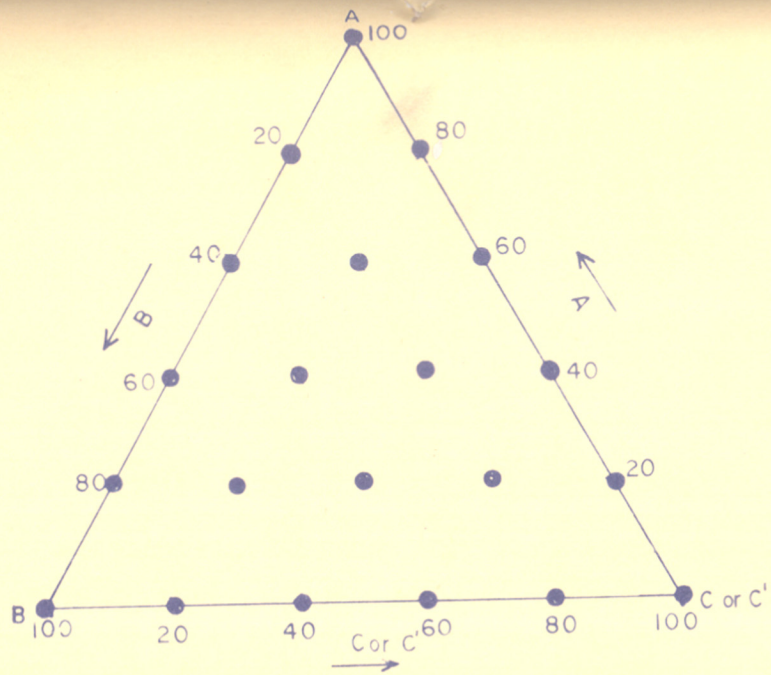

$$A = Li^{1+}_{1.0}\left[Mn^{4+}_{1.0}\ Cr^{3+}_{1.0}\right]O_4$$

$$B = Zn^{2+}_{1.0}\left[Cr^{3+}_{2}\right]O_4$$

$$C = Li^{1+}_{0.5}\ Zn^{2+}_{0.5}\left[Li^{1+}_{0.5}\ Mn^{4+}_{1.5}\right]O_4$$

$$C' = Cu^{1+}\left[Mg^{2+}_{0.5}\ Mn^{4+}_{1.5}\right]O_4$$

Fig 9. PHASE DIAGRAM REPRESENTING THE COMPOUNDS OF FIRST AND SECOND SYSTEMS

All the thirty six compounds can be represented by a phase diagram where:

$$A = Li^{1+}[Mn^{4+}Cr^{3+}]O_4$$

$$B = Zn^{2+}[Cr^{3+}]_2O_4$$

$$C = Li^{1+}_{0.5}Zn^{2+}_{0.5}[Mn^{4+}_{1.5}Li^{1+}_{0.5}]O_4$$

$$C' = Cu^{1+}[Mg^{2+}_{0.5}Mn^{4+}_{1.5}]O_4$$

The solid solutions of ABC are classified as system I and those of ABC' as system II (Fig.9).

Finely divided spectroscopically pure compounds were weighed and mixed under alcohol in an agate pestle mortar for about 3 hours to ensure the formation of a homogenous mixture. After the removal of alcohol, the mixtures are reacted in platinum crucibles at 800°C for 24 hours in oxygen atmosphere. The samples are furnace cooled, are ground for 5-6 hours, and again reacted at 900°C for 24 hours in oxygen atmosphere. The process of grinding and firing is once again repeated, this time the reaction temperature being 950°C. This alternate grinding and firing facilitate the formation of homogeneous solid solutions. Compounds rich in chromium are fired for the fourth time also at temperatures slightly above 950°C. Higher temperatures are not tried as there is a possibility for lithium to evaporate and thus reduce Mn^{4+} to Mn^{3+}. All the samples are reacted and cooled in excess oxygen to maintain the tetravalency of manganese.

2.2 X-RAY DIFFRACTION

Completion of the reaction is checked by taking the X-ray powder photographs. Compounds are analysed by X-ray diffraction technique using Cu-Kα radiation. No extra lines corresponding to unreacted oxides have been observed. From the Debye-Scherrer powder patterns, the d values are calculated in the usual manner and the unit cell dimensions are determined on the basis of their cubic symmetry. The unit cell dimension 'a' of the cubic spinel has been calculated by making use of the formula:

$$\frac{1}{d^2} = \frac{h^2 + k^2 + l^2}{a^2}$$

The mean value of 'a' has been found out from the 'd' values of all the reflections. The values of $\frac{1}{d^2}$ have then been calculated for each reflection and compared with $\frac{1}{d^2}$ values experimentally observed.

Quantitative intensity measurements are carried out for 12 compounds (six from I system and six from II system) at the Bhabha Atomic Research Centre, Trombay, Bombay. The X-ray diffractometer has a Geiger counter for directly measuring the intensity of the diffracted beam for different values of '2θ' using a copper target.

Intensities are calculated using the formula:

$$I_{hkl} = |F^2| . P. \frac{1+\text{Cos}^2 2\theta}{\text{Sin}^2\theta\text{Cos}\theta}$$

where F is the structure factor, P is the multiplicity factor and the remaining term is the combined Lorentz and polarization factor respectively for each reflection. Since the intensities

are measured by a diffractometer from a thick slab of the powder, the absorption correction factor being independent of θ, is the same for every reflection and is not included in the above calculations. We have not done corrections for thermal vibrations.

The structure factor $|F|$ for each of the reflections is calculated by making use of the ionic scattering power of different ions, $f_{Mn^{4+}}$, $f_{Cr^{3+}}$, $f_{O^{2-}}$, $f_{Zn^{2+}}$ etc. The ionic scattering factor 'f' for these different ions has been computed from the standard values given in the International Tables for the Determination of Crystal Structure Vol.II, 1935. When more than one type of ion shared a set of equivalent sites, weight average of the scattering powers of various ions at a given site is taken as the effective scattering power.

Cation Distribution

In system I the ions present are Li^{1+}, Zn^{2+}, Mn^{4+} and Cr^{3+}. The cation distribution can be written out unambiguously on the basis of well known site preference energies (Tables 1 and 2). Cr^{3+} is known to be strongly octahedral prefering cation whereas Zn^{2+} has strong tetrahedral preference. As Mn^{4+} is isoelectronic with Cr^{3+} it is supposed to have strong octahedral preference and kept at octahedral position. Moreover all the compounds reported earlier contain Mn^{4+} at octahedral position (Blasse[55]). This fixes the cation distribution unambiguously because the remaining sites are occupied only by Li^{1+} ions.

But in system II which contains Li^{1+}, Zn^{2+}, Cu^{1+}, Mg^{2+},

Cr^{3+} and Mn^{4+}, the assignment is not so straight forward. The last two ions are obviously present at octahedral position and Zn^{2+} and Cu^{1+} at tetrahedral position. But Li^{1+} and Mg^{2+} have nearly equal octahedral site preference energies -3.6 and -5.0. So either Li^{1+} can be at tetrahedral position and Mg^{2+} at octahedral position or vice versa. This ambiguity has been settled by the actual intensity calculations. The cation distribution finally arrived by us is given in Tables (18,19).

Having settled the cation distribution, the oxygen ion parameter 'u' has been determined by calculating the diffraction intensities for different values of u starting from 0.375 to 0.400 with an interval of 0.005. The reflections most sensitive to u are 111, 220, 400 and 422. The value of u at which the intensities had the best match with the observed ones are selected.

Having thus determined the 'u' value, the intensities for the rest of the reflections are calculated. After fixing the 'u' and 'a' values, the Me-Me and Me-O distances have been calculated using the following formulae:

$$Me_{oct-O} = a\sqrt{\frac{1}{16} - \frac{1}{2}n + 3n^2}$$

$$Me_{tet-O} = a\left(\frac{1}{8} + n\right)\sqrt{3}$$

$$Me_{oct}\text{-}Me_{oct} = \frac{1}{4}a\sqrt{2}$$

$$Me_{oct}\text{-}Me_{tet} = \frac{1}{8}a\sqrt{11}$$

$$Me_{tet}\text{-}Me_{tet} = \frac{1}{4}a\sqrt{3}$$

where a = cell edge and n= u- 0.375

2.3 MAGNETIC SUSCEPTIBILITY MEASUREMENTS

The magnetic susceptibility of the samples has been measured by the Gouy method. The principle involved is that if a cylindrical sample is suspended between the two poles of a magnet so that one end of the sample is in the region of large field intensity and the other end of the sample, in the region of very low field intensity then the force exerted on the sample along its length is given by:

$$f = \frac{1}{2} (K_1 - K_2)(H_1^2 - H_2^2)A$$

where K_1 is the volume susceptibility of the sample K_2=volume susceptibility of the surroundings, H_1=maximum field intensity at one end of the sample, H_2= minimum field intensity at the other end of sample, A = area of cross section of the sample.

If the length of the sample is large $H_2 = 0$, Further, volume susceptibility of the surroundings can be neglected. Hence:

$$f = 1/2\ K_1 H_1^2 A = g\ \Delta W$$

where g is the gravitational constant and ΔW is the change in weight of the substance due to application of field.

A small flat face electromagnet of one square inch cross-sectional area with a gap between the two magnetic pole pieces of about 3.5 cms. has been used. The magnet has been attached to a variable stabilized power supply of 0-200 volts DC and 0-50 amperes current. A steady magnetic field of about 5000 oersteds is obtained by passing a current of 20 amps through the coils of the magnet. Same constant field is maintained for all measurements at all temperatures. The

weight of the specimen as well as the change in weight are measured by a Mettler-make single pan balance which can read weights with 0.05 milligram accuracy.

The sample holder is a cylindrical pyrex glass tube of 20 cms. length with a uniform internal diameter of 3 mm. The tube is filled with a finely powdered sample upto the fixed mark (about 13 cms. above the bottom) and is suspended from the arm of the microbalance. A silver chain is used for suspending the tube. One end of the sample is kept exactly at the centre of the pole pieces and the other end is nearly at zero field. The specimen tube is surrounded in a glass chamber which is again kept in the special type of pyrex Dewar flask arranged in the centre of the pole pieces. When the measurements are carried out at low temperatures, dry nitrogen gas is passed continuously to avoid condensation of moisture over the specimen tube.

The susceptibility has been measured at various temperatures. The desired temperature is obtained by using suitable baths. The low temperature baths are liquid nitrogen, solid alcohol at its freezing point, solid CO_2 and ice. High temperatures are obtained by making use of a specially designed platinum wire wound furnace. Low temperatures are measured by using a copper-constantan thermocouple and high temperatures by making use of a chromel-alumel thermocouple. The emf is measured by a portable Potentiometer which can read upto the accuracy of 5μ volts.

Magnetic force acting on the sample is:

$$f = 1/2\ K_1 H_1^2 A = g\ \Delta W$$

$$\frac{\chi_1 W_1}{\chi_2 W_2} = \frac{\Delta W_1}{\Delta W_2}$$

χ_1 = Magnetic susceptibility per gm. of substance 1

χ_2 = Magnetic susceptibility per gm. of substance 2

W_1 = Wt. of substance 1

W_2 = Wt. of substance 2

ΔW_1 = Change in weight of the substance 1 in the magnetic field

ΔW_2 = Change in weight of the substance 2 in the magnetic field

Hence: $\chi_2 = \left[\frac{\chi_1 W_1}{\Delta W_1}\right] \frac{\Delta W_2}{W_2}$

If the magnetic susceptibility of the samples is measured under the identical conditions and the magnetic susceptibility of one of the compounds is known, the susceptibility of the other compounds can be easily obtained from the above relation, if

$$\frac{\chi_1 W_1}{\Delta W_1} = A,\ \chi_2 = A \frac{\Delta W_2}{W_2}$$

A = tube constant for magnetic set up.

The tube constant is found out with the aid of analar grade copper sulphate $CuSO_4.5H_2O$ whose susceptibility is known

$$\chi_{gm.} = 6.24 \times 10^{-6} \text{ at } 300^{\circ}K$$

By using this constant, magnetic susceptibility of specpure Mn_3O_4 has been determined at various temperatures. The values of Mn_3O_4 at various temperatures have been found to be in agreement with those reported by Moore *et al*[66].

The same tube has been used throughout the experiment and the susceptibility of the unknown substance has been determined, knowing the change in weight of the unknown sample under identical conditions at various temperatures.

2.4 MEASUREMENTS OF ELECTRICAL CONDUCTIVITY

Preparation of the Pellets

The compounds prepared by alternate grinding and heating, were finally ground in an automatic grinder for about 5 hours. One cc. of 2 per cent polyvinyl acetate in acetone was then added to about 1 gm. of the powder and mixed nicely for half an hour. The paste thus formed was dried for half an hour and pressed in a die of 1 cm. diameter by means of a Carver laboratory hydraulic press fitted with a calibrated pressure gauge. The pressure applied was usually 5000 p.s.i. and the pellet was about 0.2 to 0.3 cm.in thickness. Then the pellets were slowly heated in oxygen atmosphere upto 800°C (kept for 2 hours to burn away the binder) and then slowly raised upto 950°C and sintered there for 12 hours. Then the furnace was put off and the pellets were furnace cooled. By this procedure beautiful crack-free pellets were obtained.

Measurement of Electrical Conductivity

The two end faces of the pellet were made conducting by applying silver paste. This type of contact gives low resistance and high reproducibility. Electrical conductivity as a function of temperature was measured on EICO electric volt-ohm meter Model 214. The temperature was measured with a chromel-alumel thermocouple and a portable potentiometer which can read upto the accuracy of 5μ volts.

The sample holder is constructed out of 1/2 inch diameter silica tube with one end closed by a flat silica plate. A slot is made just above the closed end to give an opening of

about 1" x 1/4". The pellet is sandwiched between two platinum foils and placed on the bottom of the silica tube. The spring is placed in such a way that it does not come across in the heating zone but remains out of the furnace. Calibrated chromel-alumel thermocouple is placed very close to the pellet. The platinum wires fused to the platinum foils are insulated and taken out of the silica tube.

The furnace for high temperature measurement is constructed by winding a standard resistor kanthal wire on a silica tube of one inch inner diameter and a length of one foot, so as to obtain a constant temperature zone of about 6 inches in length. This assembly is fixed in a box made up of asbestos cement sheets lagged by asbestos powder in order to avoid heat transfer. The temperature of the furnace can be controlled by making use of a variac and suitable voltage stabilizer. Before each reading was taken, the temperature was allowed to stay at a particular value for a minimum of 15 minutes. The furnace was then heated to next higher temperature and the resistance values at different temperatures were obtained.

Electrical conductivity measurements have also been done at low temperature in some compounds which showed very low resistance at room temperature (of the order of 30-70 ohms.). Hence conductivity has been measured at temperatures down to liquid nitrogen temperature by using various fixed temperature baths such as liquid nitrogen, solid alcohol in equilibrium with liquid alcohol at its freezing point; solid CO_2, ice etc.

The sample along with the sample holder was kept under

hydrogen in order to avoid the condensation of moisture on the pellet. Copper constantan thermocouple is used to measure low temperatures.

CHAPTER - III

EXPERIMENTAL RESULTS

3.1 X-RAY RESULTS

All the compounds mentioned in Table-5 have been checked by X-ray diffraction technique. They all had cubic spinel structure and showed no tetragonal distortion. X-ray intensity calculations were done for 12 compounds as described earlier, 6 from System I and 6 from System II. Those compounds which had considerably high chromium content were selected. As the aim is to study the 90^{o} B-B interaction where the cation-cation distance plays an important role in determining the sign of exchange interactions, the Me_{oct}-Me_{oct} distances were also calculated. Moreover the 'u' and 'a' values are dependent on the size of the ions and hence the radii of octahedral and tetrahedral holes were calculated and presented along with ionic size of tetrahedral ions and octahedral ions.

In Tables 6-17 the calculated and observed intensities and the calculated and observed $1/d^2$ values are given for the 12 compounds. In Tables 18,& 19 u, a, $r_{oct.hole}$, $r_{tet.hole}$, $r_{ions.tetrahedral\ site}$, $r_{ions\ octahedral\ site}$ and charge of the ions at both the sites are given. In Tables 20 and 21 the Me_{oct}-Me_{oct} distances along with O value and percentage of manganese and chromium that occupy the octahedral position are presented. In Tables 22,&23 the observed and calculated intensities of 220 and 422 reflections are given for the sake of comparison.

From an observation of the tables it is evident that the observed and calculated intensities are in fairly good agreement. But for the 222 reflection, of the observed intensities are found

Table - 6

$Li_{0.5}Zn_{0.5}[Mn_{0.7}Cr_{1.2}Li_{0.1}]\ O_4$

u = 0.396

a = 8.2805

hkl	$\frac{1}{d^2}$ obs.	$\frac{1}{d^2}$ cal.	Int.obs.	Int.cal.
111	0.04383	0.04376	55.6	57
220	0.1166	0.1167	27.2	25
311	0.1601	0.1604	100.0	82
222	0.1751	0.1752	13.6	3
400	0.2333	0.2334	42.0	39
422	0.3496	0.3501	7.0	5
511,333	0.3936	0.3937	32.0	55
440	0.4664	0.4668	44.0	56

Table - 7

$Li_{0.4}Zn_{0.6}[Mn_{0.4}Cr_{1.6}]\ O_4$

u = 0.382

a = 8.334

hkl	$\frac{1}{d^2}$ obs.	$\frac{1}{d^2}$ cal.	Int.obs.	Int.cal.
111	0.0432	0.04310	19	20
220	0.1152	0.1151	29	24
311	0.1584	0.1566	100	103
222	0.1728	0.1733	10	1
400	0.2304	0.2313	36	46
422	0.3456	0.3461	11	9
511,333	0.3890	0.3901	37	38

Table - 8

$Li_{0.3}Zn_{0.7}[Mn_{0.5}Cr_{1.4}Li_{0.1}]O_4$

u = 0.384

a = 8.315

hkl	$\frac{1}{d^2}$ obs.	$\frac{1}{d^2}$ cal.	Int.obs.	Int.cal
111	0.04403	0.04377	17	12
220	0.1152	0.1157	37	32
311	0.1583	0.1591	100	105
222	0.1742	0.1736	7	0.5
400	0.2313	0.2314	21	33
422	0.3450	0.3471	13	12
511,333	0.3903	0.3905	32	44
440	0.4615	0.4627	85	75

Table - 9

$Li_{0.2}Zn_{0.8}[Mn_{0.2}Cr_{1.8}]O_4$

u = 0.385

a = 8.3104

hkl	$\frac{1}{d^2}$ obs.	$\frac{1}{d^2}$ cal.	Int.obs.	Int.cal
111	0.04344	0.04403	9	9
220	0.1158	0.1158	39	28
311	0.1593	0.1593	100	93
222	0.1738	0.1733	7	0.7
400	0.2317	0.2313	21	29
422	0.3475	0.3451	11	9
511,333	0.3910	0.3901	36	38
440	0.4633	0.4615	41	56

Table - 10

$Li_{0.2}Zn_{0.8}[Mn_{0.6}Cr_{1.2}Li_{0.2}]\ O_4$

u = 0.393

a = 8.314

hkl	$\frac{1}{d^2}$ obs.	$\frac{1}{d^2}$ cal.	Int.obs.	Int.cal.
111	0.04355	0.04340	15	12
220	0.1158	0.1158	43	35
311	0.1593	0.1592	100	85
222	0.1733	0.1736	8	0.5
400	0.2313	0.2315	18	26
422	0.3472	0.3472	13	9
511,333	0.3901	0.3906	34	45
440	0.4629	0.4629	30	52

Table - 11

$Li_{0.1}Zn_{0.9}[Mn_{0.3}Cr_{1.6}Li_{0.1}]\ O_4$

u = 0.395

a = 8.316

hkl	$\frac{1}{d^2}$ obs.	$\frac{1}{d^2}$ cal.	Int.obs.	Int.cal.
111	0.04355	0.04337	9	10
220	0.1158	0.1157	44	41
311	0.1583	0.1591	100	88
222	0.1742	0.1736	8	1.5
400	0.2313	0.2313	19	23
422	0.3462	0.3471	15	7
511,333	0.3901	0.3905	35	49
440	0.4615	0.4627	41	50

Table - 12

$Cu_{0.2}Li_{0.8}[Mn_{1.1}Cr_{0.8}Mg_{0.1}]O_4$

u = 0.390
a = 8.215

hkl	$\frac{1}{d^2}$ obs.	$\frac{1}{d^2}$ cal.	Int.obs.	Int.cal.
111	0.04448	0.04445	112	114
220	0.1190	0.1185	11	8
311	0.1628	0.1630	100	86
222	0.1777	0.1778	14	2
400	0.2374	0.2371	81	96
331	0.2819	0.2816	11	9
511,333	0.3999	0.4000	35	48
422			abs.	0.96

Table - 13

$Zn_{0.2}Cu_{0.2}Li_{0.6}[Mn_{0.9}Cr_{1.0}Mg_{0.1}]O_4$

u = 0.394

a = 8.232

hkl	$\frac{1}{d^2}$ obs.	$\frac{1}{d^2}$ cal.	Int.obs.	Int.cal.
111	0.04448	0.04427	82	68
220	0.1181	0.1121	19	19
311	0.1643	0.1624	100	85
222	0.1768	0.1771	14	2
400	0.2356	0.2361	50	60
422	-	-	absent	0.6
511,333	0.3985	0.3985	33	64

Table - 14

$Li_{0.2}Zn_{0.6}Cu_{0.2}[Mn_{0.5}Cr_{1.4}Mg_{0.1}]O_4$

u = 0.394

a = 8.306

hkl	$\frac{1}{d^2}$ obs.	$\frac{1}{d^2}$ cal.	Int.obs.	Int.cal.
111	0.04355	0.04348	18	15
220	0.1158	0.1160	40	35
311	0.1593	0.1594	100	86
222	0.1744	0.1740	7	1
400	0.2325	0.2319	24	24
422	0.3472	0.3478	12	10
511,333	0.3910	0.3913	31	39
440	0.4637	0.4637	37	58

Table - 15

$Zn_{0.8}Cu_{0.2}[Mn_{0.3}Cr_{1.6}Mg_{0.1}]O_4$

u = 0.395

a = 8.318

hkl	$\frac{1}{d^2}$ obs.	$\frac{1}{d^2}$ cal.	Int.obs.	Int.cal.
111	0.04355	0.04336	8	7
220	0.1158	0.1156	43	40
311	0.1583	0.1519	100	87
222	0.1733	0.1735	7	1
400	0.2313	0.2313	16	17
422	0.3472	0.3469	11	14
511,333	0.3901	0.3903	23	44

Table - 16

$Zn_{0.6}Cu_{0.4}[Mn_{0.6}Cr_{1.2}Mg_{0.2}]\ O_4$

u = 0.398

a = 8.3115

hkl	$\frac{1}{d^2}$ obs.	$\frac{1}{d^2}$ cal.	Int.obs.	Int.cal.
111	0.04355	0.04342	9.21	8
220	0.1158	0.1158	43.00	47
311	0.1593	0.1592	100.00	85
222	0.1733	0.1737	8.00	1
400	0.2320	0.2316	18.00	15
422	0.3472	0.3474	12.00	12
511,333	0.3901	0.3908	30.00	47
440	0.4629	0.4631	38.00	45

Table - 17

$Cu_{0.6}Zn_{0.4}[Mn_{0.9}Cr_{0.8}Mg_{0.3}]O_4$

u = 0.399

a = 8.305

hkl	$\frac{1}{d^2}$ obs.	$\frac{1}{d^2}$ cal.	Int.obs.	Int.cal.
111	0.04355	0.04347	14	7
220	0.1158	0.1160	43	47
311	0.1593	0.1594	100	81
222	0.1742	0.1740	7	1
400	0.2325	0.2320	18	14
422	0.3475	0.3479	11	12
511,333	0.3910	0.3914	29	43
440	0.4640	0.4637	26	43

Table - 18

Compound	u	a	$r_{oct.\ hole}$	$r_{tet.\ hole}$	$r_{ions\ tetra-site}$	$r_{ions\ oct-site}$	charge of ions tetra-site	Charge of ions oct.site
$Li_{0.5}Zn_{0.5}[Mn_{0.7}Cr_{1.2}Li_{0.1}]O_4$	0.396	8.2805	0.512	0.694	0.670	0.595	1.5	6.5
$Li_{0.4}Zn_{0.6}[Mn_{0.4}Cr_{1.6}]O_4$	0.382	8.334	0.626	0.505	0.684	0.620	1.6	6.4
$Li_{0.3}Zn_{0.7}[Mn_{0.5}Cr_{1.4}Li_{0.1}]O_4$	0.384	8.315	0.607	0.530	0.698	0.610	1.7	6.3
$Li_{0.2}Zn_{0.8}[Mn_{0.2}Cr_{1.8}]O_4$	0.385	8.3104	0.597	0.543	0.712	0.635	1.8	6.2
$Li_{0.2}Zn_{0.8}[Mn_{0.6}Cr_{1.2}Li_{0.2}]O_4$	0.393	8.314	0.540	0.658	0.712	0.600	1.8	6.2
$Li_{0.1}Zn_{0.9}[Mn_{0.3}Cr_{1.6}Li_{0.1}]O_4$	0.395	8.316	0.527	0.688	0.726	0.625	1.9	6.1

Table - 19

Compound	u	a	$r_{oct.\ hole}$	$r_{tet.\ hole}$	$r_{ions\ tetra-site}$	$r_{ions\ oct-site}$	charge of ions tetra-site	Charge of ions Oct.site
$Cu_{0.2}Li_{0.8}[Mn_{1.1}Cr_{0.8}Mg_{0.1}]O_4$	0.390	8.215	0.538	0.592	0.672	0.568	1.0	7.0
$Zn_{0.2}Cu_{0.2}Li_{0.6}[Mn_{0.9}Cr_{1.0}Mg_{0.1}]O_4$	0.394	8.232	0.514	0.653	0.700	0.588	1.2	6.8
$Li_{0.2}Zn_{0.6}Cu_{0.2}[Mn_{0.5}Cr_{1.4}Mg_{0.1}]O_4$	0.394	8.306	0.532	0.672	0.756	0.613	1.6	6.4
$Zn_{0.8}Cu_{0.2}[Mn_{0.3}Cr_{1.6}Mg_{0.1}]O_4$	0.395	8.318	0.527	0.688	0.784	0.628	1.8	6.2
$Zn_{0.6}Cu_{0.4}[Mn_{0.6}Cr_{1.2}Mg_{0.2}]O_4$	0.398	8.3115	0.505	0.731	0.828	0.605	1.6	6.4
$Cu_{0.6}Zn_{0.4}[Mn_{0.9}Cr_{0.8}Mg_{0.3}]O_4$	0.399	8.305	0.497	0.744	0.872	0.583	1.4	6.6

Table - 20

Compound	Me_{oct}-Me_{oct} distance	% of octahedral sites occupied by Cr^{3+}	% of octahedral sites occupied by Mn^{4+}	θ
$Li_{0.5}Zn_{0.5}[Mn_{0.7}Cr_{1.2}Li_{0.1}]O_4$	2.927	60	35	- 75
$Li_{0.2}Zn_{0.8}[Mn_{0.6}Cr_{1.2}Li_{0.2}]O_4$	2.938	60	30	- 84
$Li_{0.3}Zn_{0.7}[Mn_{0.5}Cr_{1.4}Li_{0.1}]O_4$	2.940	70	25	- 99
$Li_{0.4}Zn_{0.6}[Mn_{0.4}Cr_{1.6}]O_4$	2.945	80	20	-118
$Li_{0.1}Zn_{0.9}[Mn_{0.3}Cr_{1.6}Li_{0.1}]O_4$	2.940	80	15	-154
$Li_{0.2}Zn_{0.8}[Mn_{0.2}Cr_{1.8}]O_4$	2.937	90	10	-180

Table - 21

Compound	Me_{oct}-Me_{oct} distance	% of octahedral sites occupied by Cr^{3+}	% of tetrahedral sites occupied by Mn^{4+}	θ
$Cu_{0.6}Zn_{0.4}[Mn_{0.9}Cr_{0.8}Mg_{0.3}]O_4$	2.740	40	45	-13
$Cu_{0.2}Li_{0.8}[Mn_{1.1}Cr_{0.8}Mg_{0.1}]O_4$	2.71	40	55	-22
$Zn_{0.2}Cu_{0.2}Li_{0.6}[Mn_{0.9}Cr_{1.0}Mg_{0.1}]O_4$	2.716	50	45	-41
$Zn_{0.6}Cu_{0.4}[Mn_{0.6}Cr_{1.2}Mg_{0.2}]O_4$	2.742	60	30	-35
$Li_{0.2}Zn_{0.6}Cu_{0.2}[Mn_{0.5}Cr_{1.4}Mg_{0.1}]O_4$	2.74	70	25	-58
$Zn_{0.8}Cu_{0.2}[Mn_{0.3}Cr_{1.6}Mg_{0.1}]O_4$	2.744	80	15	-65

Table - 22

Compound	220 obs.	220 cal.	422 obs.	422 cal.
$Li_{0.5}Zn_{0.5}[Mn_{0.7}Cr_{1.2}Li_{0.1}]O_4$	27	25	7.41	5
$Li_{0.4}Zn_{0.6}[Mn_{0.4}Cr_{1.6}]O_4$	29	24	11.00	9
$Li_{0.3}Zn_{0.7}[Mn_{0.5}Cr_{1.4}Li_{0.1}]O_4$	37	32	13.00	12
$Li_{0.2}Zn_{0.8}[Mn_{0.2}Cr_{1.8}]O_4$	39	28	11.00	9
$Li_{0.2}Zn_{0.8}[Mn_{0.6}Cr_{1.2}Li_{0.2}]O_4$	43	35	13.00	9
$Li_{0.1}Zn_{0.9}[Mn_{0.3}Cr_{1.6}Li_{0.1}]O_4$	44	41	15.00	7

Table - 23

Compound	220 obs.	220 cal.	422 obs.	422 cal.
$Cu_{0.2}Li_{0.8}[Mn_{1.1}Cr_{0.8}Mg_{0.1}]O_4$	11	8	abs.	0.956
$Zn_{0.2}Cu_{0.2}Li_{0.6}[Mn_{0.9}Cr_{1.0}Mg_{0.1}]O_4$	19	19	abs.	0.600
$Li_{0.2}Zn_{0.6}Cu_{0.2}[Mn_{0.5}Cr_{1.4}Mg_{0.1}]O_4$	40	35	12	10.00
$Zn_{0.8}Cu_{0.2}[Mn_{0.3}Cr_{1.6}Mg_{0.1}]O_4$	43	40	11	14.00
$Zn_{0.6}Cu_{0.4}[Mn_{0.6}Cr_{1.2}Mg_{0.2}]O_4$	43	47	12	12.00
$Cu_{0.6}Zn_{0.4}[Mn_{0.9}Cr_{0.8}Mg_{0.3}]O_4$	43	47	11	12.00

to be always higher than the calculated intensities. In most of the cases the calculated intensities for 440 and (511,333) reflections are found to be higher than the observed intensities.

Another interesting feature is that there is an increase in the 220 and 422 reflections with ∅ decreasing lithium content in both the systems (Tables 22,23). This may be due to the fact that these two reflections are dependent on only the scattering factors of the A site cations and as the A sites are occupied more and more by heavier ions, the intensity also increases. In the second system, the last three compounds of Table 23 contain no lithium at tetrahedral sites and as copper and zinc have nearly same scattering power the intensities also remain same.

In Tables 18 and 19, the u, a, $r_{oct-hole}$, $r_{tet-hole}$ etc. are given. There is a regular variation in u as the charge and radius of ions on tetrahedral site increase except for the compound $Li_{0.5}Zn_{0.5}[Mn_{0.7}Cr_{1.2}Ii_{0.1}]O_4$. As the u value increases, naturally the radius of the tetrahedral hole increases and the radius of the octahedral hole decreases. Same is the case with second system.

However, not much regularity was found in the value of 'a' in both the systems. In Tables 20&21, the Me_{oct}-Me_{oct} distances are given along with the θ values obtained from magnetic susceptibility data. These results will be discussed later.

3.2 MAGNETIC SUSCEPTIBILITY MEASUREMENTS RESULTS

Paramagnetic susceptibility of all the compounds from 78°K to 600°K has been measured by the Gouy method. From the experimental results, the values of molar susceptibility (χ_M) have been calculated and $1/\chi_M$ was plotted as a function of temperature. In the higher temperature region the ~~compounds~~ plots were linear obeying Curie-Weiss law.

$$\frac{1}{\chi} = \frac{T}{C} - \frac{\theta}{C}$$

The Curie and Weiss constants C and θ are determined from the slope and the intercept of the linear $1/\chi_M$ vs. T plot. The value of C depends on the number of free electrons in an atom. The relation between the number of free spins in the ion and its C value is given by:

$$C_A = n(n+2)\frac{N_o\beta^2}{3k}$$

k = Boltzmann constant
N_o = Avagadro's number
n = number of free spins on an ion
β = Bohr magneton

Thus the values of C_A for different values of n are:

n	1	2	3	4	5
C_A	0.37	0.99	1.86	2.98	4.34

The C values are additive, i.e. $C_M = \Sigma\, n_i C_i$ where C_M is the Curie constant per mole, C_i = Curie constant per gm. atom for the i^{th} paramagnetic ion, n_i is the number of i^{th} ion in the molecule. Summation is taken over all the paramagnetic ions. The C value can be calculated for the probable spin

configuration of the ion in the molecule and compared with experimental value.

The value of θ on the other hand depends on the interaction between the neighbouring spins in the solid. The value of θ therefore gives an idea of the nature and strength of this interaction. A +ve value of θ means that the interaction is ferromagnetic in nature whereas negative value would indicate an antiferromagnetic interaction.

The values of θ, C_M observed and C_M calculated are presented for the 36 compounds in the tables given below:

Table - 24

C_M and θ Values for Compounds of I st.system

Compound	C_M (theoretical)	C_M (experimental	θ
$Li_{0.5}Zn_{0.5}[Mn_{1.5}Li_{0.5}]O_4$	2.790	2.145	+57
$Li_{0.6}Zn_{0.4}[Mn_{1.4}Cr_{0.2}Li_{0.4}]O_4$	2.976	2.162	+44
$Li_{0.7}Zn_{0.3}[Mn_{1.3}Cr_{0.4}Li_{0.3}]O_4$	3.161	2.308	+37
$Li_{0.4}Zn_{0.6}[Mn_{1.2}Cr_{0.4}Li_{0.4}]O_4$	2.976	2.222	+22
$Li_{0.8}Zn_{0.2}[Mn_{1.2}Cr_{0.6}Li_{0.2}]O_4$	3.348	2.000	+ 8

Table - 25

C_M and θ Values for Compounds of Ist System

Compound	C_M (theoretical)	C_M (experimental)	θ
$Li_{0.5}Zn_{0.5}[Mn_{1.1}Cr_{0.6}Li_{0.3}]O_4$	3.161	2.381	- 2.5
$Li_{0.9}Zn_{0.1}[Mn_{1.1}Cr_{0.8}Li_{0.1}]O_4$	3.534	2.973	- 9
$Li_{0.6}Zn_{0.4}[Mn_{1.0}Cr_{0.8}Li_{0.2}]O_4$	3.348	2.240	-10
$Li_{0.3}Zn_{0.7}[Mn_{0.9}Cr_{0.8}Li_{0.3}]O_4$	3.161	2.467	-20
$Li_{1.0}[Mn_{1.0}Cr_{1.0}]O_4$	3.720	2.500	-50
$Li_{0.7}Zn_{0.3}[Mn_{0.9}Cr_{1.0}Li_{0.1}]O_4$	3.534	2.500	-60

Table -26

C_M and θ Values for Compounds of Ist System

Compound	C_M (theoretical)	C_M (experimental)	θ
$Li_{0.4}Zn_{0.6}[Mn_{0.8}Cr_{1.0}Li_{0.2}]O_4$	3.348	2.554	- 67
$Li_{0.8}Zn_{0.2}[Mn_{0.8}Cr_{1.2}]O_4$	3.720	2.308	- 68
$Li_{0.5}Zn_{0.5}[Mn_{0.7}Cr_{1.2}Li_{0.1}]O_4$	3.534	2.400	- 75
$Li_{0.2}Zn_{0.8}[Mn_{0.6}Cr_{1.2}Li_{0.2}]O_4$	3.348	3.025	- 84
$Li_{0.6}Zn_{0.4}[Mn_{0.6}Cr_{1.4}]O_4$	3.720	2.445	- 89

Table - 27

C_M and θ Values for Compounds of Ist System

Compounds	C_M (theoretical)	C_M (experimental)	θ
$Li_{0.3}Zn_{0.7}[Mn_{0.5}Cr_{1.4}Li_{0.1}]O_4$	3.534	6.25	- 99
$Li_{0.4}Zn_{0.6}[Mn_{0.4}Cr_{1.6}]O_4$	3.720	2.513	-118
$Li_{0.1}Zn_{0.9}[Mn_{0.3}Cr_{1.6}Li_{0.1}]O_4$	3.534	3.770	-154
$Li_{0.2}Zn_{0.8}[Mn_{0.2}Cr_{1.8}]O_4$	3.720	6.250	-180
$Zn_{1.0}[Cr_2]O_4$	3.720	3.50	-350

Table - 28

C_M and θ Values for Compounds of IInd System

Compounds	C_M (theoretical)	C_M (experimental)	θ
$Cu_{1.0}[Mg_{0.5}Mn_{1.5}]O_4$	2.79	3.461	+67
$Li_{0.2}Cu_{0.8}[Mn_{1.4}Cr_{0.2}Mg_{0.4}]O_4$	2.976	2.128	+49
$Li_{0.4}Cu_{0.6}[Mn_{1.3}Cr_{0.4}Mg_{0.3}]O_4$	3.161	2.222	+40
$Zn_{0.2}Cu_{0.8}[Mn_{1.2}Cr_{0.4}Mg_{0.4}]O_4$	2.976	3.333	+40
$Li_{0.6}Cu_{0.4}[Mn_{1.2}Cr_{0.6}Mg_{0.2}]O_4$	3.348	2.095	+13
$Li_{0.2}Zn_{0.2}Cu_{0.6}[Mn_{1.1}Cr_{0.6}Mg_{0.3}]O_4$	3.161	2.546	+ 7

Table - 29

C_M and θ Values for Compounds of IInd System

Compound	C_M (theoretical)	C_M (experimental)	θ
$Li_{0.8}Cu_{0.2}[Mn_{1.1}Cr_{0.8}Mg_{0.1}]O_4$	3.534	2.200	-22
$Li_{0.4}Zn_{0.2}Cu_{0.4}[Mn_{1.0}Cr_{0.8}Mg_{0.2}]O_4$	3.348	2.500	-35
$Zn_{0.4}Cu_{0.6}[Mn_{0.9}Cr_{0.8}Mg_{0.3}]O_4$	3.161	3.333	-13
$Li_{0.6}Zn_{0.2}Cu_{0.2}[Mn_{0.9}Cr_{1.0}Mg_{0.1}]O_4$	3.534	2.258	-41
$Li_{0.2}Zn_{0.4}Cu_{0.4}[Mn_{0.8}Cr_{1.0}Mg_{0.2}]O_4$	3.348	2.439	-27

Table - 30

C_M and θ Values for the Compounds of IInd System

Compound	C_M (theoretical)	C_M (experimental)	θ
$Li_{0.4}Zn_{0.4}Cu_{0.2}[Mn_{0.7}Cr_{1.2}Mg_{0.1}]O_4$	3.534	2.321	-48
$Zn_{0.6}Cu_{0.4}[Mn_{0.6}Cr_{1.2}Mg_{0.2}]O_4$	3.348	2.679	-35
$Li_{0.2}Zn_{0.6}Cu_{0.2}[Mn_{0.5}Cr_{1.4}Mg_{0.1}]O_4$	3.534	2.222	-58
$Zn_{0.8}Cu_{0.2}[Mn_{0.3}Cr_{1.6}Mg_{0.1}]O_4$	3.534	2.167	-65

In the first four tables, the θ values of the first system (which are obtained from extrapolation of the high temperature linear portion) along with the C_M values observed and calculated are given. In the next three tables the θ values of the second system along with the C_M values are given. It is evident from the tables that θ varies regularly not only with the varying concentrations of chromium and manganese but also with the total number of magnetic ions present at the octahedral sites.

The result can be explained on the assumption that Mn^{4+}-Mn^{4+} interactions are +ve and Cr^{3+}-Cr^{3+} interactions are negative. The Table (24) contains compounds of relatively high Mn^{4+} concentration. When the octahedral sites contain more than 60 percent of Mn^{4+}, the compounds are ferromagnetic. Thus in Table 24 as the concentration of Mn^{4+} decreases the θ value also decreases. But among the last two compounds even though

Mn^{4+} content remains constant, θ decreases because there is an increase in the chromium concentration and hence in the total number of magnetic ions.

Similarly in Table 25, the compounds show the predominance of antiferromagnetic interactions, as the concentration of Mn^{4+} is less than 60 per cent of the octahedral sites. It is worth observing that in Table 25 for compounds 2,3,4 the concentration of chromium remained same and the concentration of manganese decreased, even then there is no much change in the value of θ. Whereas among compounds 4 and 5, when the concentration of chromium increased from 0.8 to 1.0 and the concentration of manganese increased from 0.9 to 1.0, but there is much change in θ value. This indicates that the Cr^{3+}-Cr^{3+} interactions are strong and -ve. Similarly the compounds 4 and 6 (Table 25) can be compared.

A similar behaviour of θ can be observed in the compounds presented in Tables 26 and 27.

In Tables 28, 29 and 30 the compounds of IInd system are presented. They contain copper ion also, regarding whose valency there is a lot of controversy. However, the results can be explained by assuming that copper is monovalent and is present at tetrahedral sites. In Table 28 all the ferromagnetic compounds are presented. The compounds are arranged in the decreasing order of manganese concentration.

From the results it is evident that the value of θ is greatly effected by the concentration of chromium ions and the total number of magnetic ions, and to a lesser extent by the concentration of manganese ions.

In general, the C_M values calculated from the slope of the

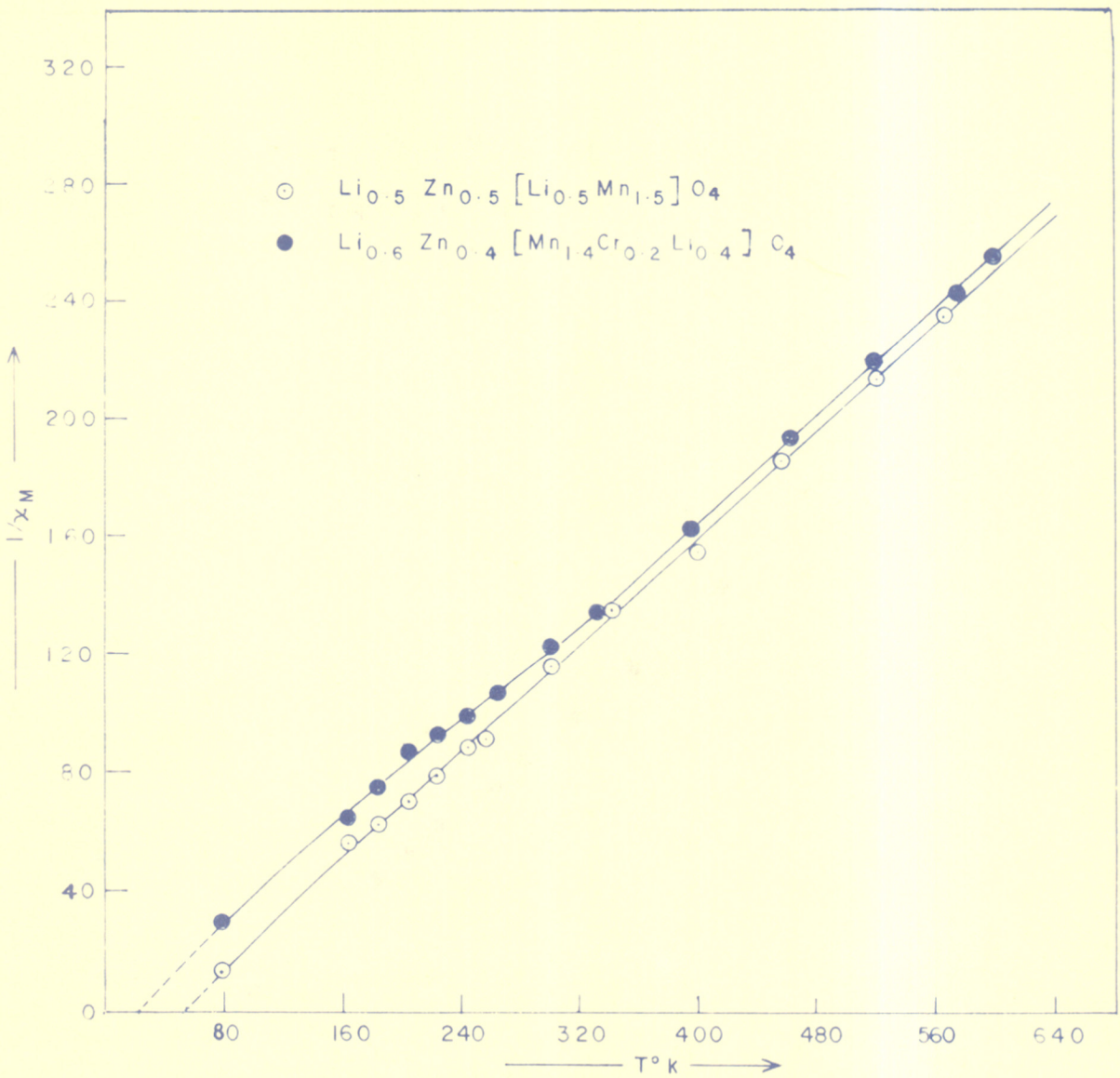

Fig 10. PLOTS OF $\frac{1}{\chi_M}$ AS A FUNCTION OF TEMPERATURE FOR FIRST SYSTEM

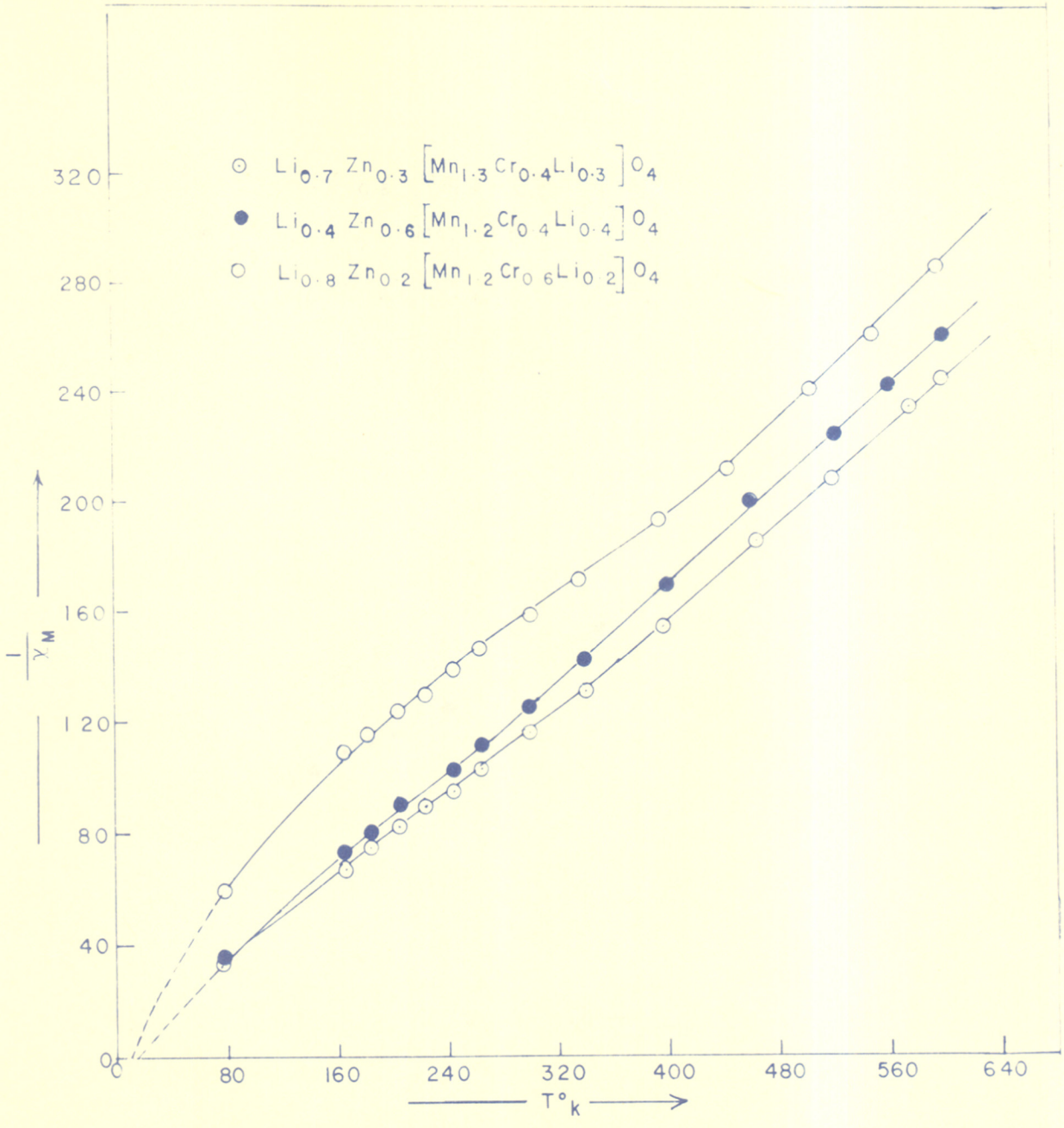

Fig11. PLOTS OF $\frac{1}{\chi_M}$ AS A FUNCTION OF TEMPERATURE FOR FIRST SYSTEM

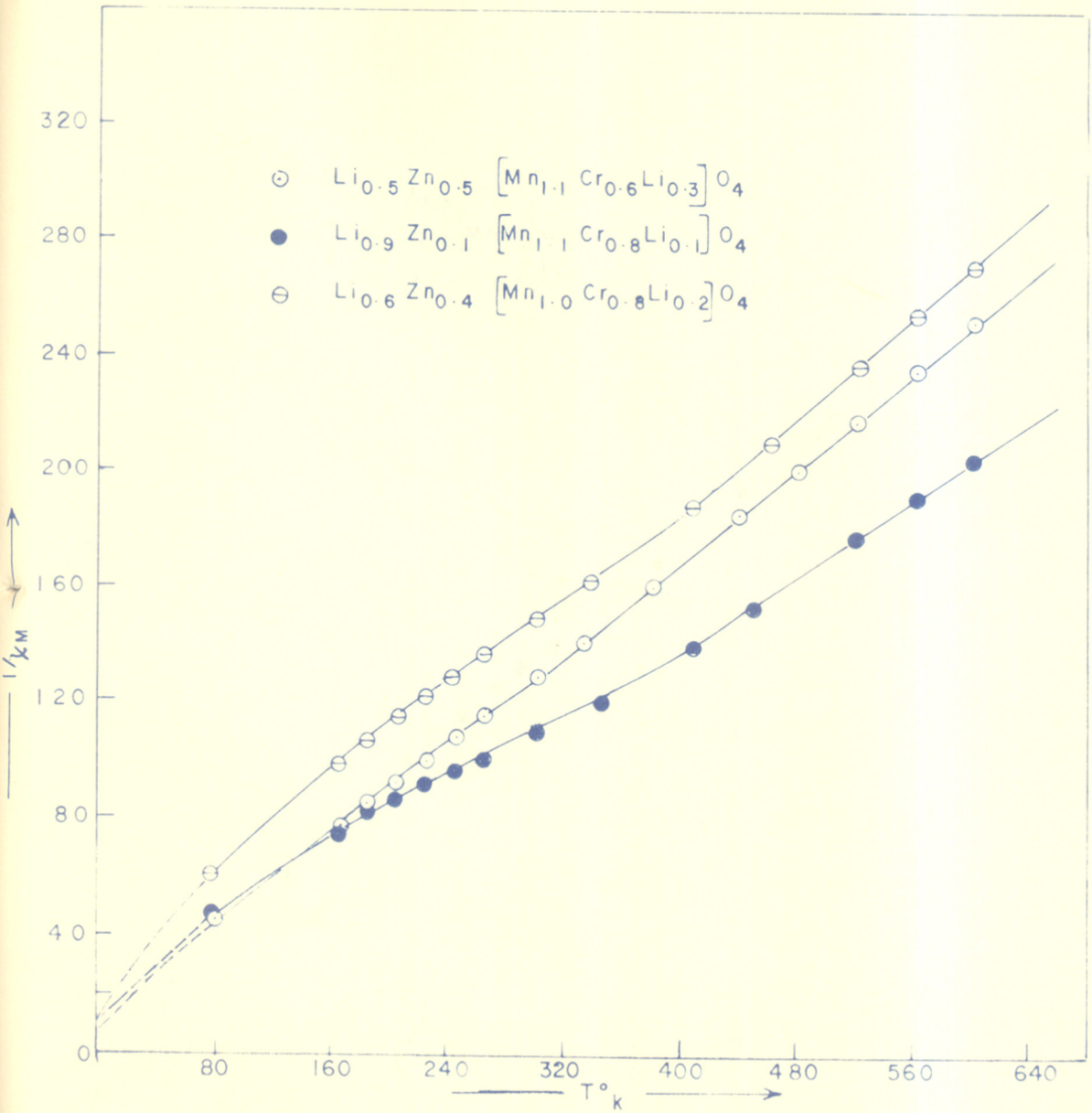

Fig12. PLOTS OF $\frac{1}{\chi_M}$ AS A FUNCTION OF TEMPERATURE FOR FIRST SYSTEM

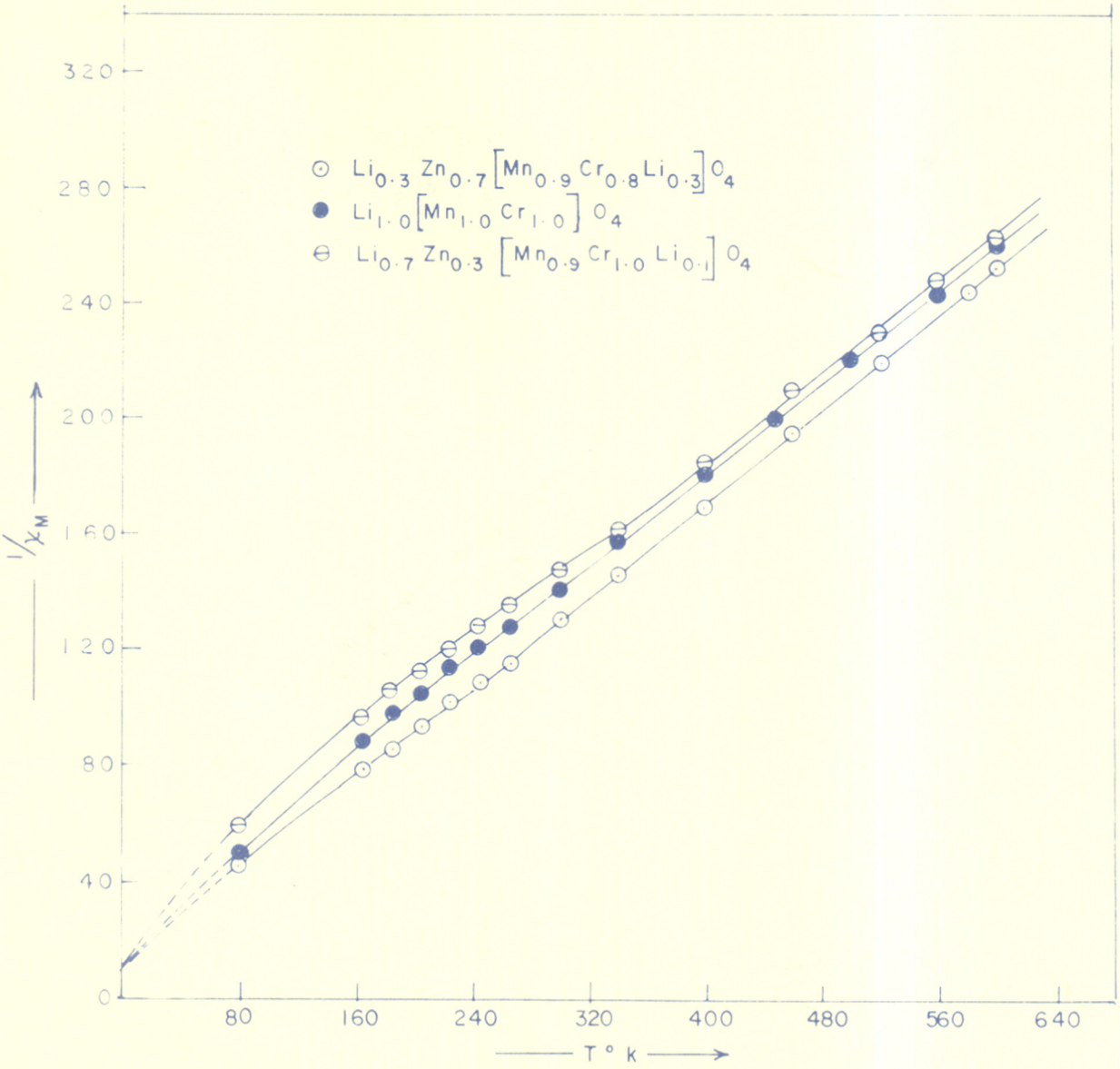

Fig 13 PLOTS OF $\frac{1}{\chi_M}$ AS A FUNCTION OF TEMPERATURE FOR FIRST SYSTEM

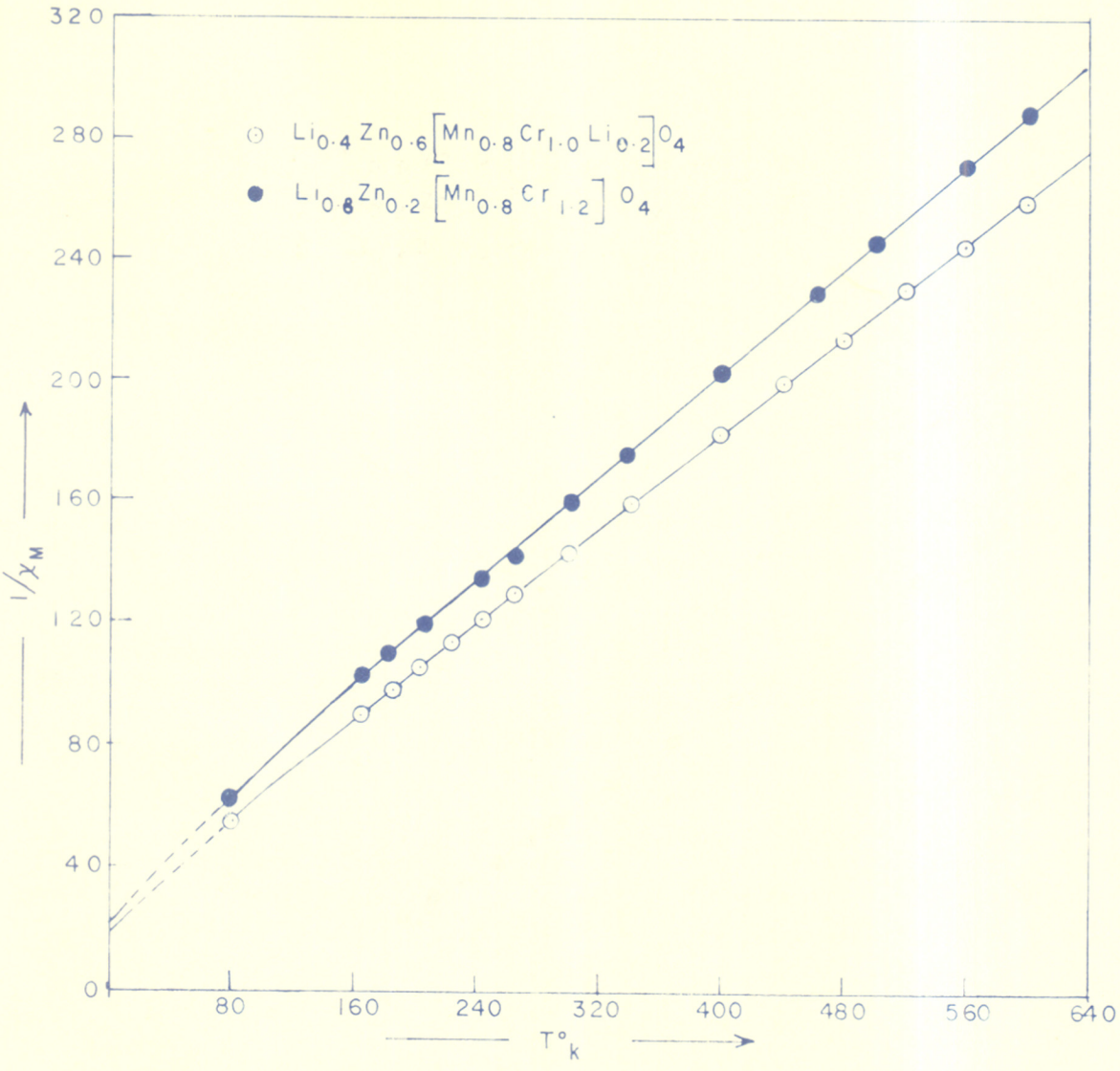

Fig 14. PLOTS OF $\frac{1}{\chi_M}$ AS A FUNCTION OF TEMPERATURE FOR FIRST SYSTEM

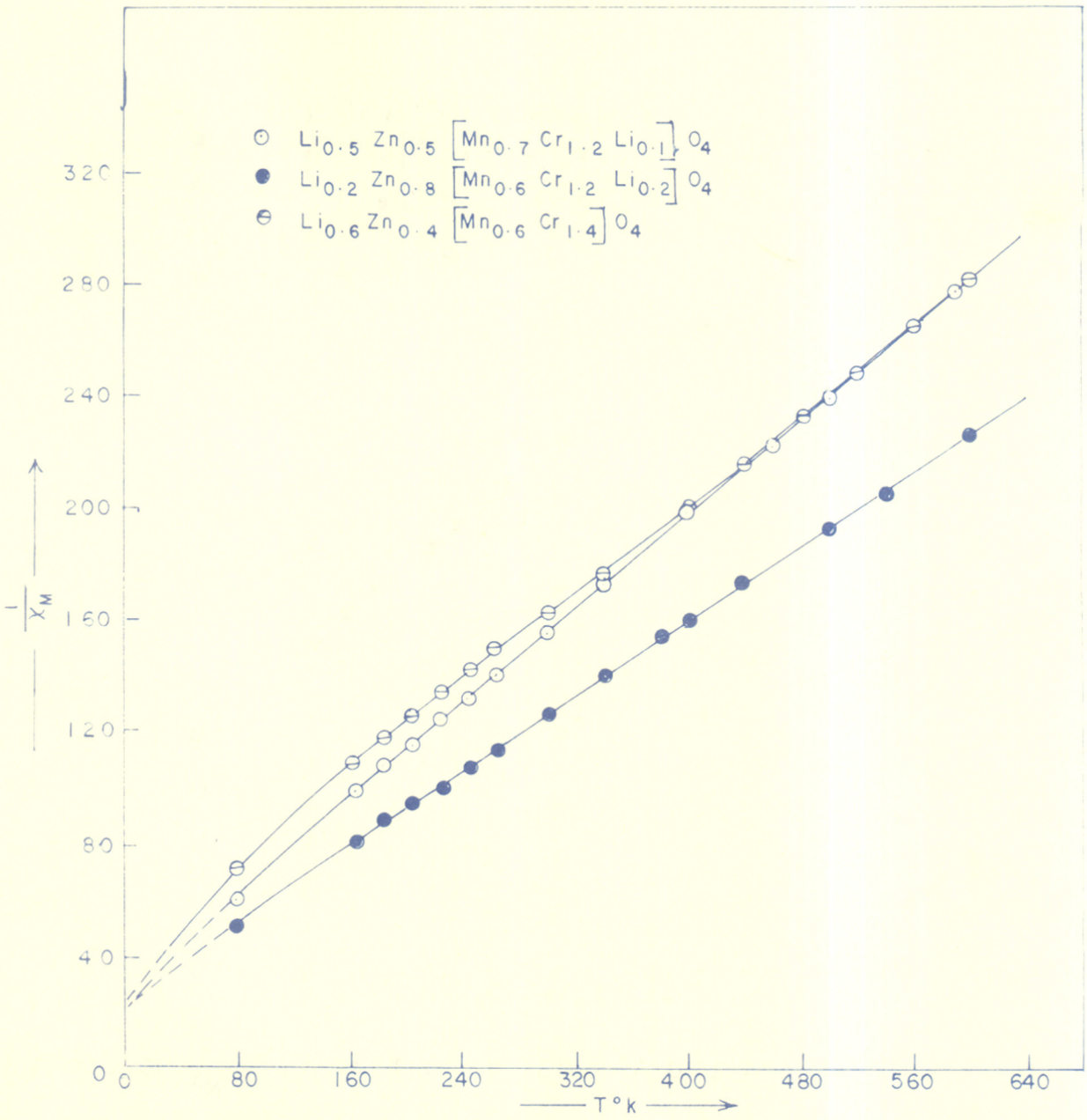

FIG.15. PLOTS OF $\frac{1}{\chi_M}$ AS A FUNCTION OF TEMPERATURE FOR FIRST SYSTEM

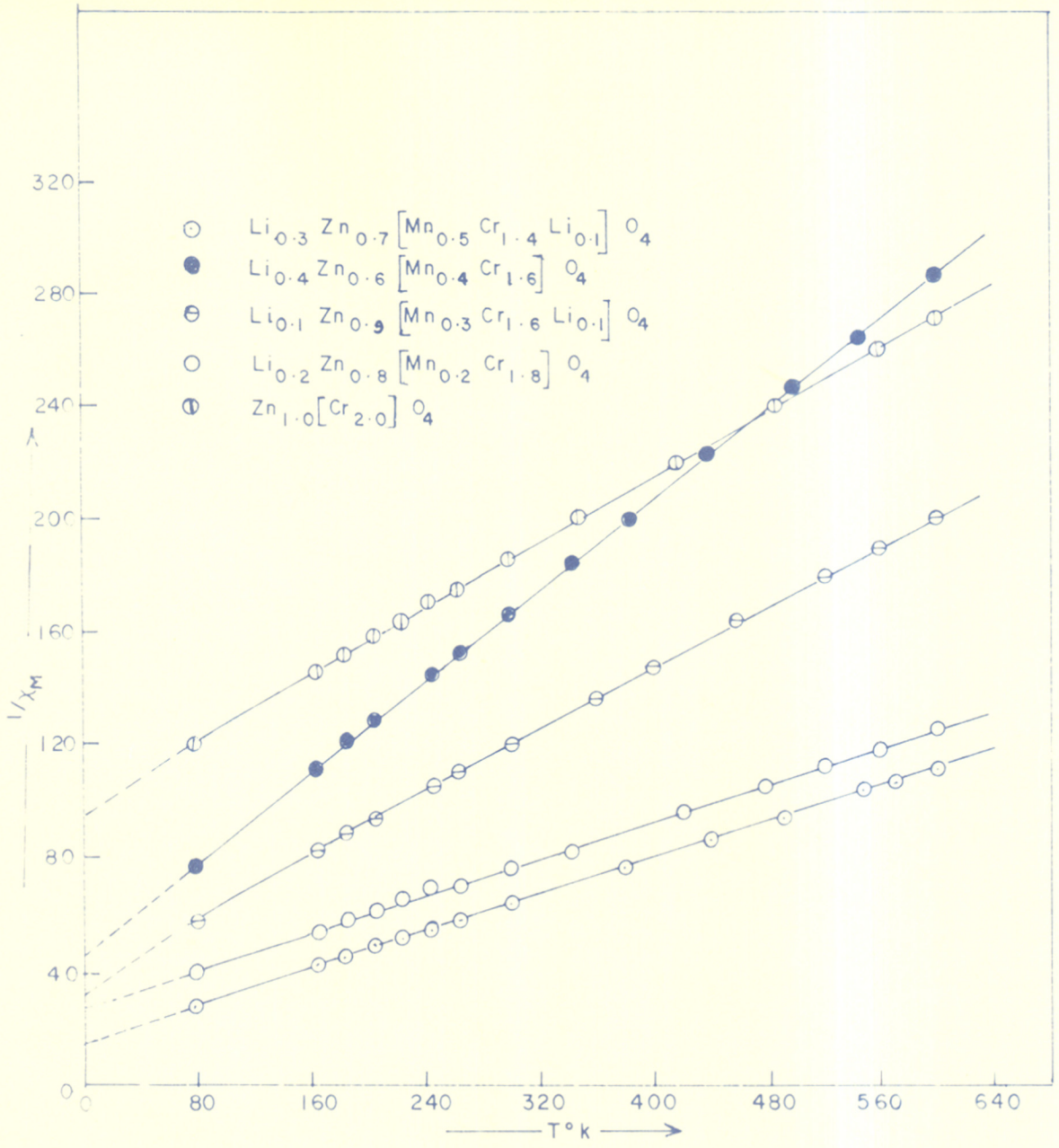

Fig 16. PLOTS OF $\frac{1}{\chi_M}$ AS A FUNCTION OF TEMPERATURE FOR FIRST SYSTEM

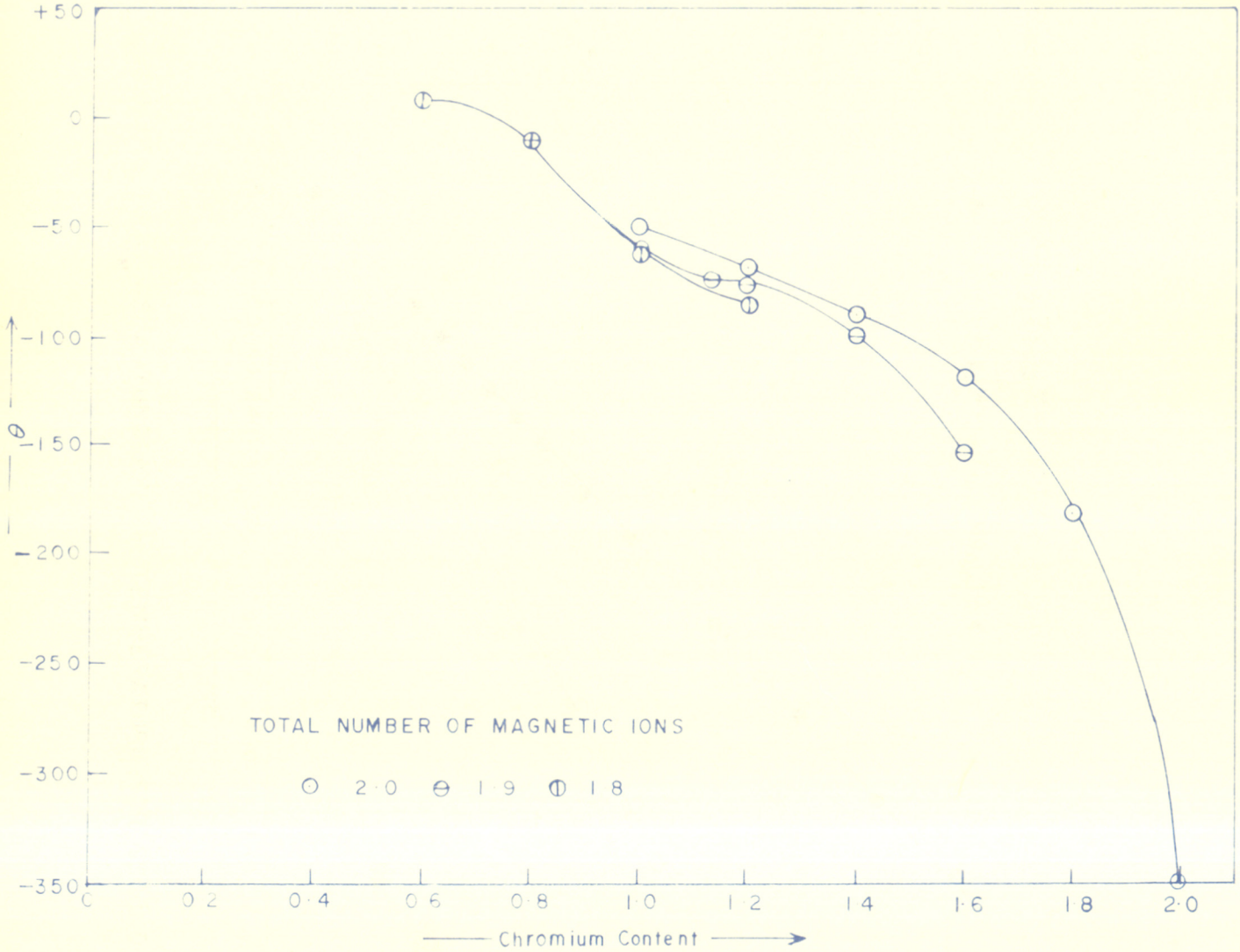

Fig 17 PLOT OF θ AS A FUNCTION OF CHROMIUM CONTENT FOR FIRST SYSTEM

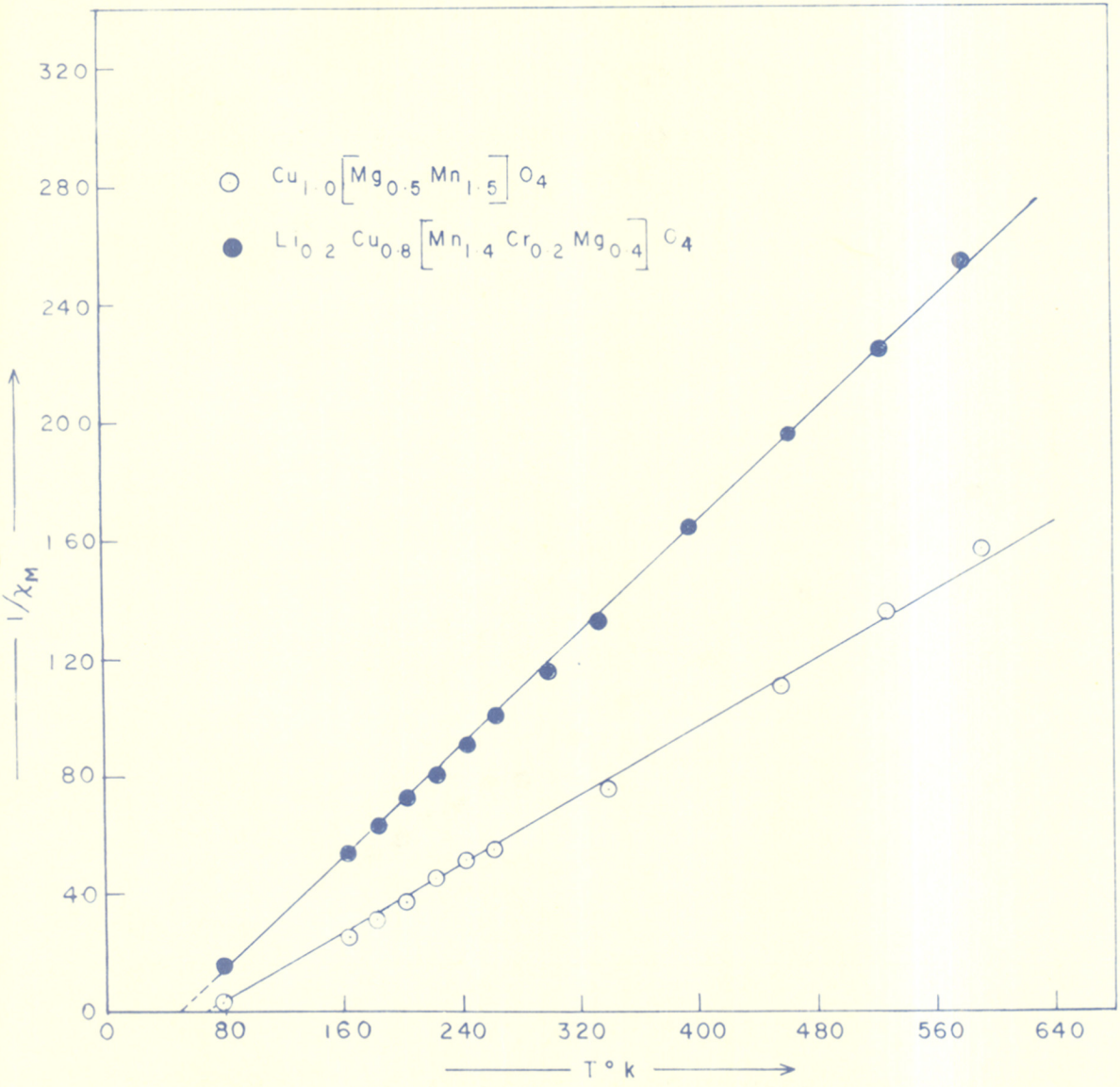

Fig 18. PLOTS OF $\frac{1}{\chi_M}$ AS A FUNCTION OF TEMPERATURE FOR SECOND SYSTEM

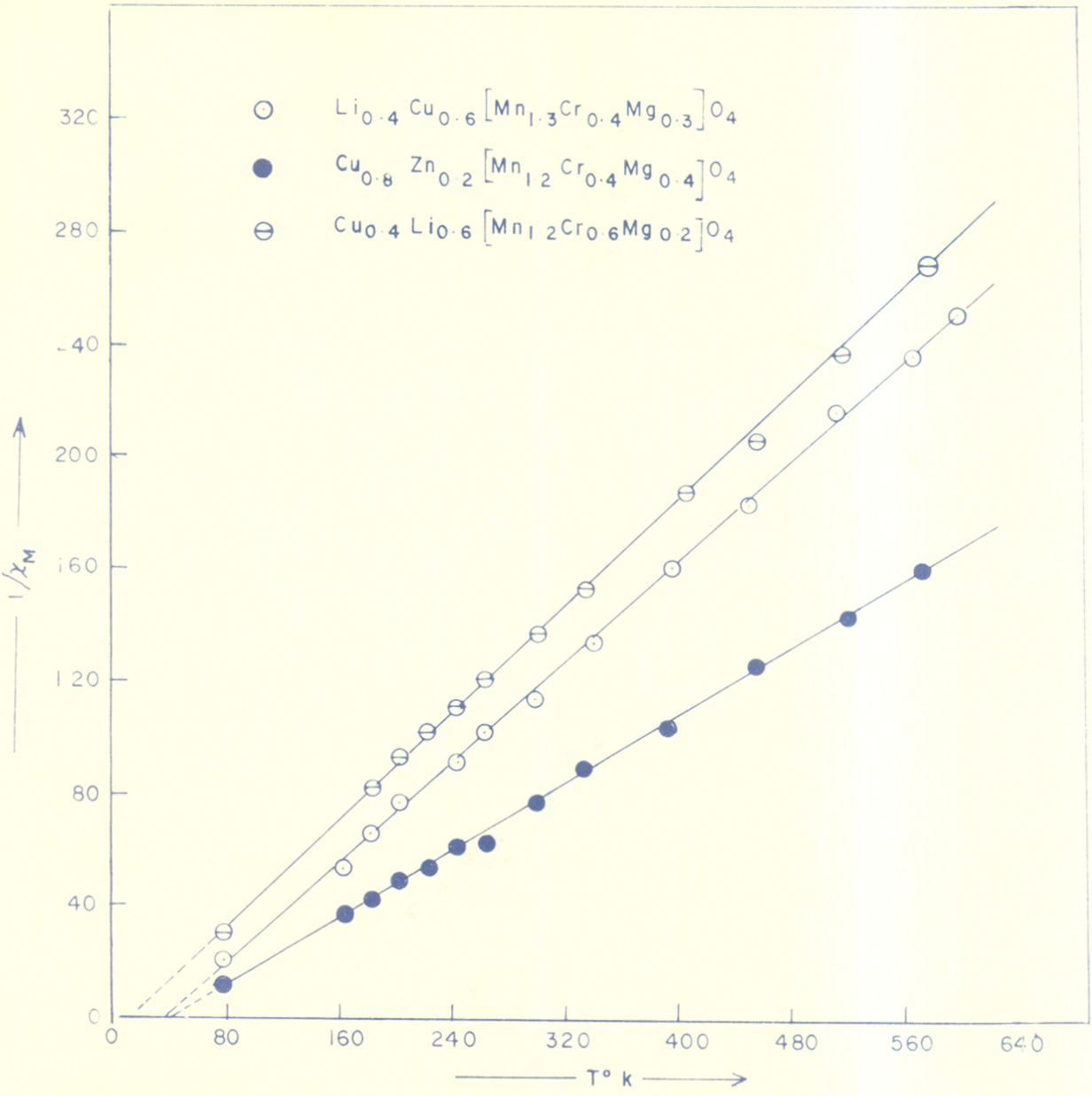

Fig19. PLOTS OF $\frac{1}{\chi_M}$ AS A FUNCTION OF TEMPERATURE FOR SECOND SYSTEM

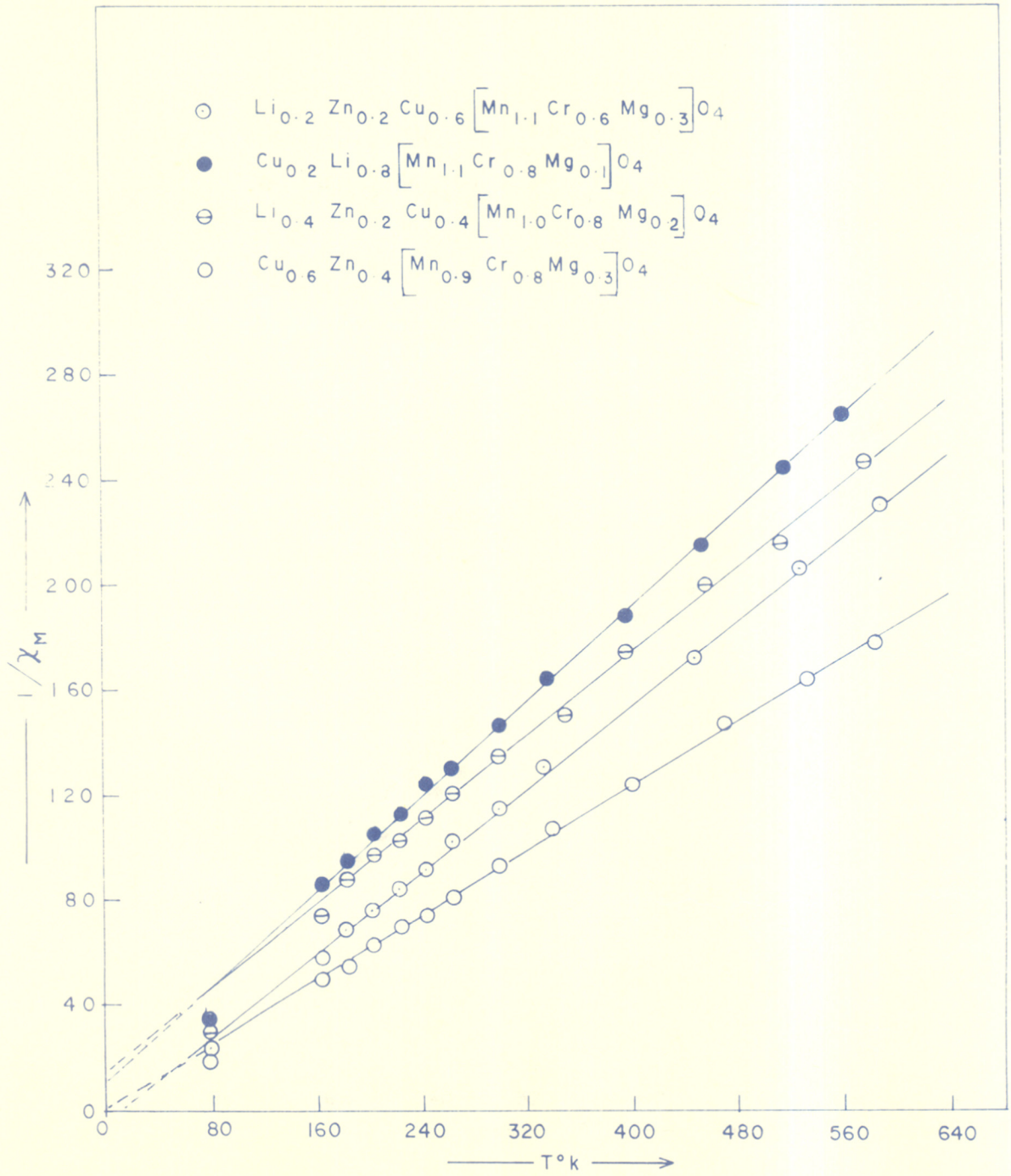

Fig 20. PLOTS OF $\frac{1}{\chi_m}$ AS A FUNCTION OF TEMPERATURE FOR SECOND SYSTEM.

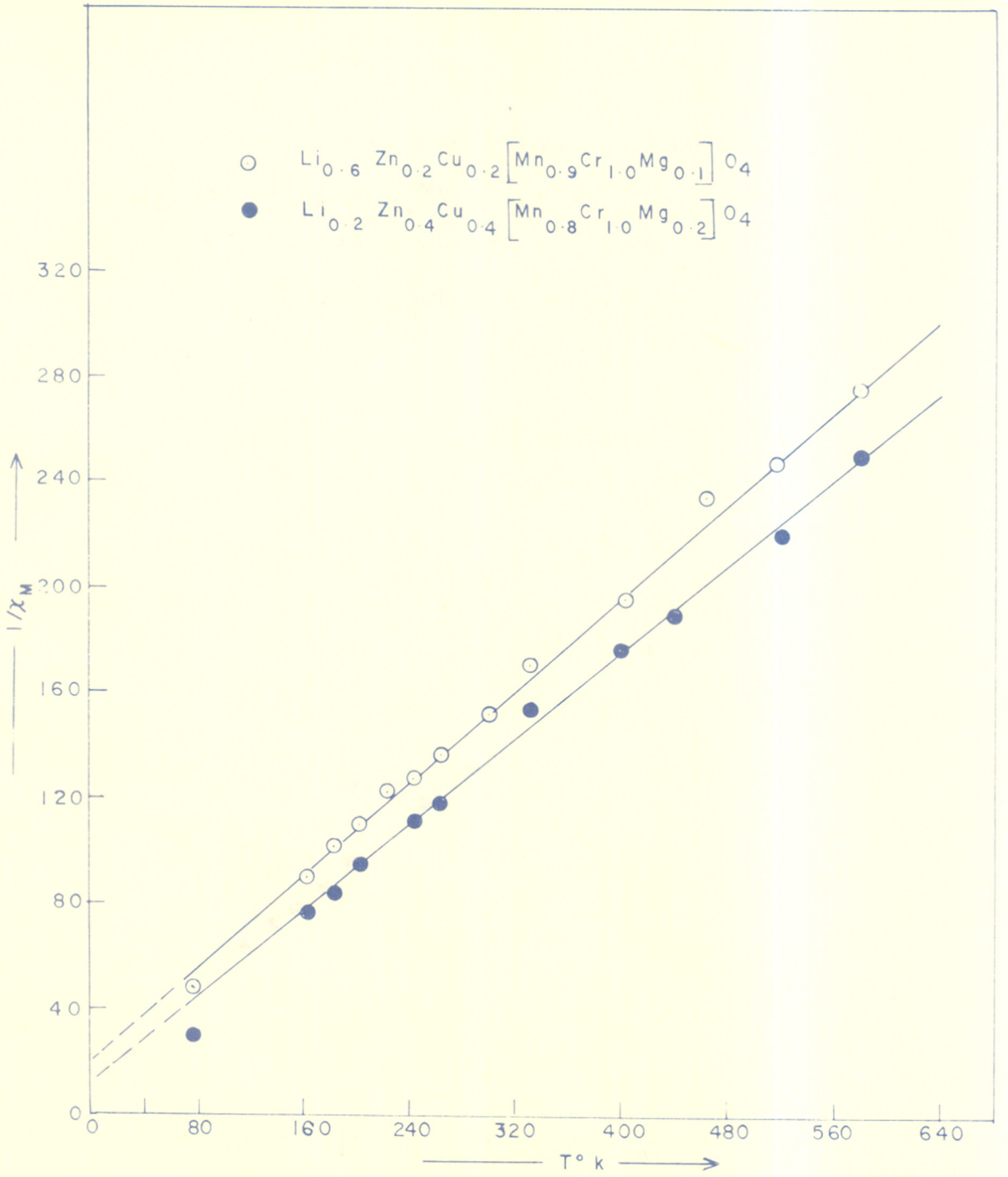

Fig.21 PLOTS OF $\frac{1}{\chi_M}$ AS A FUNCTION OF TEMPERATURE FOR SECOND SYSTEM

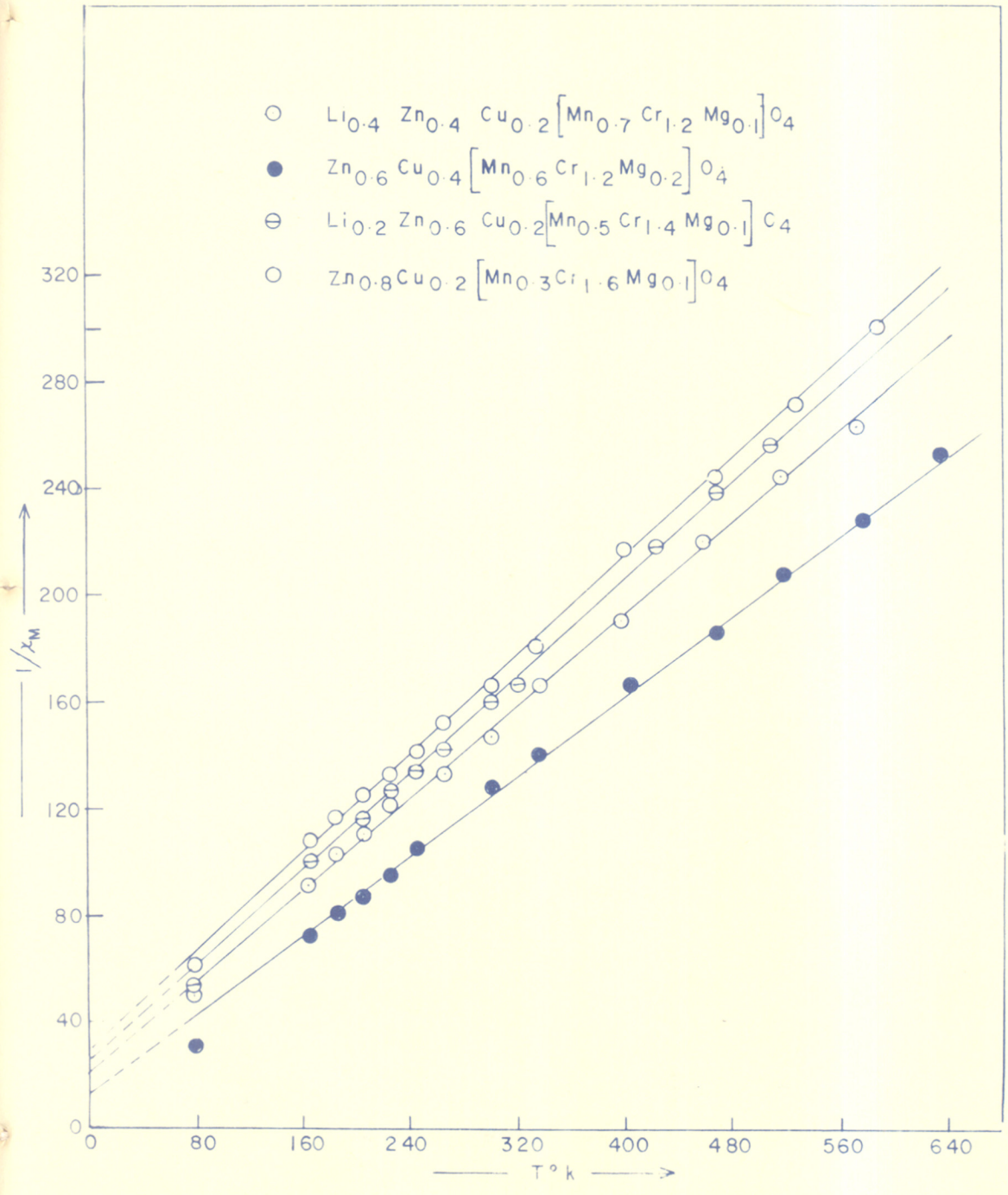

Fig 22. PLOTS OF $\frac{1}{\chi_M}$ AS A FUNCTION OF TEMPERATURE FOR SECOND SYSTEM

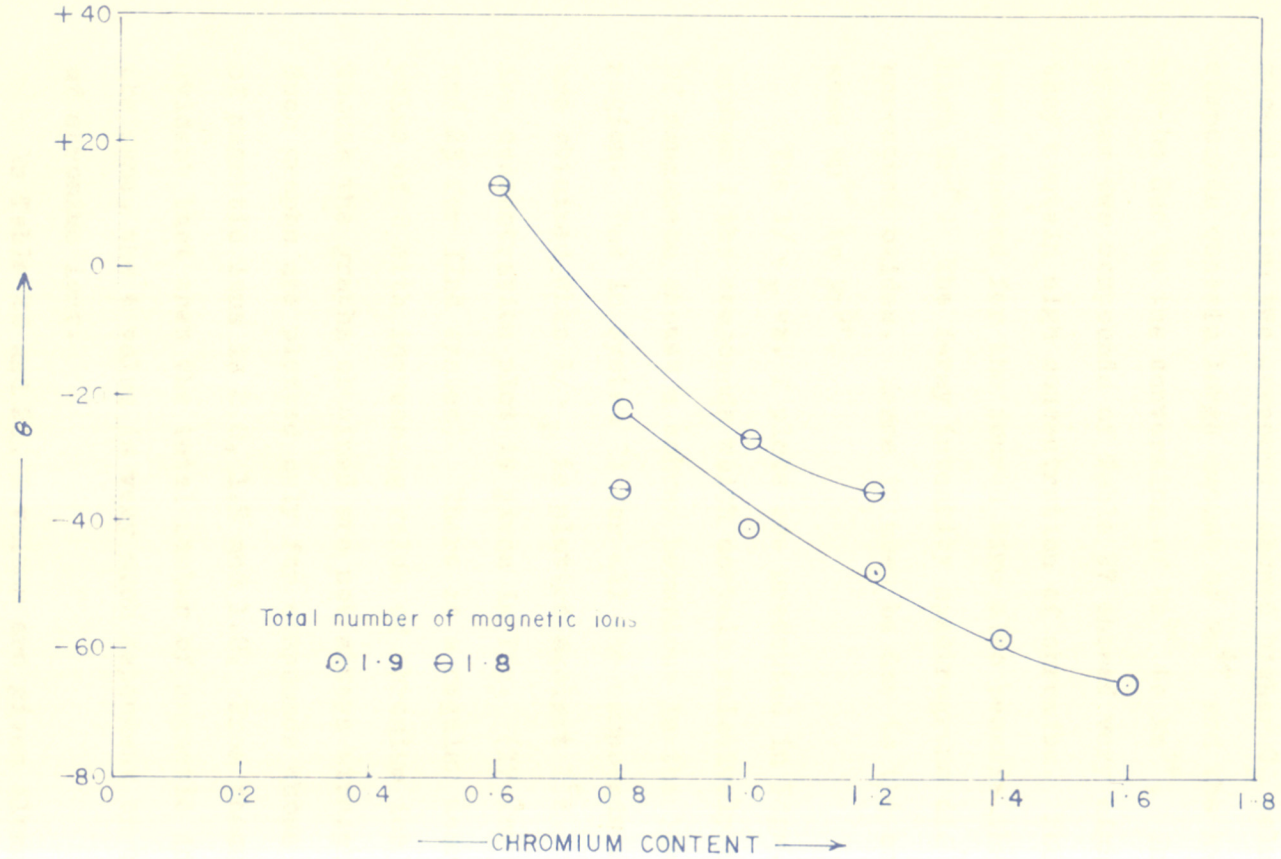

FIG.23 PLOT OF θ AS A FUNCTION OF CHROMIUM CONTENT FOR SECOND SYSTEM

curves are found to be less than the theoretical C_M values. In one or two cases higher C_M values are also obtained. In second system two compounds showed higher C_M values. Those compounds contain large amount of Mn^{4+} and the high C_M value may be due to the conversion of Mn^{4+} to Mn^{3+}. In first system two compounds of Table 27 showed very high C_M value but they contain high concentration of chromium. Those compounds were reacted for the fourth time also because they contain high Cr^{3+}. The X-ray intensity spectrograms did not show any unreacted oxides. Hence it must be due to the conversion of some Mn^{4+} to Mn^{3+}.

The $1/\chi_M$ vs. T plots are presented in Figs.10-23. In system I the compounds which contain relatively high content of manganese showed a convex behaviour in the low temperature region. But in System II for all the compounds straightlines are obtained when $1/\chi_M$ is plotted against T^oK. θ vs chromium ion concentration plot is given in Fig. (17 for Ist system and 23 for IInd system). There is a regular decrease in the value of θ with increasing value of chromium ion concentration, though the graphs obtained are not always straight lines. Such graphs are plotted only for compounds whose total number of magnetic ions is 2.0, 1.9 and 1.8. From these graphs it is evident that when the total number of magnetic ions remains the same, the θ value is very much dependent on the concentration of chromium ions.

In Table 20 and 21, θ values are given along with the Me_{oct}-Me_{oct} distance and the percentage of chromium and

manganese ions that occupy the octahedral sites. No definite conclusions can be drawn from these results as the data is inadequate to correlate the Me_{oct}-Me_{oct} distance with the θ value. Though the value of θ depends upon the Me_{oct}-Me_{oct} distance, there are various other factors. Especially the concentration of chromium influences to a very large extent the value of θ.

3.3 ELECTRICAL CONDUCTIVITY RESULTS

All the compounds mentioned earlier have been pressed in the form of pellets and sintered. The dimensions of the sintered pellets have been measured by a micrometer. Electrical resistance of the sintered pellets has been measured from room temperature to about 300°C and the specific resistance values have been found out. Log ρ has been plotted as a function of 1/T. The plots of log ρ vs. 1/T are straight lines indicating that the exponential law is obeyed

$$\sigma = \sigma_0 \exp \frac{-\Delta E}{kT}$$

$$\rho = \rho_0 \exp \frac{-\Delta E}{kT}$$

$$\therefore \log \rho = \log \rho_0 + \frac{\Delta E}{2.303kT}$$

where σ = specific conductivity

ρ = specific resistance

ΔE = Thermal activation energy

k = Boltzmann constant

T = Absolute temperature

The energy of activation for each compound has been then calculated from the slope of log ρ vs. 1/T plot. The results are given in the following tables.

Table - 31

Results of Conductivity Measurements of the Compounds of Ist System

Compound	log ρ 27°C	log ρ_o	ΔE in ev.
$Li_{0.5}Zn_{0.5}[Mn_{1.5}Li_{0.5}]O_4$	5.40	$\bar{2}.45$	0.41
$Li_{0.6}Zn_{0.4}[Mn_{1.4}Cr_{0.2}Li_{0.4}]O_4$	4.80	$\bar{2}.55$	0.37
$Li_{0.4}Zn_{0.6}[Mn_{1.2}Cr_{0.4}Li_{0.4}]O_4$	4.95	$\bar{2}.50$	0.39
$Li_{0.7}Zn_{0.3}[Mn_{1.3}Cr_{0.4}Li_{0.3}]O_4$	4.95	$\bar{2}.82$	0.37
$Li_{0.5}Zn_{0.5}[Mn_{1.1}Cr_{0.6}Li_{0.3}]O_4$	5.10	$\bar{2}.17$	0.41
$Li_{0.3}Zn_{0.7}[Mn_{0.9}Cr_{0.8}Li_{0.3}]O_4$	5.45	$\bar{2}.80$	0.40

Table - 32

Results of Conductivity Measurements of the Compounds of Ist System

Compound	$\log \rho$ 27°C	$\log \rho_o$	ΔE in ev.
$Li_{0.8}Zn_{0.2}[Mn_{1.2}Cr_{0.6}Li_{0.2}]O_4$	4.75	$\bar{2}.80$	0.36
$Li_{0.6}Zn_{0.4}[Mn_{1.0}Cr_{0.8}Li_{0.2}]O_4$	5.65	$\bar{1}.00$	0.40
$Li_{0.4}Zn_{0.6}[Mn_{0.8}Cr_{1.0}Li_{0.2}]O_4$	7.45	$\bar{1}.77$	0.45
$Li_{0.2}Zn_{0.8}[Mn_{0.6}Cr_{1.2}Li_{0.2}]O_4$	5.97	$\bar{1}.35$	0.39

Table - 33

Results of Conductivity Measurements of the Compounds of Ist System

Compound	$\log P$ 27°C	$\log P_o$	ΔE in ev.
$Li_{0.9}Zn_{0.1}[Mn_{1.1}Cr_{0.8}Li_{0.1}]O_4$	5.00	$\bar{2}.70$	0.38
$Li_{0.7}Zn_{0.3}[Mn_{0.9}Cr_{1.0}Li_{0.1}]O_4$	5.35	$\bar{2}.80$	0.39
$Li_{0.5}Zn_{0.5}[Mn_{0.7}Cr_{1.2}Li_{0.1}]O_4$	5.70	$\bar{1}.42$	0.37
$Li_{0.3}Zn_{0.7}[Mn_{0.5}Cr_{1.4}Li_{0.1}]O_4$	6.70	$\bar{1}.20$	0.45
$Li_{0.1}Zn_{0.9}[Mn_{0.3}Cr_{1.6}Li_{0.1}]O_4$	7.10	$\bar{1}.82$	0.43

Table - 34

Results of Conductivity Measurements of the Compounds of Ist System

Compound	log P 27°C	log P_o	ΔE in ev.
$Li_{1.0}[Mn_{1.0}Cr_{1.0}]O_4$	5.80	$\bar{1}.00$	0.41
$Li_{0.8}Zn_{0.2}[Mn_{0.8}Cr_{1.2}]O_4$	5.97	$\bar{1}.30$	0.40
$Li_{0.6}Zn_{0.4}[Mn_{0.6}Cr_{1.4}]O_4$	6.65	$\bar{1}.75$	0.41
$Li_{0.4}Zn_{0.6}[Mn_{0.4}Cr_{1.6}]O_4$	7.45	$\bar{0}.60$	0.41
$Li_{0.2}Zn_{0.8}[Mn_{0.2}Cr_{1.8}]O_4$	8.85	$\bar{1}.92$	0.53
$Zn_{1.0}[Cr_2]O_4$	-	$\bar{5}.00$	0.99

Table - 35

Results of Conductivity Measurements of the Compounds of IInd System

Compound	log ρ 27°C	log ρ_o	ΔE in ev.
$Cu_{1.0}[Mg_{0.5}Mn_{1.5}]O_4$	1.85	$\bar{1}.00$	0.17
$Li_{0.2}Cu_{0.8}[Mg_{0.4}Cr_{0.2}Mn_{1.4}]O_4$	1.45	$\bar{3}.80$	0.22
$Zn_{0.2}Cu_{0.8}[Mn_{1.2}Cr_{0.4}Mg_{0.4}]O_4$	1.62	$\bar{2}.30$	0.20
$Li_{0.4}Cu_{0.6}[Mn_{1.3}Cr_{0.4}Mg_{0.3}]O_4$	1.45	$\bar{3}.95$	0.21
$Li_{0.2}Zn_{0.2}Cu_{0.6}[Mn_{1.1}Cr_{0.6}Mg_{0.3}]O_4$	1.45	$\bar{2}.15$	0.20
$Zn_{0.4}Cu_{0.6}[Mn_{0.9}Cr_{0.8}Mg_{0.3}]O_4$	1.80	$\bar{2}.12$	0.22

Table - 36

Results of Conductivity Measurements of the Compounds of IInd System

Compound	log ρ 27°C	log ρ_o	ΔE in ev.
$Li_{0.6}Cu_{0.4}[Mn_{1.2}Cr_{0.6}Mg_{0.2}]O_4$	1.62	$\bar{2}.10$	0.21
$Li_{0.4}Zn_{0.2}Cu_{0.4}[Mn_{1.0}Cr_{0.8}Mg_{0.2}]O_4$	1.75	$\bar{2}.42$	0.20
$Li_{0.2}Zn_{0.4}Cu_{0.4}[Mn_{0.8}Cr_{1.0}Mg_{0.2}]O_4$	1.90	$\bar{2}.37$	0.21
$Zn_{0.6}Cu_{0.4}[Mn_{0.6}Cr_{1.2}Mg_{0.2}]O_4$	2.70	$\bar{1}.00$	0.20

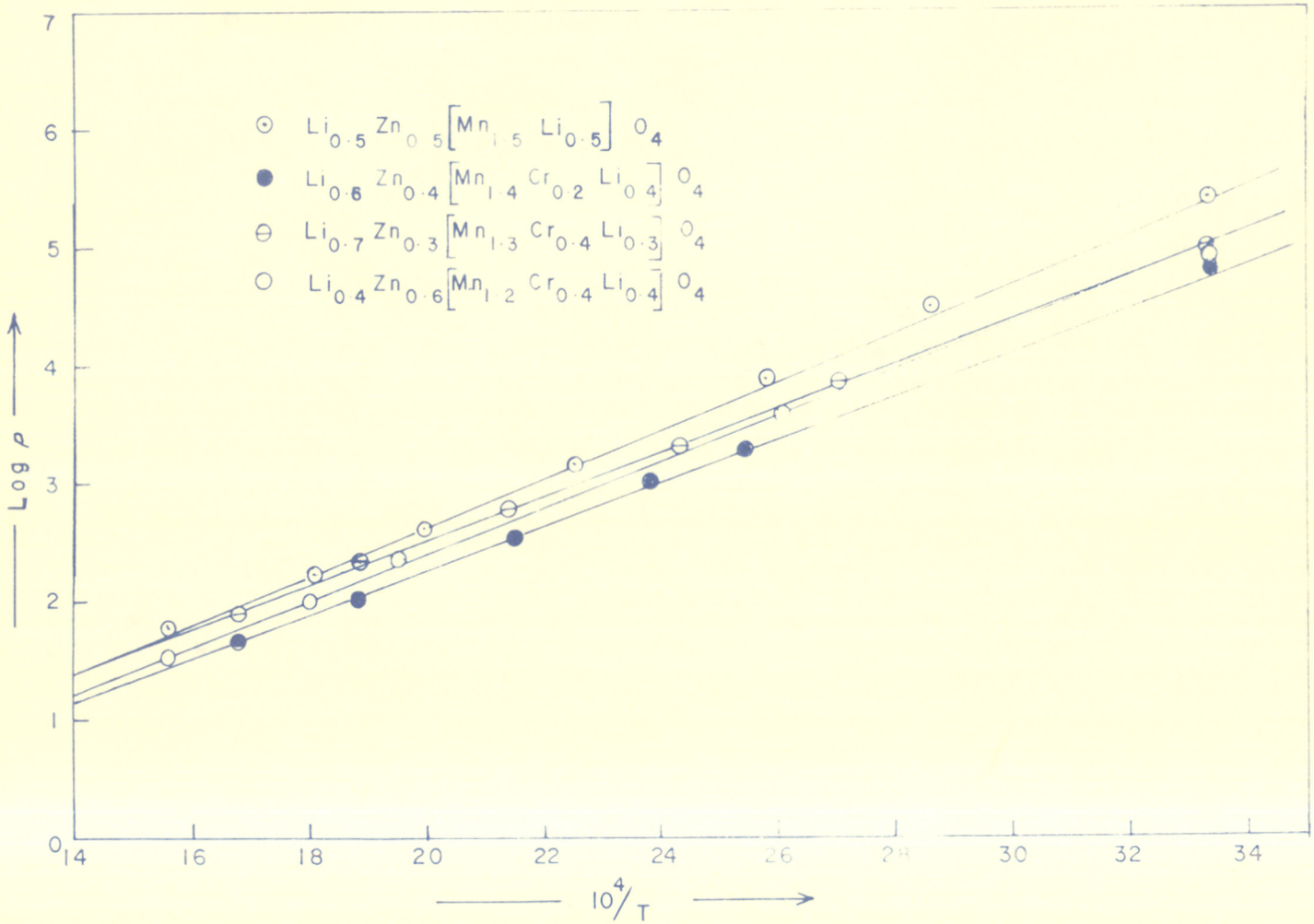

Fig24. PLOTS OF LOG ρ AS A FUNCTION OF RECIPROCAL TEMPERATURE FOR FIRST SYSTEM

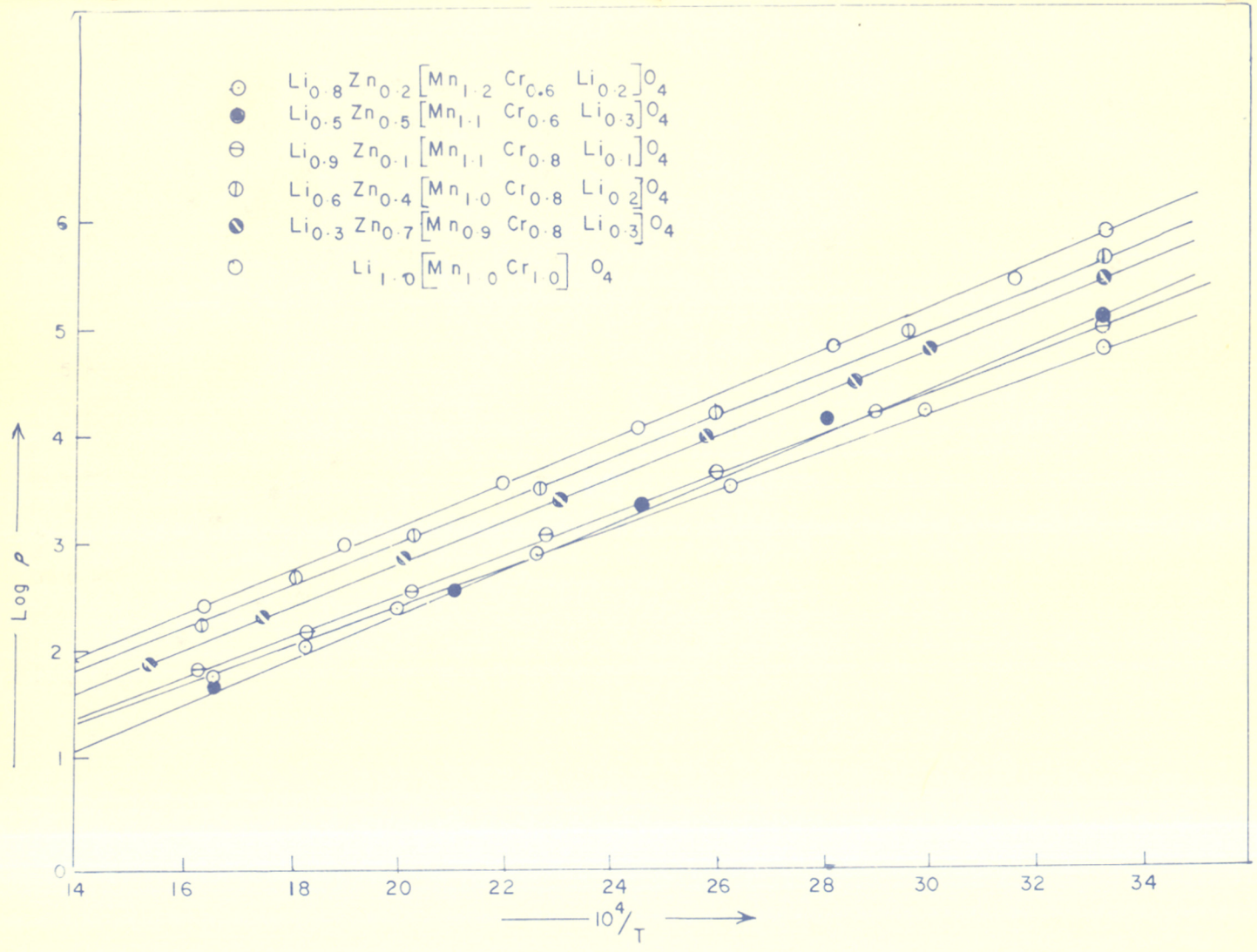

Fig 25 PLOTS OF LOG ρ AS A FUNCTION OF RECIPROCAL TEMPERATURE FOR FIRST SYSTEM

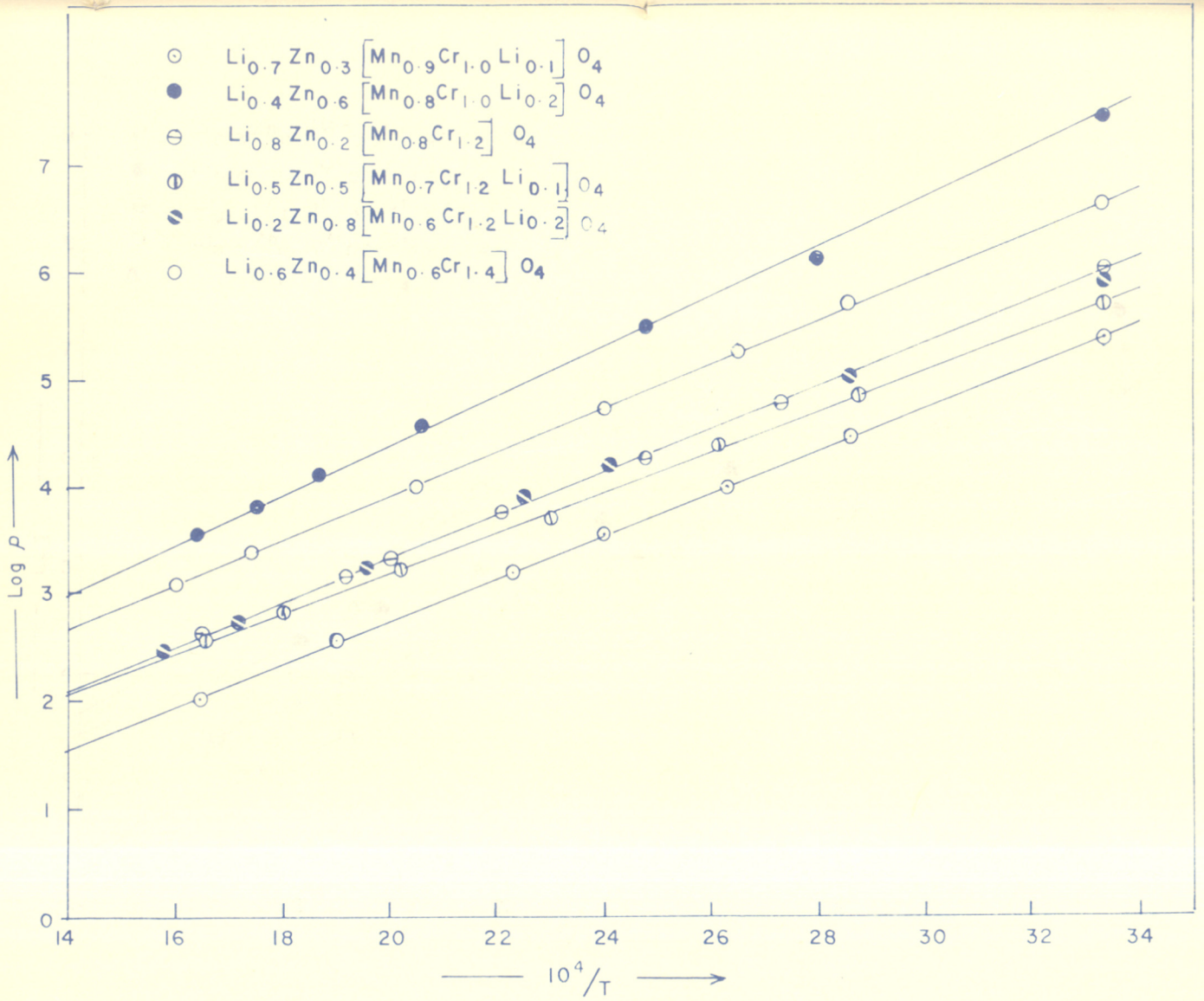

Fig.26 PLOTS OF LOG ρ AS A FUNCTION OF RECIPROCAL TEMPERATURE FOR FIRST SYSTEM

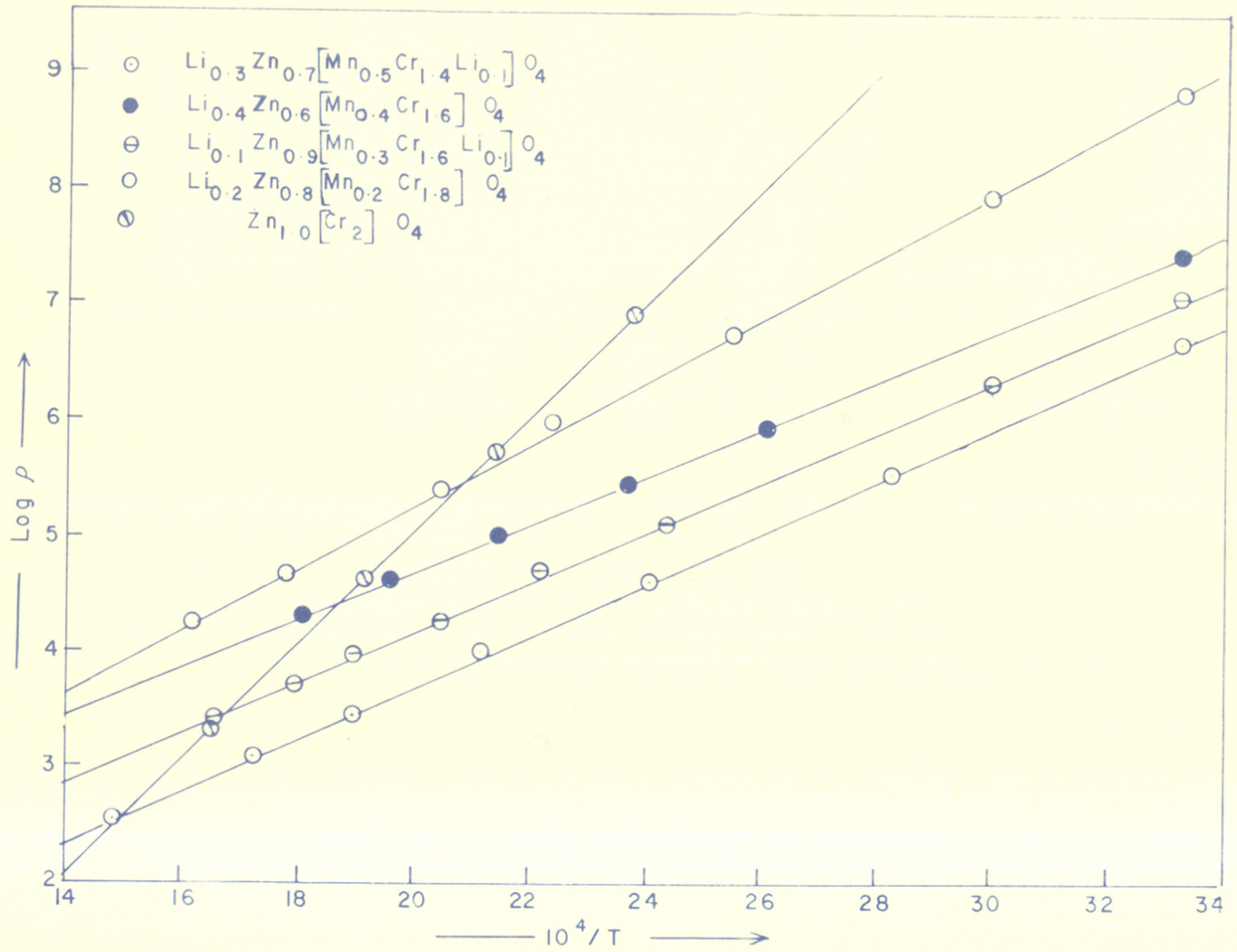

Fig 27. PLOTS OF LOG ρ AS A FUNCTION OF RECIPROCAL TEMPERATURE FOR FIRST SYSTEM

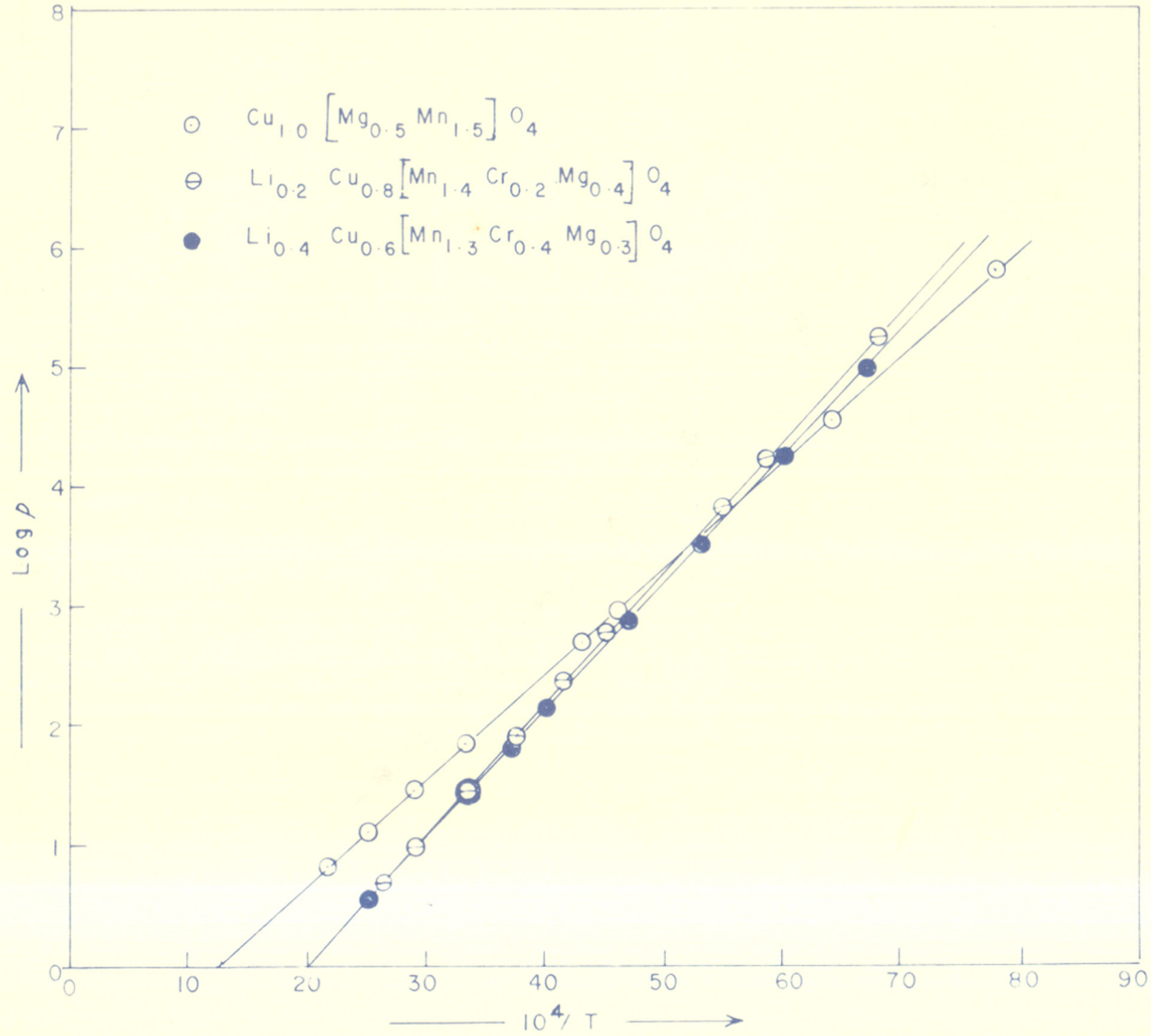

Fig 28 PLOTS OF LOG ρ AS A FUNCTION OF RECIPROCAL TEMPERATURE FOR SECOND SYSTEM

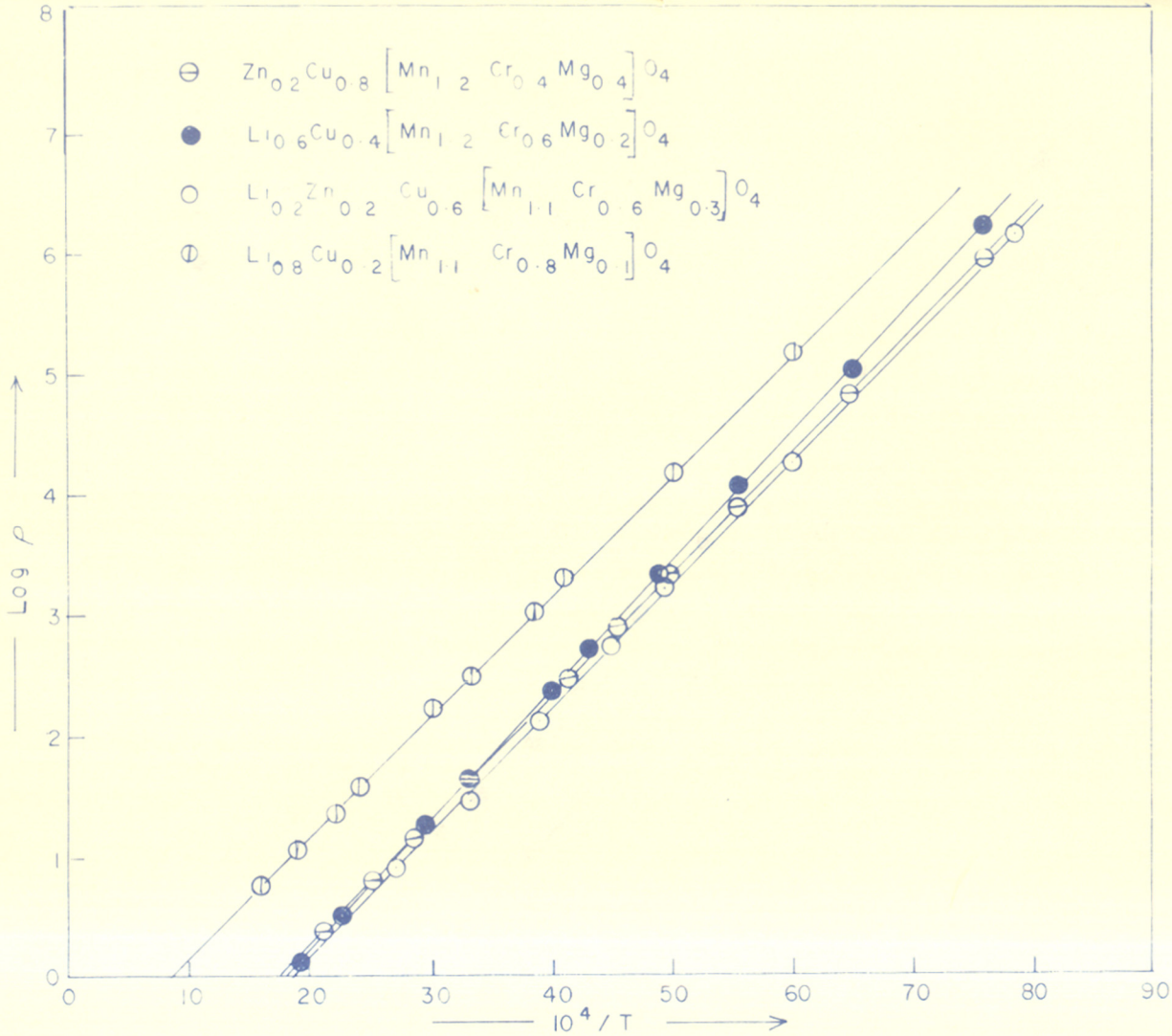

Fig 29. PLOTS OF LOG ρ AS A FUNCTION OF RECIPROCAL TEMPERATURE FOR SECOND SYSTEM

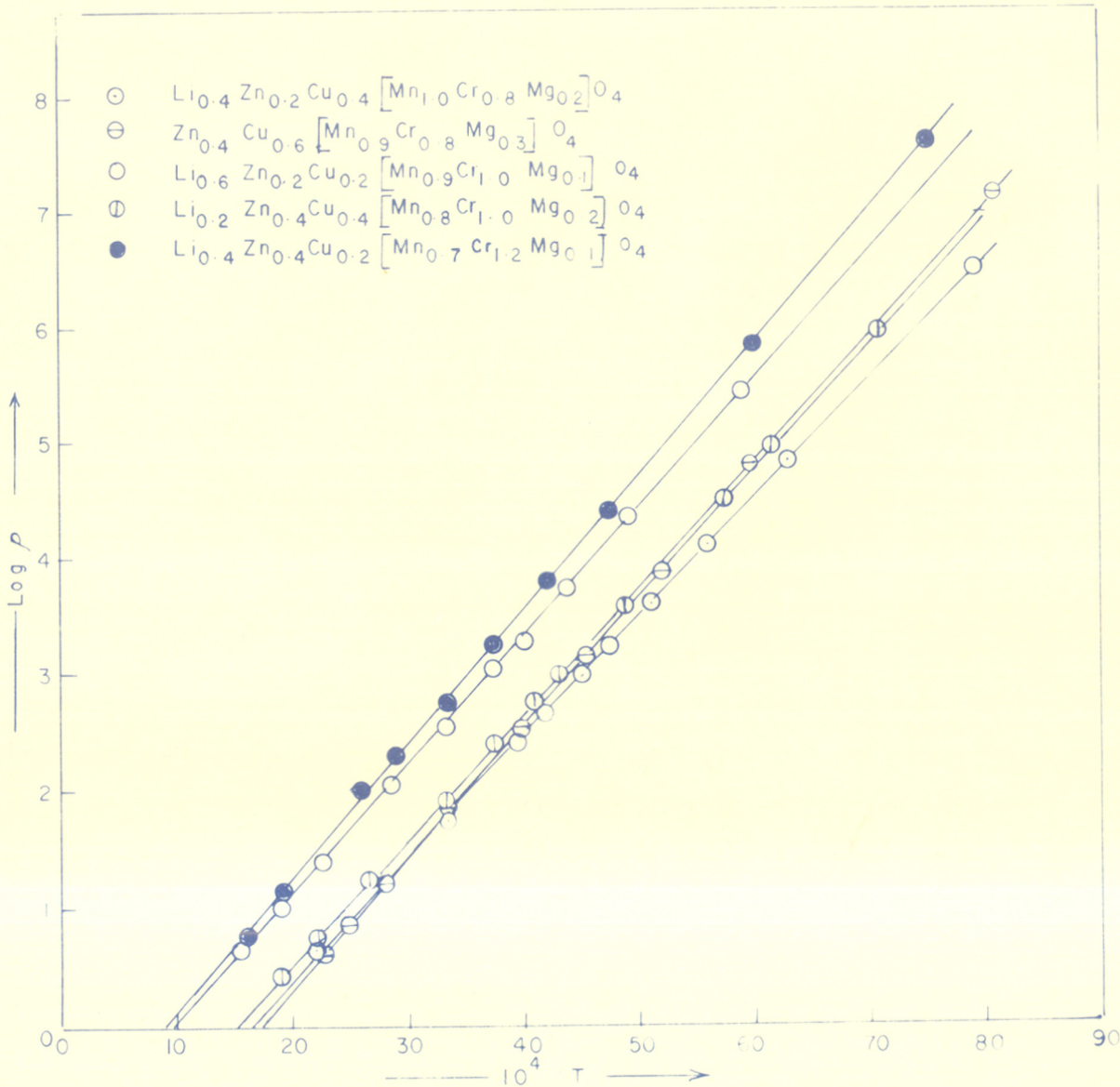

Fig. 30 PLOTS OF LOG ρ AS A FUNCTION OF RECIPROCAL TEMPERATURE FOR SECOND SYSTEM

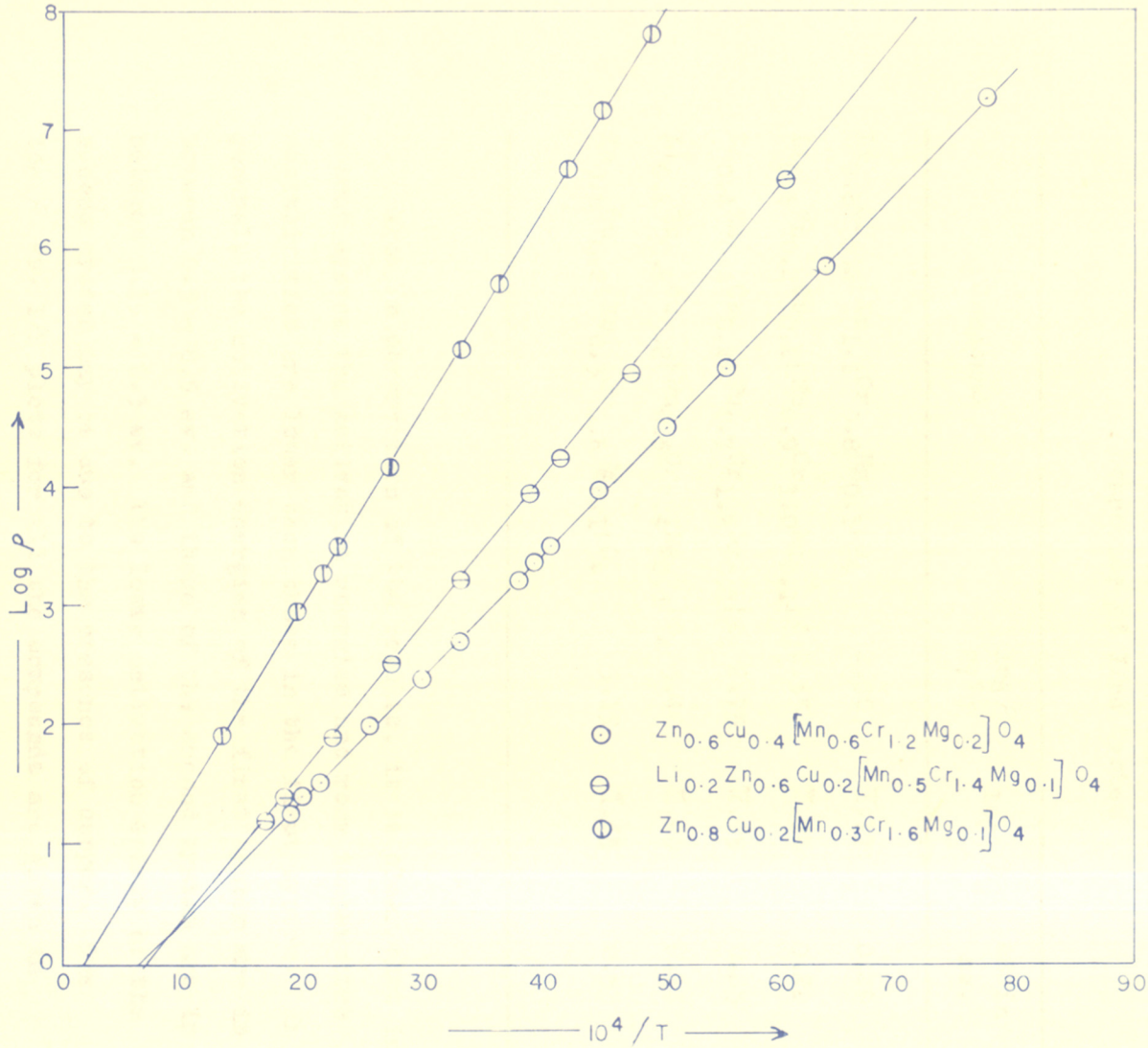

Fig.31. PLOT OF LOG ρ AS A FUNCTION OF RECIPROCAL TEMPERATURE FOR SECOND SYSTEM

Table - 37

Results of Conductivity Measurements of the Compounds of IInd System

Compound	log ρ 27°C	log ρ_o	ΔE in ev.
$Li_{0.8}Cu_{0.2}[Mn_{1.1}Cr_{0.8}Mg_{0.1}]O_4$	2.50	$\bar{1}.17$	0.20
$Li_{0.6}Zn_{0.2}Cu_{0.2}[Mn_{0.9}Cr_{1.0}Mg_{0.1}]O_4$	2.55	$\bar{2}.92$	0.22
$Li_{0.4}Zn_{0.4}Cu_{0.2}[Mn_{0.7}Cr_{1.2}Mg_{0.1}]O_4$	2.75	$\bar{2}.95$	0.23
$Li_{0.2}Zn_{0.6}Cu_{0.2}[Mn_{0.5}Cr_{1.4}Mg_{0.1}]O_4$	3.40	$\bar{2}.80$	0.24
$Zn_{0.8}Cu_{0.2}[Mn_{0.3}Cr_{1.6}Mg_{0.1}]O_4$	5.15	$\bar{1}.65$	0.33

From an observation of the results, it is clear that in the second system the activation energies and room temperature resistivities are lower than those in the first system. In general, the activation energies of the first system are in between 0.3 - 0.5 ev. and those of the second system are in between 0.15 - 0.3 ev. The lower activation energy of the second system may be due to the presence of copper. The log ρ vs. 1/T plots for all the compounds are given in Figures (24-31).

CHAPTER - IV

DISCUSSION

A careful study of the χ_M^{-1}- T curves of different compounds presented in Fig.Nos.(10-23) reveals some interesting features. The work may be divided into two systems, the first system containing Li^{1+} and Zn^{2+} at tetrahedral sites and Mn^{4+}, Cr^{3+} and Li^{1+} at octahedral sites; and the second system containing Cu^{1+}, Li^{1+} and Zn^{2+} at tetrahedral sites and Mn^{4+}, Cr^{3+} and Mg^{2+} at octahedral sites.

In first system, the compound $Li^{1+}_{0.5}Zn^{2+}_{0.5}[Mn^{4+}_{1.5}Li^{1+}_{0.5}]O_4$ shows a perfect linear $1/\chi_M$-T plot with an asymptotic Curie temperature of 57°K, indicative of a ferromagnetic ordering below the curie temperature. However, the next compound with 10 per cent chromium at octahedral site shows a marked departure from linearity in the $1/\chi_M$-T plot in the low temperature region. This tendency continues until 40 per cent of the octahedral sites are occupied by chromium. In the remaining compounds when chromium concentration is higher, the compounds give again straight χ_M^{-1}—T lines with negative θ values showing the predominance of antiferromagnetic behaviour below the ordering temperature. There is a regular change in the value of θ with increasing chromium concentration. In Fig.(17) the variation of θ with Cr ion concentration is presented graphically. As the value of θ depends also on the total number of magnetic ions, three curves are drawn each having a constant value of total number of magnetic ions.

The second system is more complicated than the first because it contains five different icns and in addition copper,

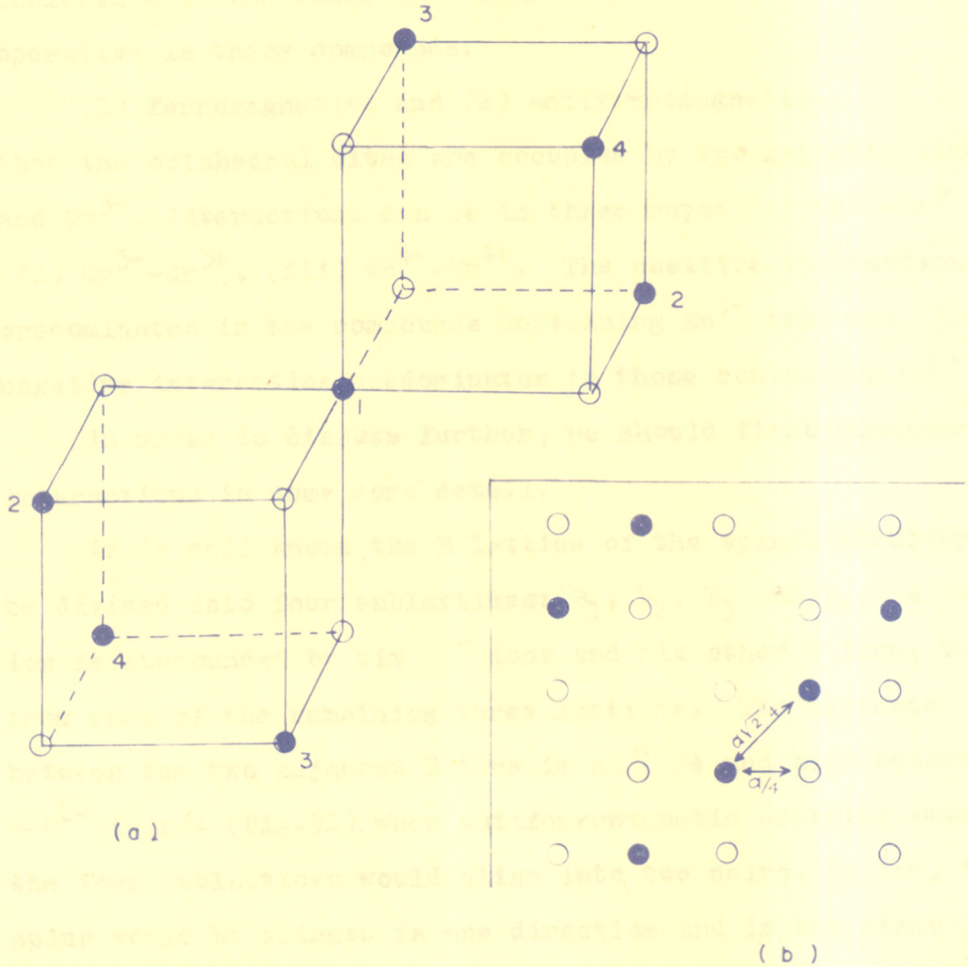

FIG. No. 32 SIX NEAREST METAL ION NEIGHBOURS OF AN OCTAHEDRAL METAL ION

● — METAL ION

○ — OXYGEN ION

which can be present either as Cu^{1+} at tetrahedral site, or Cu^{2+} at octahedral site or both. In the second system almost all the graphs are close to straight lines. The gradual transition from ferromagnetic to antiferromagnetic ordering is indicative of the facts that there are two interactions operative in these compounds:

(1) ferromagnetic, and (2) antiferromagnetic.

When the octahedral sites are occupied by two magnetic ions Mn^{4+} and Cr^{3+}, interactions can be in three ways: (i) Mn^{4+}-Cr^{3+}, (ii) Cr^{3+}-Cr^{3+}, (iii) Mn^{4+}-Mn^{4+}. The positive interaction predominates in the compounds containing Mn^{4+} ions and the negative interaction predominates in those containing Cr^{3+} ions.

In order to discuss further, we should first consider 90^{o} interactions in some more detail.

As is well known, the B lattice of the spinel structure can be divided into four sublattices: B_1, B_2, B_3 and B_4. A 'B' ion is surrounded by six O^{2-} ions and six other B ions, two from each of the remaining three lattices. The distance between the two adjacent B ions is $a\sqrt{2}/4$ and that between B-O^{2-} is a/4 (Fig.32). When antiferromagnetic ordering sets in, the four sublattices would align into two pairs, in one, the spins would be aligned in one direction and in the other it would be in the opposite direction.

In the present system the magnetic ions are isoelectronic and have the $3d^3$ configuration and the sign of interaction itself is changed as we go from Mn^{4+} to Cr^{3+}. The interactions in these compounds can arise (i) due to the interaction of t_{2g}

electrons of the neighbouring B ions and (ii) due to the indirect interaction between the two d^3 ions via the intervening oxygen ion, the B-O-B angle being 90°.

In the case of half filled overlapping orbitals between any pair of ions at a distance R-R', there is only one transfer integral $b_{R-R'}$, which is proportional to the orbital overlap. The exchange parameter for the cation-cation contribution is given by:

$$J_{ij}^{C-C} \text{ (two half filled orbitals)} = -2\, b_{ij}^2\, U^{-1}$$

which is negative. In a substance with n unpaired d electrons per cation, the exchange integral for the total cation spin $S = n/2$ is,

$$J_{ij}^{C-C} \text{ (half filled - half filled)} = -\frac{2b_{ij}^2}{4S^2U}$$

The transfer integrals b_{ij} carry an electron from one ion to another without change of spin. Since the overlapping orbitals are half filled and the Pauli exclusion principle limits a given orbital to one electron of each spin this means that the interacting electrons must be antiparallel if the transfer is to take place. This leads to antiferromagnetic alignment. The parameter b_{ij} is proportional to the orbital overlap and so must increase exponentially with decreasing cation-cation separation.

In the present case the magnetic ions Cr^{3+} and Mn^{4+} have half filled t_{2g} orbitals and empty e_g orbitals. The e_g orbitals are directed towards the near neighbour anions and the d_{xy},

d_{yz}, d_{zx} orbitals are pointing towards the near neighbour cations (Fig.5). Now as the t_{2g} orbitals are half filled direct B-B interactions are possible and they are strongly negative. Goodenough[32,33] has pointed out that cation-cation interactions will be significant if octahedral site cations have the outer electron configuration $3d^m$ ($m < 5$) and the occupied octahedra share a common face or common edge and if $m < 3$ the cation-cation interaction may be as strong as or stronger than the c-a-c interactions. This tendency is enhanced by the fact that an absence of e_g electrons allows a minimal separation of cations sharing a common anion octahedron face or edge.

If the cation-cation separation is $R > R_c$, the electrons can be treated as localized and weak cation-cation interactions will occur. If $R < R_c$ then the cation electrons are delocalized and strong cation-cation interactions will occur. If two half filled t_{2g} orbitals overlap, optimum binding occurs for that configuration of t_{2g} electron spins, that permit the maximum amount of electronic charge in the overlapping region midway between the positive cation cores. If the electrons have parallel spins they exclude one another from this region. Therefore the antiferromagnetic correlation between the electrons on neighbouring cations stabilizes the binding.

Till now we have considered direct interactions between cations. Now let us see the interactions via the anion intermediary. As was mentioned earlier in Introduction, in d^3-d^3 the delocalization super exchange between t_{2g}-t_2g gives

antiferromagnetic interactions and between t_{2g}-e_g gives ferromagnetic interactions. Correlation superexchange via s orbitals is antiferromagnetic but via $p\sigma$, $p\pi$ or via $p\sigma$, $p\sigma'$ is ferromagnetic[43]. Because of the smaller radial extension of the s orbitals this contribution is smaller. It was proved[67] that in octahedral environment Cr^{3+} with a $3d^3$ configuration can only form magnetic $p\pi$ bonds, so the super exchange via the anion intermediary in case of d^3 electrons gives ferromagnetic interactions.

So both the direct interactions J^d and superexchange interactions J^s_{90} contribute to the 90° B-B interaction J_{90} in spinels. We have seen that J^d is negative and is highly dependent on the cation-cation separation. Now before considering the sign reversal of interactions let us consider the relative importance of both the interactions.

Miyahara *et al*[56] calculated the asymptotic Curie temperature neglecting the more distant exchange interactions and assuming that J_{90} is composed of J^s_{90} and J^d

$$\theta \text{ or } T_N = \frac{2S(S+1)(Z^sJ^s + Z^dJ^d)}{3k}$$

where S is the spin quantum number, k is the Boltzmann constant and Z^s and Z^d stand for the number of super and direct exchange paths. In the case of a normal spinel the number of paths of superexchange interaction (Z^s) are 12 and the number of nearest neighbour cations (Z^d) is 6. In 90° case the octahedral interstices of two neighbouring cations share a common edge and $\frac{Z^s}{Z^d} = 2$. They defined a normalized asymptotic Curie

temperature $\overline{\theta}$ as a measure of the exchange interactions by:

$$\overline{\theta} = \frac{6}{Z^s}\ \theta$$

In the table given below the dependence of $\overline{\theta}$ on Cr-Cr distance is evident.

Table - 38

Compound	Cr-Cr	Cr-O	Angle Cr-O-Cr	$\overline{\theta}$	θ
$ZnCr_2O_4$	2.94	1.99	95.4	-196	-392
$MgCr_2O_4$	2.95	2.00	95.5	-175	-350
$CdCr_2O_4$	3.04	1.99	99.9	- 42	- 83

The above data has been explained by the fact that the contribution of J^d at M-O-M angles of $\sim 90^o$ is important in the case of chromium. As J^d is very sensitive to the cation-cation separation when Cr-Cr distance increases the contribution of J^d falls rapidly and hence $\overline{\theta}$ of $CdCr_2O_4$ is -42 and that of $ZnCr_2O_4$ is -196.

Many workers have studied the 90^o B-B interaction in spinels containing chromium. The data on oxide spinels show that the interactions are highly negative whereas in sulphides and chlorides the interactions are positive. Menyuk, Dwight et al[52] have worked on several spinels of the type ACr_2X_4 where A is non magnetic zinc or cadmium and X is O, S or Se and held the view that the nearest neighbour Cr^{3+}—— Cr^{3+}

interaction is a combination of an antiferromagnetic direct interaction which is strongly sensitive to cell size and a less sensitive ferromagnetic superexchange interaction. They have plotted asymptotic Curie temperature vs. Cr-Cr distance for zinc and cadmium spinels. For a given A site ion there is a strong dependence of T_A on lattice size but the quantitative variation is quite different depending on whether the A site ion is zinc or cadmium. Since T_A is proportional to the sum of all the magnetic exchange interactions this indicates that the diamagnetic A site cation has a significant effect on these interactions.

The data on sulphide spinels given in Introduction further emphasizes the importance of Me_{oct}-Me_{oct} distance in the determination of sign of interactions.

Several workers are of the opinion that not only n-n interactions but n-n-n interactions must also be considered. Menyuk *et al*[52] when they considered the non linearity of $1/\chi$ vs T curves of the zinc containing spinels, tried to explain by assuming that the cell size decreases with decreasing temperature. They measured the cell dimensions at 300°K and 84°K and found that the cell length of $ZnCr_2Se_4$ decreases from 10.497 Å at 300°K to 10.485 Å at 84°K, and the cell size of $ZnCr_2S_4$ decreased from 9.986 Å at 300°K to 9.965 Å at 89°K. These changes were found to be too small to support the behaviour of zinc spinels and so they assumed that n-n-n interactions play an important role. It was shown by Anderson[68] that n-n interactions alone cannot lead to long range antiferromagnetic order in a cubic spinel with nonmagnetic

A site ions. P.K.Baltzer et al[50,51] considered 30 B-B interactions in spinels and argued that the large number of distant interactions could out-weigh the small number of stronger nearest neighbour interactions.

Till now we have considered the data on chromite spinels. In order to explain the sign reversal in chromites, Kanamori[42] proposed two mechanisms. In the first mechanism, he took into account the direct exchange interaction J^d between neighbouring cations. J^d may be negative when the orbitals of cations are mutually non orthogonal. If the sign of 90^o superexchange interaction J^s_{90} is independent of the kind of the anion and is +ve in case of Cr^{3+} then J_{90} between Cr^{3+}'s is positive in chlorides and negative in oxides on account of the larger separation of neighbouring Cr^{3+}'s in chlorides than in oxides. In the second mechanism, he neglected the J^d and considered a mechanism in which the sign of J^s varies with the kind of anion. In case of d^3 configuration (eg Cr^{3+}) the contribution of S-orbitals of anion to J^s_{90} is negative and the total contribution of the p orbitals will be positive. Therefore J_{90} between Cr^{3+}'s can be negative in some cases in which the contribution of S-orbitals is larger than that of p-orbitals.

The work of Blasse[55] on spinels containing tetravalent manganese shows the predominance of ferromagnetic interactions between Mn^{4+}—Mn^{4+}. So the first mechanism which considers both direct exchange and superexchange can better explain the results than the second mechanism which neglects the direct exchange and assumes that the sign of J^s_{90} varies with the kind of anion. Our results can be explained as follows.

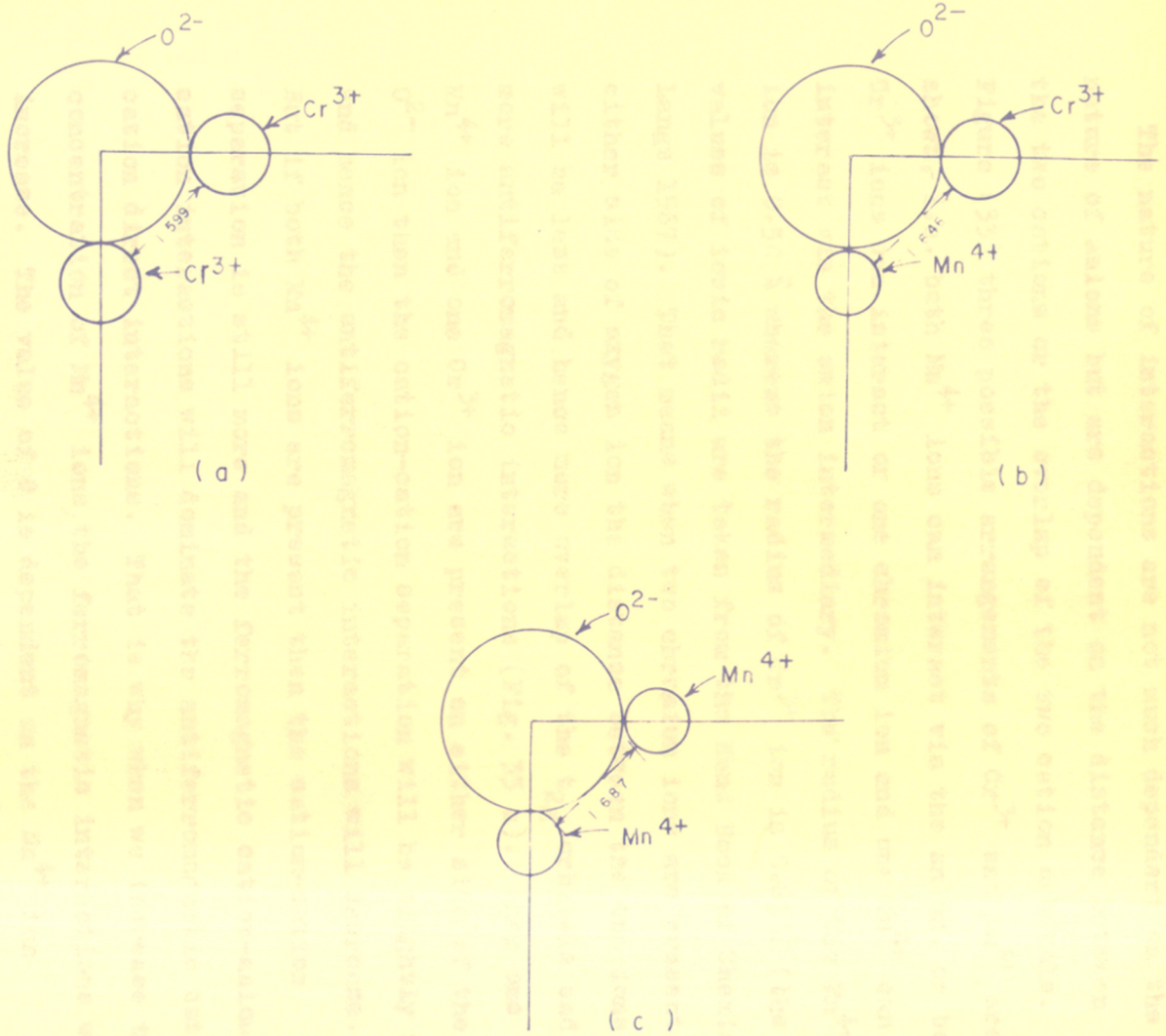

FIG-33 THE GEOMETRICAL CONFIGURATION OF O^{2-} AND Cr^{3+} AND Mn^{4+} IN THE CASE OF 90° INTERACTION THE RADIUS OF EACH CIRCLE IS PROPORTIONAL TO THE IONIC RADIUS.

The nature of interactions are not much dependent on the nature of anions but are dependent on the distance between the two cations or the overlap of the two cation orbitals. In Figure (33) three possible arrangements of Cr^{3+} and Mn^{4+} are shown, i.e. both Mn^{4+} ions can interact via the anion, or both Cr^{3+} ions can interact or one chromium ion and one Mn^{4+} can interact via the anion intermediary. The radius of the Mn^{4+} ion is 0.50 Å whereas the radius of Cr^{3+} ion is 0.65 Å (the values of ionic radii are taken from the Hand Book of Chemistry, Lange 1967). That means when two chromium ions are present on either side of oxygen ion the distance between the two ions will be less and hence more overlap of the t_{2g} orbitals and more antiferromagnetic interactions (Fig. 33 a). When one Mn^{4+} ion and one Cr^{3+} ion are present on either side of the O^{2-} ion then the cation-cation separation will be slightly more and hence the antiferromagnetic interactions will decrease. But if both Mn^{4+} ions are present then the cation-cation separation is still more and the ferromagnetic cation-anion-cation interactions will dominate the antiferromagnetic cation-cation direct interactions. That is why when we increase the concentration of Mn^{4+} ions, the ferromagnetic interactions will increase. The value of θ is dependent on the Mn^{4+} ion concentration but is more affected by the Cr^{3+} ion concentration because Mn^{4+}-Cr^{3+} and Cr^{3+}-Cr^{3+} interactions both are negative whereas only Mn^{4+}-Mn^{4+} interactions are positive.

The Me_{oct}-Me_{oct} distance varies with the change in the value of 'a' and as Me_{oct}-Me_{oct} distance increases the compounds

should become more ferromagnetic in behaviour. But in the case of these compounds the situation is complicated by the fact that there are many ions present and each will have its influence on 'u' and 'a' value. It is very difficult to correlate the magnitude of interactions with Me_{oct}-Me_{oct} distance because even when the distance remains the same if we put Cr^{3+} in place of Mn^{4+} there will be a lot of increase of antiferromagnetic interactions because of the difference in ionic radii. The value of θ can be correlated with the value of Me_{oct}-Me_{oct} distance, only in a cases where the octahedral ions are same but the distance between them is varied by putting some other anion, just as in the case of oxides, sulphides, selenides and chlorides of chromium.

It is clear from the above discussion that in our compounds both ferromagnetic and antiferromagnetic interactions are present. In the case of Mn^{4+}-O^{2-}-Mn^{4+} the superexchange interaction exceeds the direct exchange, and hence ferromagnetic behaviour would result. In the case of Cr^{3+}, the superexchange Cr^{3+}-O^{2-}-Cr^{3+} is exceeded by the direct exchange Cr^{3+}-Cr^{3+} and hence antiferromagnetic behaviour would result. Similarly in the case of Mn^{4+}-Cr^{3+} also antiferromagnetic interactions may result. So the final magnetic behaviours of the compound is a sum of ferromagnetic interactions between Mn^{4+}-O^{2-}-Mn^{4+} and antiferromagnetic interactions between Mn^{4+}-O^{2-}-Cr^{3+}, and Cr^{3+}-O^{2-}-Cr^{3+}. Though the nature of interactions can be predicted from this work it is not possible to make a quantitative estimate of the magnitudes of the interactions.

The C_M Values of the Compounds

The C_M values have been calculated from the slope of the high temperature region of $1/\chi_M$-vs-T curve. The C_M values for all the compounds have been given in Tables (24-30). The observed C_M values are much lower than the theoretical spin only values.

Low moments in chromites below Néel temperature were explained by P.K.Baltzer and P.J.Wojtowicz[69] as due to spin quenching. They argued that when chromium ion is present in a B site and if the B site is given a sufficient tetragonal or trigonal distortion, the doublet state having a spin of $\frac{1}{2}$ and a moment of one Bohr magneton becomes the ground state. They emphasised that a macroscopically distorted phase is not required for this effect and it is only necessary that a distribution of distorting neighbours be present, sufficient in numbers, to alter the symmetry about, and hence spin quench at least a fraction of chromium ions. The existence of spin quenched Cr^{3+} explains the moments of essentially all the chromites at temperatures below their Curie temperature. But they mentioned that the paramagnetic susceptibilities of all the chromites are high indicating that the Cr^{3+} exists in its high spin state above Curie temperature.

Actually in our compounds there are no distorting magnetic ions. If some of the Mn^{4+} had been present as Mn^{3+} to cause local Jahn-Teller distortion we could have got still higher C_M values, because Mn^{3+} contains four free spins. The observation of low C_M values itself proves the absence of

Mn^{3+} ions.

The low C_M values observed can be explained by assuming cluster formation. D.B.Rogers and R.W.Germann[70] have proposed that Mn^{3+} ions on a lattice of non Jahn-Teller ions may cluster due to a dynamic or static Jahn-Teller effect. Elastic energies associated with Jahn-Teller stabilizations, static or dynamic, are reduced by a clustering of the Jahn-Teller ions. Clustering introduces regions of slightly different M_s. They have presented some indirect evidence for clustering in lithium spinels of the type $M^{3+}[Li_{0.5}Mn^{3+}_{1.5}]O_4$ in which Mn^{3+} ions are partially substituted for M^{3+}. They have chosen the spinel system $M^{3+}[Li_{0.5}Mn^{3+}_{x}\ M^{3+}_{1.5-x}]O_4$ where M^{3+} is Fe^{3+}, Ga^{3+} and Al^{3+}. They have summarized approximate values for the critical concentrations (x_c) of these three ions, at which long range order is removed in the lithium spinel systems of iron, gallium and alluminium. They found that the critical concentration of manganese is less than that of the other ions. On the basis of octahedral site preference Mn^{3+} should be least effective since the expected preference decreases in the order Rh^{3+} > Cr^{3+} > Mn^{3+}. Therefore they proposed that the mechanism by which Mn^{3+} removes octahedral order is not only the forced migration of lithium to the A sites, but also the formation of manganese clusters that interrupt long range order. They have also explained the compositional dependence of the lattice parameters for the system $Li_{0.5}Fe_{2.5-x}Mn_xO_4$. Initially the substitution of manganese occurs randomly and an expansion of the lattice results in the normal way by introduction of larger

ion. But at a value of $x < x_c$ the concentration of manganese is sufficiently high that some of the substituted manganese can migrate at the reaction temperature to form clusters. Since this clustering results in a reduction of the elastic energies associated with Jahn-Teller stabilization, the effective radius of the manganese ion will be reduced. Thus a nonlinear lattice parameter dependence is anticipated for compositional ranges in which the manganese occurs both randomly and clustered. At a critical concentration x_c the clusters are sufficiently large and numerous that essentially all of the manganese ions are included in them and further substitutions result in a linear dependence of the lattice parameters.

G.Blasse[55a] has explained the low C_M values observed in $ZnMn_tFe_{2-t}O_4$ on the basis of clustering of Mn^{3+} ions at high values of t. He observed that the Curie constant is far too low compared with the spin only value and in some cases it is equal to the Curie constant calculated for Fe^{2+} and Mn^{4+}. He explained this on the basis of clustering of Mn^{3+} ions on octahedral sublattice. The question of Fe^{2+} and Mn^{4+} being present does not arise as the resistivity and crystallographic measurements point to the trivalent ions. He has done a simple calculation showing the relation between p the probability for a nearest-neighbour ion of a fixed Mn^{3+} ion in $Zn[Mn_{0.5}Ga_{0.5}]O_4$ to be Mn^{3+} and the Curie constant. He pointed out that in the system $ZnMn_tFe_{2-t}O_4$, the low Curie constants may arise due to any one of the following reasons:

(1) If there is a small amount of Fe^{3+} ions on A sites

magnetic clusters are formed due to strong Fe^{3+}-Fe^{3+} AB interactions. Clusters are also formed by Fe_A^{3+}-Mn_B^{3+} AB interactions.

(2) There may be some Mn^{3+} ions on A sites so that Mn_A^{3+}-Fe_B^{3+} clusters are possible.

(3) The cation distribution may change with temperature

(4) At higher temperatures the combination Fe^{2+} and Mn^{4+} may become occupied.

So he expressed the opinion that the interpretation of Curie constants of compounds with more than one kind of paramagnetic ions is quite complicated and must be done with care.

The low C_M values observed in our compounds can also be explained by assuming cluster formation. The spin pairing of Cr^{3+} ions does not seem reasonable because the spin pairing energy is known to be larger than the crystal field splitting. Moreover in the paramagnetic region the chromium compounds reported earlier showed the C_M values equal to the theoretical spin only values. So the possibility of spin quenching is ruled out in the case of our compounds.

The compounds contain Cr^{3+}, Mn^{4+} as paramagnetic ions at octahedral site and Mg^{2+} or Li^{1+} as diamagnetic ions. The percentage of paramagnetic ions is quite large at octahedral sites and the probability of each magnetic ion having another magnetic ion as its nearest neighbour is quite high. So the clusters can be formed at octahedral sites due to strong B-B interactions between Cr^{3+}-Cr^{3+} and Mn^{4+}-Mn^{4+} as compared to Mn^{4+}-Cr^{3+}. The energy is expected to be lower when there are clusters of Cr^{3+} ions and/or of Mn^{4+} ions than when both the

ions are distributed at random.

In the former cases the interaction would be between Cr^{3+}-Cr^{3+} and Mn^{4+}-Mn^{4+} and in the latter case between Cr^{3+}-Mn^{4+}. The former being much stronger we expect that cluster formation would lower the total energy of the system.

The cluster formation can be further supported by the fact that there is a strong deviation from the straight line in the plots of $1/\chi_M$ Vs.T in the low temperature region. Especially this behaviour is much pronounced in the first system where all the compounds show convex behaviour which can be explained by cluster formation.

4.2 ELECTRICAL PROPERTIES OF THE COMPOUNDS

Before discussing the electrical conductivity results, let us consider the various conduction mechanisms proposed for transition metal oxides.

Conduction Mechanism in Transition Metal Oxides

Transition metal oxides show a wide range of electrical conductivities, at one end having a typical insulator such as MnO ($\sigma \approx 10^{-15}\ \Omega^{-1}cm^{-1}$) and at the other extreme having a very good conductor such as ReO_3 ($\sigma \approx 10^{5}\ \Omega^{-1}cm^{-1}$). The electrical properties of solids can generally be explained on the basis of one of the two theories: (1) the Bloch-Wilson's Band theory, (2) the Heitler-London localised electron theory.

According to Bloch-Wilson's Band theory, in the case of crystalline solids, the allowed electronic states form bands of closely spaced energy levels separated by forbidden energy gaps. When all the bands are either completely full or entirely empty at $0^{o}K$, the substance is an insulator and a material with a partially filled band must be metallic. In case of insulators at higher temperatures some electrons can be promoted to the conduction band creating an equal number of holes in the valence band. The number of holes in the valence band (n_h) and the number of electrons in conduction band (n_e) at temperature T is given by:

$$n_e = n_h = \frac{1}{4}\left[\frac{2KT}{\pi\hbar^2}\,(m_e^{*}\, m_n^{*})^{1/2}\right]^{3/2} \exp -Eg/2KT$$

where m_e^* and m_h^* are the effective masses of electron and hole respectively. The conductivity is given by:

$$\sigma = n_e e\mu_e + n_h e\mu_h$$

where n_e and n_h are the concentrations of free electrons and holes respectively and μ_e and μ_h are the electron and hole mobilities. The temperature dependence of mobility is algebraic and is much weaker than exponential dependencies in n_e and n_h. Thus conductivity can be written as:

$$\sigma = \sigma_o(T)\ \exp^{-Eg/2KT}$$

where $\sigma_o(T)$ is an algebraic function of temperature. Thus a plot of $\ln \sigma$ Vs 1/T gives the value for the energy gap E_g provided the energy gap does not vary with temperature. Such plots are expected to be linear.

In the case of transition metal oxides, the only states in the vicinity of Fermi energy are those in the d bands and hence the d electrons are generally responsible for the electrical properties. The predictions of Band theory fail in the case of most of the transition metal oxides. For example, MnO has a partially filled band and thus should be metallic whereas actually it is an insulator ($\sigma_{RT} \approx 10^{-15}\ \Omega^{-1}cm^{-1}$). There are a large number of oxides predicted to be metallic by the band theory but they turn out to be insulating. This can be explained in one way that the d bands are too narrow to support metallic conductivity. However, there are a good number of oxides which show very good conductivity only with d band electrons ($ReO_3 \approx 10^5\ \Omega^{-1}cm^{-1}$).

Many workers tried to improve Band theory by introducing interactions between electrons. It was proposed by Slater[71] that antiferromagnetic interactions should be considered while calculating the ground state energy and in that case the self consistent potential in the Hartree-Fock equation cannot have full translational symmetry of the lattice. So the doubly periodic exchange potential splits the first Brillouin zone into half and introduces an energy separation at the surface between the new sub-zones. Antiferromagnetism can therefore lead to an insulating ground state for a large class of crystals which would otherwise be metallic (NiO, MnO).

Another improvement of Band theory was done by considering the crystalline distortion. According to this model the spontaneous crystallographic distortion to a lower symmetry at low temperatures introduces an energy gap. Adler[72] has considered both antiferromagnetic exchange interactions and crystallographic distortion to a lower symmetry, and observed that in that model the parameters were such as to give a second order transition for an antiferromagnetic case and a first order transition in a crystal distortion case. The gaps introduced by deformation of this type are of the order of tenths of electron volts and hence the distortions will occur only when the original band widths are of the order of tenths of electron volts or smaller. Therefore extremely narrow band materials with partially filled bands can lower their ground state energy by a crystalline structure distortion.

Eventhough Band theory with its modifications explains the

insulating ground state, it does not provide an explanation for the finite temperature behaviour of many materials. The reason for the failure of Band theory is the neglect of electron correlations, which are very important in narrow energy bands. Moreover the polar character of the ionic oxide structure causes a strong electron lattice interaction and modifies the electron band structure seriously.

The fact that electron correlations must be considered was first proposed by Mott[73]. He suggested that localization of electrons may arise due to the coulomb repulsion between two 3d electrons of opposite sign on the same ion. Hubbard[74] in a series of papers presented a relatively simple model that includes a large part of the correlations. He first considered the theory with the case of an S band having two states per atom (up and down spin states) because of mathematical simplicity involved in it. He obtained an approximate solution of the correlation problem for the model using a Green function technique. The solution has the property of reducing to the exact atomic solution in the approximate limit and to the ordinary uncorrelated Band picture in the opposite limit. In his later work he extended the simplest approximation to the case of d bands.

Localized Electron Model

The localized electron model is similar to the Heitler-London approach for the hydrogen molecule and assumes that the crystal consists of an assembly of fixed and independent ions sitting at their lattice positions and the overlap of the

electronic orbitals is very small. DeBoer and Verwey[75] made the first attempt to explain the mechanism of electrical conduction in oxide semiconductors. They assumed that a high potential barrier exists between any two transition metal ions in the crystal. If the life time of an excited state in which an electron can tunnel through the barrier is much shorter than the tunneling time, the electrons can be considered to be localized. Thus the material would be insulating at low temperatures and the energy required to go from the ground state to the conducting state can be identified as the activation energy for conduction.

Verwey[76] *et al* applied this model to lithium doped NiO. For every Li atom introduced in place of nickel atom, one Ni^{3+} ion and one Li^{1+} ion are produced and the extra hole on each Ni^{3+} ion should conduct in a narrow energy band. It was noted that this hole is initially attracted to the Li^{1+} ion, and the activation energy was the work required to separate the hole on the Ni^{3+} ion from the vicinity of Li^{1+}.

Heikes and Johnston[77] have extended the theory and noted that if Verwey's model is correct, when sufficient lithium atoms were added so that each nickel ion would be expected to have at least one lithium ion as a nearest neighbour, the activation energy should vanish. They were the first to ascribe the localization of holes to Landau trapping and they noted that activation energy is associated with mobility rather than carrier concentration.

These theories were later developed into *Polaron theory*

by Yamashita Kurosowa[78], Holstein[79], Frölich[80] and many others.

When an electron is slowly moving then as a result of electron lattice interaction, the surrounding lattice particles will be displaced to new equilibrium positions. If the potential well provided by the induced displacements is sufficiently deep, the electron will occupy a bound state, unable to move unless accompanied by the well. The unit consisting of the electron together with its induced lattice deformation is called Polaron. Its effective mass is larger than that of the Bloch electron. If the size of the Polaron is larger than lattice constant, it is called a large Polaron and if it is confined to distances less than the unit cell edge it is called small Polaron.

The large Polaron Hamiltonian was first derived by Frölich and according to that the excess electron interacts with a dielectric continuum instead of a crystal lattice consisting of +ve and -ve ions. The Polaron mobility decreases exponentially with increasing temperature and the description of large Polaron conduction is based on band model.

Small Polaron model is applicable when the electronic bands are narrow. The conduction can occur either by small Polaron hopping or by small Polaron band conduction.

Yamashita and Kurosowa[78] assumed the electron wave function to be localized around an ion and they have shown that there exists a certain probability of such electrons jumping from one ion to another neighbouring ion due to perturbation caused by such neighbours. This type of transition of electrons is accompanied by emission or absorption of phonons. The process

is therefore a thermally activated process and the mobility of charge carriers is associated with a thermal activation energy. At very low temperatures when the lattice is fixed Polaron band conductivity dominates. They calculated Polaron band width as a function of temperature. For reasonably high temperatures the Polaron band width decreases exponentially as the temperature is raised. At high temperatures Polaron band becomes so narrow that the band picture breaks down and electrons can be described by localized models. The mobility in this case increases exponentially with increasing temperature.

Holstein[79] carried out a more complete calculation using a perturbation theory on the Boltzmann equation. He emphasized the importance of small Polaron band conduction at low temperatures and at temperatures below about half the Debye temperature θ_D, Polaron band conductivity dominates. But because of the decreasing band width, the mobility of Polarons in this region decreases sharply with increasing temperature. For temperatures greater than about half the Debye temperature, the band width becomes zero and conductivity occurs by means of uncorrelated hopping of Polarons. In this region mobility increases exponentially with temperature.

D.Adler[81] in his article on insulating and metallic states in transition metal oxides has considered the applicability of various models to the actual experimental results of transition metal oxides. He concluded that neither the uncorrelated hopping of small Polarons nor Polaron band conductivity can explain the transport properties. He remarked that the electron

phonon interaction is probably less than what has been anticipated. Moreover, there is no evidence for the formation of small Polaron in any of the material. He mentioned that Hubbard's narrow energy band theory which predicts a splitting of 3d band into many narrow bands is the most reasonable one, if the electron-phenon coupling is not very large. But the transport properties of Hubbard model are not yet calculated in detail. This model can account for a material of any crystal symmetry being either a metal or a semiconductor with an energy gap. Our results can be explained as follows.

The specific resistance ρ has been measured on sintered pellets at temperatures upto 600°K. The plots of log ρ vs.1/T are given in (Fig.24-31). All the plots are straight lines and from the slope of the line the activation energies of the compounds were calculated (Tables 31-37). The activation energies of the compounds containing copper have been found to be lower than those of the compounds which do not contain copper. There has been a lot of controversy regarding the valence of copper in the compound $CuMn_2O_4$. Copper manganite was found to have the normal cubic spinel structure by Sinha *et al*[12] and they assigned the formula $Cu^{1+}[Mn^{3+}Mn^{4+}]O_4$--(1) This formula was supported by Blasse's study of paramagnetic susceptibility. Sabane[62] did the electrical conductivity and thermoelectric coefficient measurements of copper manganite as a function of temperature and supported a formula close to $Cu^{1+}[Mn^{3+}Mn^{4+}]O_4$. - (2).

But Miyahara[83] and Baltzer and Lopatin[61] supported the

formula $Cu^{2+}[Mn^{3+}]_2O_4$ ←(2). They argued that Cu^{2+} ions at tetrahedral sites tend to distort the structure with $c/a < 1$ whereas the Mn^{3+} ions tend to distort the structure with $c/a > 1$. The two effects mutually balanced and hence the cubic structure is maintained.

The X-ray absorption edge measurements made by A.Miller[64] supports the formula $Cu^{2+}[Mn^{3+}]_2O_4$. Sheftel et al[65] have found that depending on the preparation condition, copper manganite can show a slight departure from normal spinel structure and they have ascribed the formula to the compound

$$Cu^{2+}_{x}\ Mn^{2+}_{1-x}\qquad \left[\ Cu^{2+}_{1-x}\ Mn^{4+}_{1-x}\ Mn^{3+}_{2\ x}\ \right]\ O_4 \qquad -\ (3)$$

where $0 < x < 0.33$

The calculated C_M values for the three formulas are (1) 4.84, (2) 6.95 and (3) 7.2 - 7.11. The work of Bull[82] on magnetic susceptibility of copper manganite as a function of temperature gave a C_M value of 4.75 which strongly supports the formula (1). Moreover the high conductivity of copper manganite cannot be explained by [2]. Shet[16] has studied the solid solutions $CuCrMnO_4$ and found that the conductivity of the system $CuCr_{2x}Mn_{2-2x}O_4$ increases with x upto x = 0.5 where it is maximum. After x = 0.5 the value starts decreasing again. He explained the results by assuming the formula (1) to be correct and that electron exchange between Cu^{1+} and Cu^{2+} at tetrahedral site also contributes to conductivity. The high conductivity of $CuCrMnO_4$:

$$Cu^{1+}_{0.5}\ Cu^{2+}_{0.5}[Mn^{3+}_{0.5}\ Mn^{4+}_{0.5}\ Cr^{3+}_{1.0}]\ O_4$$

is attributed to conduction taking place both at the octahedral and tetrahedral sites.

If the entire copper is present as Cu^{1+} then manganese would have to be present as Mn^{4+}. In this case conduction by hopping is not possible. Only mechanism would be the band conduction in Cu^{1+} band. Although the concentration of Cu^{1+} remains the same, the electrical conductivity decreases as we go down the table (Table 37). This clearly brings out the fact that it is Cu-Mn couple which is responsible for a high conductivity in spinels and not copper or manganese alone. Many copper containing spinels are known e.g. copper chromite, ferrite etc. but they do not show the high order of conductivity as $CuMn_2O_4$. Similarly the copper free manganites have very high resistance. On the other hand all manganites containing both copper and manganese invariably show high conductivity. Furthermore, from the results of the present study it can be seen that some compounds have relatively low concentration of copper but still they show high conductivity. Band formation at such low concentrations of copper is considered unlikely. Another point to notice is that a relatively small amount of copper is required to impart conductivity to these manganites whereas a relatively larger amount of manganese concentration is required to get the same result. This can be interpreted to mean that the conduction takes place in the manganese level and copper is required to create the required charge carriers in manganese levels. The only way in which this can be achieved

is by electron exchange between copper and manganese ions so that a mixture of Mn^{3+}, Mn^{4+} ions are created at the manganese sites. The conduction can then take place by electron exchange between the manganese ions. Conduction can also take place in the copper levels. It is not unlikely that Cu^{1+} levels (d^{10}) would interact to form a broad band. Any electron transfer from Cu to Mn levels would create some Cu^{2+} ions i.e. some holes in this band so that we will have a partially filled Cu^{1+} band and a partially filled Mn level. This can happen if the broad d band of copper overlaps with narrow band of the Mn^{3+}. The fermilevel is such that it leaves both the broad copper band and the narrow Mn^{3+} band partially filled. The conductivity can then be explained as hole conduction in the Cu^{1+} band and due to the electron exchange between Mn^{3+} and Mn^{4+} ions.

S U M M A R Y

S U M M A R Y

When the tetrahedral A sites of a spinel structure are occupied by diamagnetic ions, the 90° B-B interactions become quite significant. The Cr^{3+}- Cr^{3+} interactions in chromites are known to be antiferromagnetic whereas the Mn^{4+}-Mn^{4+} interactions in manganites are known to be ferromagnetic. In order to investigate this difference in the behaviour of isoelectronic ions Cr^{3+} and Mn^{4+} with a $3d^3$ configuration, this work was taken up.

Compounds containing diamagnetic ions at tetrahedral sites and Mn^{4+} and Cr^{3+} ions at octahedral sites have been prepared. The work is divided into two systems. The first system compounds contain Li^{1+} and Zn^{2+} at tetrahedral sites and Mn^{4+}, Cr^{3+} and Li^{1+} at octahedral sites. The second system compounds contain Li^{1+}, Zn^{2+} and Cu^{1+} at tetrahedral sites and Mn^{4+}, Cr^{3+} and Mg^{2+} at octahedral sites. The compounds were prepared by mixing the oxides under alcohol and firing the mixtures in oxygen atmosphere at 800, 900 and 950°C with intermediate cooling and grinding.

The completion of the reaction was checked by X-ray diffraction studies. All the compounds showed cubic spinel structure and no tetragonal distortion was observed. Quantitative X-ray intensity measurements were done for 12 compounds and the agreement between the values of observed and calculated intensities was found to be fairly good.

Paramagnetic susceptibility of all the compounds has been measured by the Guoy method in the temperature range 80-600°K

and $1/\chi_M$ was plotted as a function of temperature. The θ values were calculated from the high temperature linear portion of the curve. It was found that there is a gradual transition from ferromagnetic behaviour to antiferromagnetic behaviour in compounds, as the concentration of Cr^{3+} is increased or the concentration of Mn^{4+} is decreased.

It was concluded that the reason for the difference in behaviour of Cr^{3+} and Mn^{4+} is the difference in their ionic radii. Both direct exchange and superexchange contribute to J_{90}° and as Cr^{3+} ion is larger than Mn^{4+} ion, direct interaction which is strong and negative predominates in compounds rich in chromium, and hence they are antiferromagnetic. But in compounds rich in Mn^{4+} ion, the positive superexchange exceeds the -ve direct exchange and hence compounds are ferromagnetic.

The electrical conductivity of the pellets has been measured at various temperatures from room temperature to about $300^{\circ}C$. The log ρ is plotted against 1/T and the activation energies of all the compounds have been calculated. It is observed that the activation energies of compounds containing copper are less than the activation energies of the compounds which do not contain copper. The various mechanisms of conduction have been discussed.

REFERENCES

REFERENCES

1. Bragg, W.H. Nature, 95, 561 (1915)
2. Barth, T.F.W. and Posnjak, F. Zeitschur F.Krist 82, 325 (1932)
3. Verwey, E.J.W. and Heilmann, E.L. J.Chem.Physics, 15, 174 (1947)
4. Verwey, E.J.W., DeBoer, F. and Vansanten, J.H. J.Chem. Physics, 16, 1091 (1948)
5. Gorter, E.W. Philips Res.Reports, 9, 229, 295, 321, 403 (1954)
6. Goodenough, J.B. and Loeb, A.L. Physical Review, 98, 391 (1955)
7. Dunitz, J.D. and Orgel, L.E. J.Phys.and Chem.Solids, 3, 20 (1957)
8. Dunitz, J.D. and Orgel, L.E. J.Phys.and Chem.Solids, 3, 318 (1957)
9. McLure, D.S. J.Phys.and Chem.Solids, 3, 311 (1957)
10. Miller, A. J.Applied Physics, 30, 24S (1959)
11. Goodenough, J.B. Magnetism III (Rado and Suhl) p.1
12. Sinha, A.P.B., Sanjana, N.R., Biswas, A.B. Acta Crysallographica, 10, 439 (1957)
13. Bongers, P.F. Thesis, University of Leiden (1957)
14. Wickham, D.G. and Croft, W.J. J.Phys.Chemistry Solids, 7, 351 (1958)
15. Blasse, G. J.Phys.and Chem.Solids, 27, 383 (1966)
16. Shet, S.G. Thesis, University of Poona (1969)
17. Blasse, G. J.Inorg.Nucl.Chem. 25, 743 (1963)
18. Jogalekar, P.P. and Sinha, A.P.B. Indian Jour.of Pure and Appl.Physics. 5, 9, 208 (1967)

19. Ghare, D.B. and Sinha, A.P.B. J.Phys.and Chem.Solids, 29, 885 (1968)

20. Néel, L. Ann.Phys.(Paris), 3, 137 (1948)

21. Borovik, A.S - Romanov and Orlova, M.P. Soviet Phys. J.E.T.P. 5, 1023 (1957)

22. Yafet, Y. and Kittel, C. Phys.Rev. 87, 290 (1952)

23. Prince, E. Acta Crystallographica, 10, 554 (1957)

24. Jacobs, I.S. J.Applied Physics Suppl. 30, 301S (1959)

25. Lotgering, F.K. Philips Res.Reports, 11, 190,337 (1956)

26. Dwight, T.K. and Menyuk, N. Physical Review, 119, 1470 (1960)

27. Kaplan, T.A. Physical Review, 116, 888 (1959)

28. Lyons, D.H., Kaplan, T.A., Dwight,K. and Menyuk, N. Physical Review, 126, 540 (1962)

29. Hastings, J.M. and Corliss, L.M. Physical Review, 126, 556-565 (1962)

30. Sinha, A.P.B. and Sinha, K.P. J.Phys.Soc.Japan,Suppl. 17B1, 218 (1962)

31. Rosenberg, M. and Nicolae, I. Proceedings of International Conference on Magnetism, U.K. 561,(1964)

32. Wickham, D.G. and Goodenough, J.B. Physical Review, 115, 1156 (1959)

33. Goodenough, J.B. Physical Review, 117, 1442 (1960)

34. Zener, C. Phys.Review, 81, 440 (1951); 82, 403 (1952)

35. DeGennes, P.G. Phys.Review, 118, 141 (1960)

36. Heikes, R.R., McGuire, T.R. and Happel, R.J. Phys.Rev. 121, 703 (1961)

37. Anderson, P.W. and Hasegawa, H. Phys.Review, 100, 675 (1955)

38. Goodenough, J.B. Phys.Rev. 100, 564 (1955)

39. Wollan, E.O. and Koehler, W.C. Phys.Rev., 100, 545 (1955)

40. Kramers, H.A. Physica. 1, 182 (1934)

41. Anderson, P.W. Phys.Review, 79, 350 (1950)

42. Kanamori, J. J.Phys.Chem.Solids, 10, 87 (1959)

43. Goodenough, J.B. Magnetism and the Chemical Bond, 1968 Interscience Publishers, New York

44. Blasse, G. Philips Res.Reports, 18, 383 (1963)

45. Bertaut, E.F., Vu Van Qui, R.Pauthenet et. A.Murasik. J.Phys.Radium. 25, 516 (1964)

46. McGuire, T.R and Howard, L.N. Ceramic Age, 60, 22 (1952)

47. McGuire, T.R and Howard, L.N. Phys.Rev. 86, 599 (1952)

48. Lotgering, F.K. Proceedings of the International Conference on Magnetism. Nautingham, U.K. 1964 p.533

49. Anderson, P.W. Magnetism (Rado and Suhl) 25 (1963)

50. Baltzer, P.K., Lehman, H.W. and Robbins, M. Phys.Rev. Letters, 15, 493 (1965)

51. Baltzer, P.K., Wojtowicz, P.J, Lopatin, E. and Robbins, M. Phys.Rev. 151, 367 (1966)

52. Menyuk, N., Dwight, K, Arnott, R.J and Wold, A. J.Appl. Phys. 37, 1387 (1966)

53. Bongers, P.F. and Van Meurs, F.R. J.Appl.Physics, 38, 944 (1967)

54. Blasse, G. Philips Res.Reports, 18, 400 (1963)

55. (a) Blasse, G. Philips Res.Reports, 20, 528-555 (1965)
(b) Blasse, G. Solid State Communication, 3, 67 (1965)

56. Motida, K. and Miyahara, S. J.Phys.Soc. Japan, 28, 1188 (1970)

57. Motida, K and Miyahara, S. J.Phys.Soc. Japan, 29, 516-517 (1970)

58. Larson, E.G, Arnott, R.J. and Wickham, D.G. J.Phys.and Chem.Solids, 23, 1771 (1962)

59. Rosenberg, M. and Nicolau, P., Manaila, R. and Pausescu, P. J.Phys.Chem.Solids, 24, 1419-1434 (1963)

60. Sabane, C.D. Thesis University of Poona (1960)

61. Lopatin, E. and Baltzer, P.K. Phys.Letters, 22, 380 (1966)

62. Sabane, C.D, Sinha, A.P.B. and Biswas, A.B. Indian Journal of Pure and Applied Physics, 4, 187 (1966)

63. Naik and Sinha, A.P.B. Ind.Journal of Pure and Applied Physics, 7, 170 (1969)

64. Miller, A. J.Phys.Chem.Solids, 29, 633 (1968)

65. Sheftel, I.T, Zaslavskii, A.I and Kurlina, E.V. Soviet Physics Solid State, 3, 1979 (1962)

66. Moore, T.E., Meryllin, E and Selwood, P.W. J.A.C.S. 72, 856 (1950)

67. Shulman, R.G. and Knox, K. Phys.Rev.Letters, 4, 603 (1960)

68. Anderson, P.W. Phys.Review, 102, 1008 (1956)

69. Baltzer, P.K. and Wojtowicz, P.J. J.Appl.Physics Supplement, 30, 27S (1959)

70. Rogers, D.B., Germann, R.W. and Arnott, R.J. J.Appl. Physics, 36, 2338 (1965)

71. Slater, J.C. Phys.Rev. 82, 538 (1951)

72. Adler, D. and Brooks, H. Phys.Rev. 155, 826 (1967)

73. Mott, N.F. Proc.Phys.Soc.(London) A62, 416 (1949), Nuovo Cimento Suppl. 7, 312 (1958); Phil.Mag. 6, 287 (1961)

74. Hubbard, J. Proc.Royal Soc. A 276, 238 (1963); A277, 237 (1964); A281, 401 (1964) ; A285, 542 (1965); A296, 82, 100 (1966)

75. DeBoer and Verwey. Proc.Phys.Soc.A. 49, Suppl.59 (1937)

76. Verwey, E.J.W., Haajiman, P.J. and Romejin, F.C. Philips Res.Reports, 5, 173 (1950)

77. Heikes, R.R. and Johnston, W.D. J.Chem. Physics, 26, 582 (1957)

78. (a) Yamashita, J. and Kurosawa, T. J.Phys. Soc. Japan, 15, 802 (1960)

(b) Kurosawa, T. J.Phys. Soc. Japan, 15, 1211 (1960)

79. Holstein, T. Ann. Phys. N.Y. 8, 325, 343 (1959)

80. Frölich, H. Adv. Physc. 3, 325 (1954)

81. Adler, D. Solid State Physics, Vol.21, 1 (1968) Academic Press, New York-London

82. Buhl, R. J.Phys. Chem. Solids, 30, 805 (1969)

83. Miyahara, S. J.Phys. Soc. Japan, 17B1, Suppl. 181 (1962)

ooooOOOooooo